Factors affecting the non-structural functions of Rubella virus capsid

by

Steven Derald Willows

A thesis submitted in partial fulfillment of the requirements for the degree of

Doctor of Philosophy

Department of Cell Biology
University of Alberta

Abstract

During infection, the host cell environment must be altered to accommodate viral replication. These alterations include hijacking cellular membranes as well as other components to form viral replication compartments and attenuating the host defenses to prevent virus detection and elimination. While DNA viruses can encode single purpose proteins dedicated for these functions, RNA viruses have a more limited coding capacity and instead utilize proteins with multiple functions. Rubella virus, a single-stranded, positive-sense RNA virus in the family *Togaviridae*, is one example. The capsid protein of this virus, which forms the protective protein shell around the genomic RNA in the virion, also fulfils several non-structural roles during infection. While previous studies have revealed several host proteins that are associated with these non-structural roles, more work is needed in order to fully understand how capsid alters the host cell environment.

In this thesis, I investigated factors that affect the ability of capsid to inhibit apoptosis, a mechanism used to limit viral replication and eliminate infected cells within multicellular organisms. I found that phosphorylation and membrane association of capsid are important for its anti-apoptotic function, with both being necessary to prevent sequestration of capsid in RNA rich regions of the

cell. Furthermore, I discovered that a canonical binding site for protein phosphatase 1 (PP1) is important for the anti-apoptotic function of capsid as well as its role in virion assembly. Finally, I showed that the capsid protein antagonizes innate immune signaling, a function that is dependent on its PP1-binding site.

Acknowledgements

First and foremost, I would like to thank my mentor Tom. I am grateful for the opportunity he has given me to work in his lab and for the advice, patience and encouragement which have been so essential for my development as a scientist.

I would also like to thank the members of my supervisory committee, Dr. Thomas Simmen and Dr. Ing Swie Goping. Their guidance and input was vital for the progress of my research. I would also like to thank the other members of my examining committee, Dr. Maya Shmulevitz and Dr. François Jean, for taking the time to read and evaluate my thesis.

A special thanks goes out to all members of the Hobman lab, past and present. I would especially like to thank Dr. Cezar Stoica and Dr. Carolina Ilkow for taking me under their wing early in my studies. I would also like to thank Valeria Mancinelli and Eileen Reklow for their excellent technical help throughout my entire time in the Hobman lab.

I would like to extend my gratitude to our collaborators Dr. Charles Holmes, Dr. Tamara Arnold and Phuwadet Pasarj for help with reagents and advice that have been so important for the second project in my thesis.

Finally, I would also like to thank my friends and family for their love and support throughout the years. Most of all, I would like to thank my wife, Catherine, for being there for me through every part of this journey. Without her, none of this would be possible.

Table of Contents

List of Tables

List of Figures

List of Symbols and Abbreviations

°C	degrees Celsius
AIF	apoptosis inducing factor
AKAP	A-kinase anchoring protein
Bad	Bcl-2-associated death promoter
Bak	Bcl-2-associated k protein
Bax	Bcl-2-associated x protein
Bcl-2	B-cell lymphoma-2
Bcl-XL	B-cell lymphoma-extra large
BH	Bcl-2 homology domain
BHK-21	Baby hamster kidney-21 cells
Bid	BH3 interacting domain death agonist
bp	base pair
BSA	bovine serum albumin
cDNA	complementary DNA
cm	centimeters
CPI	complete protease inhibitor
CRS	congenital rubella syndrome
CT	C-terminus
CTD	c-terminal domain
DAPI	4',6-diamidino-2-phenylindole
DCP1	decapping protein 1
DD	death domain
DISC	death-inducing signaling complex
DMEM	Dulbecco's modified Eagle's medium
DMSO	dimethyl sulfoxide
DNA	deoxyribonucleic acid
dNTP	deoxynucleoside triphosphate
dsRNA	double stranded RNA
DTT	dithiothreitol
ECM	extracellular matrix
EDTA	ethylenediaminetetraacetic acid
EGFP	enhanced GFP
eIF	Eukaryotic Initiation Factor
ER	endoplasmic reticulum
EYFP	enhanced yellow fluorescent protein
FADD	Fas-associated death domain protein
FBS	fetal bovine serum
FL	gull length
g	gram

g	gravitational force
G3BP	Ras-GAP SH3 domain binding protein
GFP	green fluorescent protein
GST	glutathione-S-transferase
HBV	hepatitis B virus
HCMV	human cytomegalovirus
HCV	hepatitis C virus
HDM2	human double minute homolog 2
HEK 293T	human embryonic kidney 293T
HEPES	4-(2-hydroxyethyl)-1-piperazineethanesulfonic acid
HIV	human immunodeficiency virus
HSP	heat shock protein
HUVEC	Human umbilical vein endothelial cells
HV	high voltage
iASPP	inhibitory member of the apoptosis-stimulating proteins of the p53 family
IB	immunoblot
IFN	interferon
IFNR	interferon receptor
Ig	immunoglobulin
IP	immunoprecipitation
IRES	internal ribosome entry site
IRF	interferon regulatory factor
ISG	interferon stimulated gene
ISRE	interferon stimulated response element
JAK	janus kinase
kbp	kilo-base pairs
kDa	kilodalton
M	mole
MAM	mitochondria associated ER-membrane
MAVS	mitochondrial antiviral signaling protein
MC	microcystin
MDA5	melanoma differentiation-associated protein 5
MEM	minimal essential medium
mg	milligram
mL	millilitre
mm	millimetre
mM	millimolar
MMR	Measles Mumps Rubella
MOI	multiplicity of infection
MOT	multiplicity of transduction

mPTP	mitochondrial membrane permeability transition pore
mRNA	messenger RNA
NEAA	non-essential amino acid
NF-κB	nuclear factor kappa-light-chain-enhancer of activated B cells
ng	nanogram
nm	nanometre
NP-40	Nonident P-40
nsP	non-structural protein
NT	N-terminus
OMM	outer mitochondrial membrane
ORF	Open reading frame
PABP	poly-A binding protein
PAGE	polyacrylamide gel electrophoresis
Par-4	Prostate apoptosis response gene-4
PBS	phosphate-buffered saline
PBSCM	phosphate-buffered saline plus calcium magnesium
PBST	phosphate-buffered saline plus Tween
PCR	polymerase chain reaction
PD	pulldown
PFA	paraformaldehyde
PI3K	phosphatidyleinositol-4,5-bisphosphate 3-kinase
PKR	protein kinase R
poly(A)	polyadenosine
poly(I:C)	polyinosinic:polycytidylic acid
PP1	protein phosphatase 1
PVDF	polyvinylidene difluoride
qPCR	quantitative polymerase chain reaction
Rb	retinoblastoma protein
RER	rough endoplasmic reticulum
RIG-I	retinoic acid-inducible gene 1
RK-13	Rabbit kidney-13
RNA	ribonucleic acid
RV	Rubella virus
SARS-CoV	severe respiratory syndrome coronavirus
SDS	sodium dodecyl sulphate
SIM	structured illumination microscopy
SP	signal peptide
STAT	signal transducer and activator of transcription
TA	tail-anchored
Tat	trans-activator of transcription

tBID	truncated Bid
TEMED	N,N,N',N'-tetramethylethylenediamine
TLR	toll-like receptor
TMRM	tetramethylrhodamine methyl ester
TNF	tumor necrosis factor
TOM	translocase of the outer membrane
TRAIL	tumor necrosis factor-related apoptosis inducing ligand
U	units
UPR	Unfolded protein response
UTR	untranslated region
V	volts
v/v	volume/volume
vIBO	viral inhibitor of Bak oligomerization
VLP	virus like particle
vMIA	viral mitochondrial inhibitor of apoptosis
VSV	vesicular stomatitis virus
w/v	weight/volume
WNV	West Nile virus
Wt	wild type
µF	micro-Farad
µg	microgram
µL	microlitre

CHAPTER 1
Introduction

1.1 Rubella virus biology

Rubella virus (RV) is the causative agent of the disease Rubella, also known as the German measles, which is generally a mild, self-limiting disease. From a public health perspective, though, RV is most important due to the range of birth defects it causes when contracted during the early stages of pregnancy, collectively known as congenital rubella syndrome (CRS). While first characterized in 1815 as a rash separate from scarlet fever (Maton, 1815), RV's teratogenic effects were first discovered in 1941 by Norman Gregg, who noticed a history of German measles in mothers of children with unusual congenital cataracts (Gregg, 1941). Since this discovery, several vaccination programs have been conducted, resulting in the elimination of Rubella from several regions, including complete eradication from the Americas since 2009 (World Health Organization Rubella Fact Sheet, 2014). Despite the availability of effective vaccines, it is estimated that more than 100 000 babies are born with CRS every year. This is mostly due to poor vaccine coverage in several areas, especially South-East Asia and Africa.

While many RV infections are subclinical (Edlich *et al.*, 2005), common symptoms include low-grade fever, sore throat, lymphadenopathy and a maculopapular rash (Hobman, 2013). Typically, RV spreads through aerosols, with the virus initially replicating in the upper-respiratory tract and nasopharyngeal lymphoid

tissue (Banatvala *et al.*, 2004). Viremia is established 8-14 days after infection, with several organs, including the placenta, being affected (Banatvala *et al.*, 2004). The rash begins approximately 14 days after infection, signaling induction of the humoral response and termination of viraemia. Just before the onset of the rash, virus shedding occurs from the nasopharynx for 1 to 2 weeks or longer, although virus can be recovered from the nasopharynx up to 1 week before the onset of rash.

RV infection is associated with several complications after post-natal exposure, among them joint problems, thrombocytopenia and encephalopathy. While RV-associated arthropathy is rare in young children, up to 52% of females and 8.7% of males over the age of 11 years develop acute arthritis (Tingle *et al.*, 1986). Furthermore, nearly 30% develop recurrent arthropathy as late as 18 months post-infection. Although a transient reduction in thrombocyte counts are common during RV infection, more serious complications such as thrombocytopenic purpura and hemolytic anemia can occur, although rarely (Ueda *et al.*, 1985, Hobman, 2013). Encephalitis, which occurs in 1 per 5000-6000 cases, is the most serious complication with a mortality rate of up to 20% (Tyor *et al.*, 2014).

Several live-attenuated RV vaccines have been used and/or are currently in use. The first vaccine strain, HPV-77, was made through serial passage of RV in African green monkey kidney cells (Parkman *et al.*, 1966). This was followed quickly by the production of the Cendehill strain through passage of RV in primary rabbit kidney cells (Peetermans *et al.*, 1967) and the RA27/3 strain made by passage of RV in the human fibroblast cell line WI-38 (Plotkin *et al.*, 1967). Although more widely used initially, the HPV-77 strain was largely replaced with RA27/3 due to lower susceptibility to reinfection by wild type RV in the latter (Plotkin *et al.*, 1973). Since 1971 in the United States, the RV vaccine strains have been included as component of a trivalent vaccine with both measles and mumps, termed the MMR vaccine (Lievano *et al.*, 2012). While generally seen as safe, the RA27/3 vaccine has been reported to cause adverse effects when administered after childhood. Most adverse reactions are rather mild and include fever, rash, and injection site reaction (Lievano *et al.*, 2012, Sukumaran *et al.*, 2015). In females over the age of 11 though, acute and recurrent arthropathy were relatively common (Tingle *et al.*, 1986). Although immunization during pregnancy is not recommended, the RA27/3 strain was found to not be highly teratogenic (Preblud *et al.*, 1985).

1.1.1 Rubella and CRS

The most pressing problem caused by RV is its high teratogenicity, evident by its membership in TORCH: a group of infectious agents responsible for a large portion of birth defects, infant mortality and morbidity (Neu *et al.*, 2015). The risk of transmission of RV from the mother to the fetus is highest in the first trimester, with 81% of fetuses infected when exposed at this stage. The risk of transmission drops during the second trimester to 25%, but then increases again to 60% at 31-36 weeks and nearly 100% afterwards (Webster, 1998). Infection during the first 16 weeks appears to be the most teratogenic. In contrast, relatively few birth defects are observed when infection occurs five months or more after gestation. Fetal infection occurs after establishment of viraemia in the mother, with virus entering the placenta and ultimately passing to the fetus through damaged cells in the chorion (Tondury *et al.*, 1966). The virus then remains in the developing fetus regardless of the time of infection, with nearly 80-90% of infants having detectable RV in the first month after birth (Webster, 1998, Banatvala *et al.*, 2004).

The most common defect associated with CRS is sensorineural deafness, with up to 80% of children with CRS exhibiting this symptom (Wild *et al.*, 1989). In one study, over 80% of children with CRS exhibited cardiac defects, while almost half presented with cataracts (Horstmann, 1965). Brain damage and fetal growth

inhibition are also common in fetuses infected before 16 weeks of gestation (Webster, 1998). Additionally, CRS is associated with delayed onset type 1 diabetes, with nearly 20% of patients exhibiting diabetes by the time they were 30 (Menser *et al.*, 1978). Furthermore, patients are more likely to develop type 2 diabetes and thyroid disorders by the time they are 60 (Forrest *et al.*, 2002). Viral persistence is thought to play a role in pathogenesis (Rawls *et al.*, 1966). Infected cells readily establish persistent RV infections but often exhibit little cytopathic effect, however growth of the infected cells is significantly affected. This effect may be particularly relevant considering infants with CRS exhibit smaller birth size and abnormally low numbers of cells in various organs (Naeye *et al.*, 1965). Persistent infection of human fetal endothelial cells has also been observed in cell culture (Perelygina *et al.*, 2013) and it is tempting to speculate that the characteristic vascular defect seen in CRS infants is related to this phenomenon (Esterly *et al.*, 1967). Disruption of the mitochondria and cytoskeleton may also be a factor in teratogenesis (reviewed in Lee *et al.*, 2000).

1.1.2 Classification and life cycle

By the Baltimore classification system, RV is a type IV virus, containing a positive sense single stranded RNA genome (Baltimore, 1971). It belongs to the family of enveloped viruses called *Togaviridae* and is the sole member of its genus,

Rubivirus. The other genus in *Togaviridae*, *alphavirus*, is a group of arthropod-transmitted viruses that can be divided into "old world" viruses including Sindbis, Ross River and Chikungunya viruses whose infections are associated with rash and arthralgia and "new world" viruses that cause encephalitis, such as Eastern, Western and Venezuelan equine encephalitis viruses (reviewed in Zacks *et al.*, 2010, Suhrbier *et al.*, 2012). Unlike alphaviruses, which are transmitted by arthropod vectors, the only known reservoir for RV is humans (Hobman, 2013). While the comparison between RV and Alphaviruses is predominantly due to similar genomic features and replication strategies, their sequences are in fact quite dissimilar (Frey, 1994). Although only one serotype exists, RV is divided up into two clades, RGI and RGII (Health Section of the Secretariat of the League of Nations, 2005). RGI circulates predominantly in Europe, Japan, and the Western hemisphere while RGII, the more genetically diverse of the two, is limited to Asia and Europe (Zheng *et al.*, 2003).

Similar to most viruses, the RV life cycle begins by binding of the virion to a cellular receptor (Figure 1.1). Recently, myelin oligodendrocyte glycoprotein was identified as a receptor for RV (Cong *et al.*, 2011). However, expression of this protein is mostly limited to the central nervous system and, given the widespread cell tropism of RV, it is likely that there are other receptors. Membrane phospholipids and glycolipids are known to be important for viral

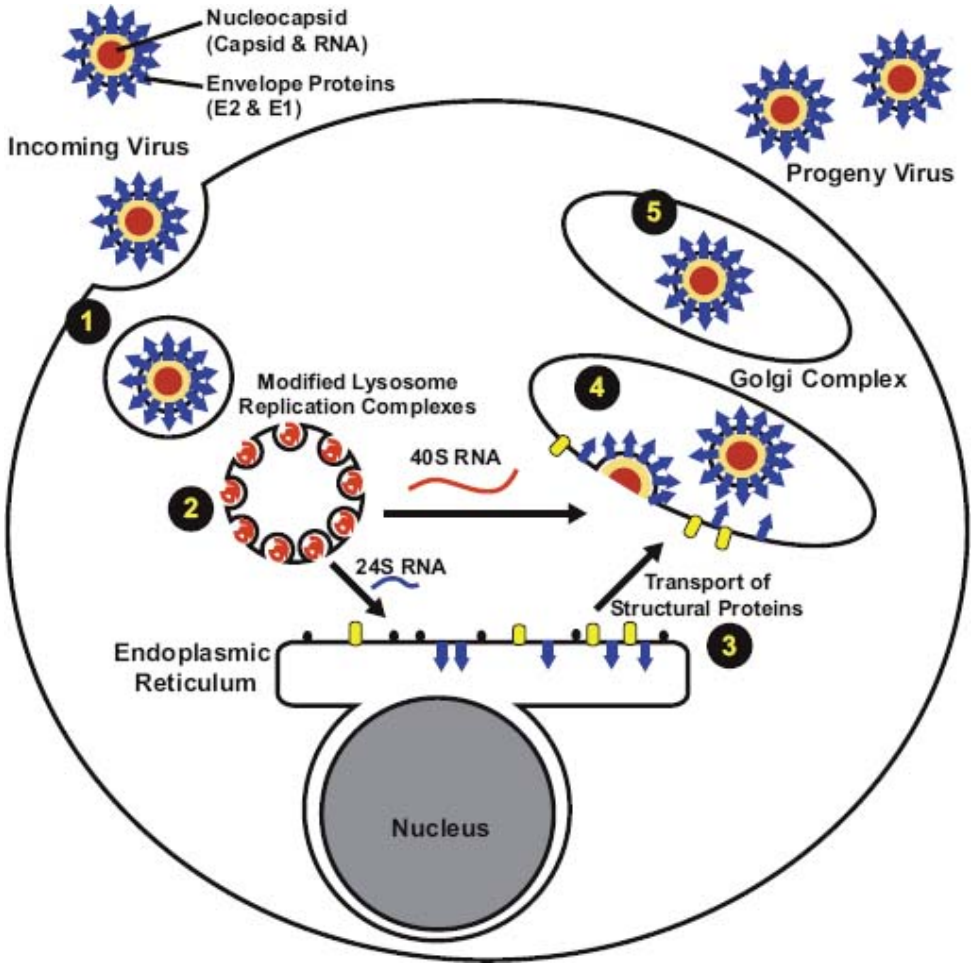

Figure 1.1 Rubella virus life cycle. 1. The RV virion binds to a membrane receptor and enters the cell through receptor-mediated endocytosis. The low pH of the endosome/lysosome results in release of the viral genome into the cytoplasm. 2. Viral replication complexes form from modified endosomes/lysosomes. These complexes act as the site of viral genomic replication and subgenomic RNA production. 3. The structural proteins are synthesized as a polyprotein precursor in association with ER membranes, which is then cleaved into capsid, E2 and E1 by host cell signal peptidase. 4. Structural proteins traffic to the Golgi compartment where viral assembly takes place. 5. After a maturation process in the Golgi, virions are released. Adapted from Hobman (2013).

entry as evidenced by the observation that treatment of cells with phospholipases A2 or C, beta-N-acetyl-D-glucosaminidase, alpha-glucosidase or beta-galactosidase reduced infection by RV (Mastromarino *et al.*, 1990). Similarly, addition of different phospholipids or glycolipids directly to cells impaired infection. Both E1 and E2 are able to induce viral entry in pseudotypes of lentiviral vectors, an activity which is enhanced by the capsid protein (Claus *et al.*, 2006). After attachment, virions enter the host cell through a clathrin-mediated endosomal pathway (Petruzziello *et al.*, 1996, Kee *et al.*, 2004). As is common among viruses that enter through receptor-mediated endocytosis, the low pH environment of the late endosome causes a conformational change in the envelope and capsid proteins of the RV virion, releasing the viral RNA into the cytoplasm (Katow *et al.*, 1988, Mauracher *et al.*, 1991). The positive strand RNA genome can then be directly translated to produce the viral replicase proteins.

Similar to all positive strand RNA viruses, replication of the RV RNA genome occurs on altered cellular membranes called replication complexes (Lee *et al.*, 1992). These replication complexes are formed from modified lysosomes, as double stranded RNA (dsRNA), an indicator of single stranded RNA virus replication, overlaps with several lysosomal markers (Magliano *et al.*, 1998). Replication complexes appear as large vacuoles in the cytoplasm with regularly

interspersed vesicles or spherules 60nm in size attached to the inner face of the vacuolar membrane (Lee *et al.*, 1992). These spherules are continuous with the cytoplasm through thin membranous necks and are the actual sites of viral replication (Lee *et al.*, 1994, Kujala *et al.*, 1999). A recent study has indicated more diverse structures where viral replication occurs, including large vesicles and "straight elements" that are also continuous with the cytoplasm (Fontana *et al.*, 2010). RV infection induces a clustering of various organelles around replication complexes, including the rough endoplasmic reticulum (RER), mitochondria, and Golgi complex (Lee *et al.*, 1992, Lee *et al.*, 1996a, Risco *et al.*, 2003). This is thought to enhance exchange of metabolites, RNA and proteins between the replication compartment and these organelles by reducing the distance between them. Unlike alphaviruses, which also cause organelle clustering, RV induces the formation of electron dense plaques between apposing membranes of the ER and mitochondria (Lee *et al.*, 1996a). After genomic replication and viral protein production, virions bud into the Golgi cisternae, although budding directly from the plasma membrane may occur to a lesser extent (von Bonsdorff *et al.*, 1969). The viral nucleocapsid assembly takes place at the same time as virion budding and nucleocapsids are only rarely seen in the cytoplasm (Lee *et al.*, 1999). This is in stark contrast to alphaviruses, which form their nucleocapsids in the cytoplasm and bud from the plasma membrane (reviewed in Simons *et al.*, 1980).

1.1.3 Rubella virus in cell culture and animal models

Most studies of RV done before 1979 used BHK-21 cells, although Vero and RK-13 cell lines are now commonly used (Frey, 1994). Titers of RV are significantly lower than those seen in alphavirus-infected cells but under optimal conditions can approach 10^7pfu/mL in BHK-21 cells and 10^8pfu/mL in Vero cells (Maes *et al.*, 1966, Vaheri *et al.*, 1967, Bardeletti *et al.*, 1979). RV replicates relatively slowly with virus titers not peaking until 48hrs (Hemphill *et al.*, 1988). It has been suggested that this may be due to the high GC content of the viral genome, which is thought to result in greater stability of RNA secondary structure and suboptimal codon usage (Frey, 1994). Generally, infected cell cultures exhibit little cytopathic effect, with most cells remaining alive 96 hours post-infection (Hemphill *et al.*, 1988). Interestingly, RV infection exhibits particularly low cytopathic effect in fetal and joint tissues and often establishes persistent infections (Miki *et al.*, 1992, Adamo *et al.*, 2004, Perelygina *et al.*, 2013). Synchronous infection is not possible in cultured cells, possibly due to fluctuation of a limiting cellular component during the cell cycle (Hemphill *et al.*, 1988, Frey, 1994). Recently though, it was found that when high MOIs were employed nearly synchronous infection in HUVEC cells resulted with most cells exhibiting RV antigen 24hrs post-infection (Perelygina *et al.*, 2013). Since two of the cells lines that produce the highest RV titers (Vero and BHK-21) lack a functional interferon

system, it has been suggested that RV is particularly sensitive to interferon (Mifune *et al.*, 1970, Frey, 1994). Indeed, addition of interferon significantly reduces viral replication (Wong *et al.*, 1967, Mifune *et al.*, 1970, Stanwick *et al.*, 1974). Furthermore RV does induce interferon expression and the induction of an anti-viral state in infected cells (Wong *et al.*, 1967). During infection, interferon expression drops rapidly after 2 days post-infection to much lower, but persistent levels. Despite these observations, extracellular viral titers were found to be slightly higher in the interferon competent A549 cells than Vero cells, calling into question the importance of interferon in viral replication in a tissue culture system (Perelygina *et al.*, 2013).

RV infection has characteristic effects on host cell replication and metabolism. For example, infection is associated with an increase in O_2 uptake: at first transiently during the first hour after infection and again later reaching a peak by 24hrs (Bardeletti, 1977). RV infection also changes both the amount and composition of lipids in host cells (Bardeletti *et al.*, 1976, Voiland *et al.*, 1980). Unlike many viruses, RV infection generally does not inhibit host cell translation on a global level at least early in the infection (Maes *et al.*, 1966, Vaheri *et al.*, 1967, Chantler *et al.*, 1980, Hemphill *et al.*, 1988). Results are more controversial in later infection though, with some studies reporting moderate to total translational inhibition 48hrs post-infection (reviewed in Frey, 1994). RV

infection is known to slow cell growth, an effect seen in both established, primary, and fetal cell cultures (Maassab *et al.*, 1966, Rawls *et al.*, 1966, Vaheri *et al.*, 1967, Boue *et al.*, 1969). One notable exception is human fetal endothelial cells, which show no difference between cell numbers in infected and uninfected cells (Perelygina *et al.*, 2013).

Investigation of RV pathogenesis has been limited by the lack of a working animal model. While African Green Monkeys can develop viremia and shed virus, infection is generally asymptomatic (Horstmann, 1969). Some CRS-like manifestations have been reported in offspring of infected rats, rabbits and monkeys, however the incidence is lower than that observed in human fetal infections (Delahunt *et al.*, 1967, Cotlier *et al.*, 1968, Kono *et al.*, 1969). Furthermore, others studies have shown no effects in these animals or inconsistent results (Webster, 1998). Due to these limitations, most understanding of the pathology of CRS has come from studies of aborted fetuses.

1.1.4 Viral genome

The viral genome is a single stranded RNA of positive polarity that can be directly translated by host ribosomes. Complete and partial RV genome sequences have been determined for several strains, including the wild type strains Therien (Frey *et al.*, 1986, Frey *et al.*, 1988, Dominguez *et al.*, 1990) and M33 (Clarke *et al.*,

1987), as well as the vaccine strains RA27/3 (Nakhasi *et al.*, 1989), Cendehill (Lund *et al.*, 2000) and HPV77 (Zheng *et al.*, 1989). Several sequences for various RV isolates are also available on Genbank. The viral RNA is both 5' capped and 3' polyadenylated (Oker-Blom *et al.*, 1984) and is 9757 nucleotides long when the polyA tail is excluded (Dominguez *et al.*, 1990). RV is known to have one of the most GC rich viral RNA genomes, with G/C bases making up 69.5% of the genome (Dominguez *et al.*, 1990). The RV genome contains two non-overlapping open reading frames (ORF): a 5' 6656 nucleotide ORF that codes for the non-structural proteins and a 3' 3189 nucleotide ORF that codes for the structural proteins (Figure 1.2). In addition to the genomic RNA, which has a sedimentation coefficient of 38-40S (Hovi *et al.*, 1970, Sedwick *et al.*, 1970), infected cells also contain a 24S subgenomic RNA that corresponds to the 3' structural gene ORF (Oker-Blom *et al.*, 1984). Similar to the genomic RNA, the subgenomic RNA is both capped and polyadenylated.

The RV genome contains several elements that are thought to play a role in replication, packaging, and interaction with host cell factors. There are three untranslated regions (UTRs): a 5' 40bp UTR, a 59bp 3' UTR, and a 123 nucleotide UTR between the non-structural and structural ORFs (Hobman, 2013). Two stem loop structures, one in the 5' untranslated region and one in the 3' untranslated region, were found to stimulate translation (Pogue *et al.*, 1993). The 123bp inter-

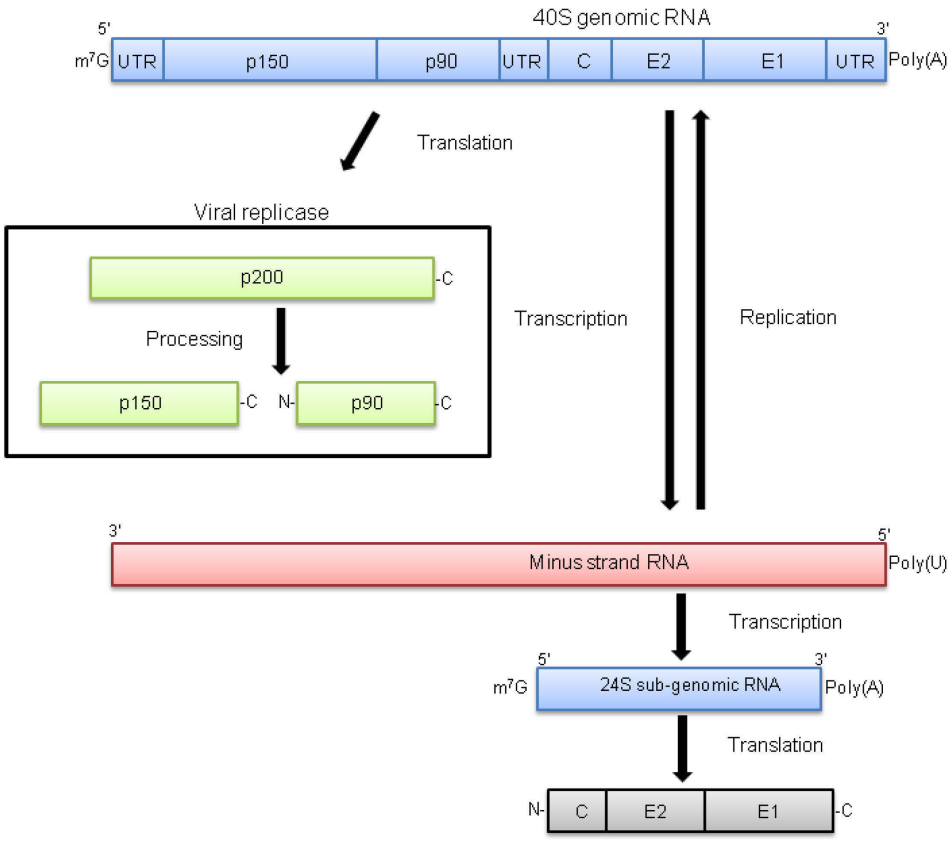

Figure 1.2 Rubella virus genome. The Rubella virus genome contains five genes and three untranslated regions (UTRs). The 5' ORF of the positive sense, 40S, genomic RNA is translated to produce the viral replicase polyprotein p200 that is later cleaved by a protease domain in the p150 protein. The replicase proteins, p150 and p90 transcribe the positive strand RNA into a minus strand that is used as a template to produce plus sense genomic and subgenomic RNAs. The subgenomic RNA is translated in association with ER membranes into the structural proteins capsid (C), E2 and E1. Adapted from Ilkow *et al* (2010b).

ORF UTR is also predicted to contain several stem loop structures and is known to affect translation of the subgenomic RNA in conjunction with 3' UTR elements (Pappas *et al.*, 2006, Hobman, 2013). Strangely, a predicted stem loop downstream of the starting site of the structural gene ORF has an inhibitory effect on translation (Pappas *et al.*, 2006). The complex stem loop structures in the 3' UTR not only affect translation but are also required for positive strand synthesis (Chen *et al.*, 2004a) and bind to several host proteins (Nakhasi *et al.*, 1994, Chen *et al.*, 1999). A stretch of nucleotides between 347 and 375 bind to the capsid protein and serves as the encapsidation signal (Liu *et al.*, 1996).

1.1.5 Non-structural proteins

The non-structural proteins are translated directly from the full length genomic RNA as a precursor polypeptide, p200, that is later cleaved into p90 and p150 (Marr *et al.*, 1994). Together these proteins form the viral replicase and are responsible for genome replication. The p150 protein contains a methyltransferase domain that is thought to be responsible for capping the genomic RNA, and a papain-like protease domain responsible for cleavage of the p200 polyprotein (Gorbalenya *et al.*, 1991, Rozanov *et al.*, 1992, Koonin *et al.*, 1993, Yao *et al.*, 1998). p150 also contains a poorly characterized X-domain, which has been shown to be important for activity of the protease domain but only when supplied in *trans* (Liang *et al.*, 2000b). Interestingly, this domain is

highly conserved in viruses with papain-like cysteine proteases and is one of the few regions highly conserved between RV and alphaviruses (Gorbalenya *et al.*, 1991). The p90 protein contains the RNA-dependent RNA polymerase and helicase motifs (Hobman, 2013). The cleavage of p200 is necessary for replication and triggers the switch from production of negative strand template RNA to positive strand genomic and subgenomic RNA (Liang *et al.*, 2000a, Liu *et al.*, 2000).

Predictably, a large pool of p150 and p90 localize to replication complexes in infected cells (Fontana *et al.*, 2007). Additionally, p150 and p90 localize to cytoplasmic fibers later in infection and these sites appeared to be a location of viral RNA replication (Forng *et al.*, 1995, Kujala *et al.*, 1999, Matthews *et al.*, 2009). The importance of these fibers is unknown, as inhibiting their formation did not significantly alter viral replication (Matthews *et al.*, 2010). p90 may also have functions unrelated to its replicase activities and has been reported to bind the host cell proteins Citron-K kinase (Atreya *et al.*, 2004) and the retinoblastoma tumor suppressor protein (Atreya *et al.*, 1998, Forng *et al.*, 1999). Furthermore, p90 expression induces tetraploidy in cells, possibly through a Citron-K kinase related inhibition of cytokinesis (Atreya *et al.*, 2004). While the significance of these interactions is unclear, they may be related to the slowed growth seen in RV infected cells.

1.1.6 Structural genes

Three structural proteins are involved in formation of the virion: the two envelope proteins E1 and E2 and the capsid protein. Virion particles range in size from 56-73nm in diameter and contain an electron dense nucleocapsid core surrounded by a lipid envelope (Murphy *et al.*, 1968). E2 and E1 form the spikes seen on the lipid envelope while the capsid protein binds to the RNA genome to form the nucleocapsid (Hobman, 2013). A recent electron tomography study revealed that RV virions are highly variable in size and shape, exhibiting what the authors describe as a "spherical" structure notably different from the typical icosahedral shape exhibited by alphaviruses (Battisti *et al.*, 2012). The virion is sensitive to heat, detergents and both protein and DNA damaging agents (Hobman, 2013). Infectivity is also lost with prolonged storage at -20°C and virions must be stored at temperatures below -60°C or lyophilized at 4°C.

The structural genes are translated as a single polypeptide from the 24S subgenomic RNA in the order NH_2-Capsid-E2-E1-COOH (Oker-Blom, 1984). This polyprotein is translated in association with RER membranes and is cleaved into its constituents by the host signal peptidase (Hobman *et al.*, 1988, Hobman *et al.*, 1989, Marr *et al.*, 1991). When the three structural proteins are expressed alone in cells, they form virus-like particles (VLP) that closely resemble RV virions

(Hobman *et al.*, 1994, Qiu *et al.*, 1994). This shows that viral RNA is not necessary for viral particle assembly.

1.1.6.1 The envelope proteins E1 and E2

As already mentioned, the E1 and E2 proteins form the viral spikes on the virion envelope and are responsible for receptor binding, internalization and membrane fusion. Although both proteins are present on the outer face of the viral envelope, E1 is the immunodominant antigen (Katow *et al.*, 1985, Waxham *et al.*, 1985a, Waxham *et al.*, 1985b). The E1 protein is a 481 amino acid protein and migrates as a discrete band between 55 and 62kDa by SDS-PAGE (Frey, 1994). E2 is a 282 amino acid protein and runs as two occasionally indistinguishable bands between 42kDa and 54kDa. The reason for this may be due to variability in glycosylation of E2. Indeed, both E1 and E2 are glycosylated at multiple asparagines (Hobman *et al.*, 1991, Lundstrom *et al.*, 1991, Qiu *et al.*, 1992) whereas E2 is heavily glycosylated on multiple serine/threonine residues (Lundstrom et al, 1987). Both proteins contain C-terminal transmembrane regions that anchor them to membranes (Clarke *et al.*, 1987, Hobman *et al.*, 1988). While E1, like the fusion proteins of alphaviruses, is a class 2 fusion protein (DuBois *et al.*, 2013), it is unique in that it is the only known viral fusion protein whose activity is $Ca2^{+}$ dependent (Dube *et al.*, 2014).

E2 protein appears to be responsible for correct targeting of the other structural proteins to the site of viral assembly, the Golgi complex. When expressed alone, E1 accumulates in a pre-Golgi compartment (Hobman *et al.*, 1992), and capsid remains associated with the ER (Hobman *et al.*, 1990, Baron *et al.*, 1992). The E2 protein, which contains a Golgi-targeting signal (Hobman *et al.*, 1995), masks an ER retention signal on E1 when the two proteins dimerize (Hobman *et al.*, 1997). This dynamic is thought to retain E1 in the ER to ensure proper folding before targeting to the Golgi (Hobman *et al.*, 1993). Ultimately, both the E2 transmembrane domains and the capsid transmembrane domain are important for proper targeting of these proteins (Garbutt *et al.*, 1999, Law *et al.*, 2001).

1.1.6.2 Capsid protein

As mentioned previously, capsid's primary structural role is to bind the viral genomic RNA and form the nucleocapsid in the center of the virion. It is a 300 amino acid protein that runs at an apparent molecular size of 33 to 35kDa during SDS-PAGE (Hobman, 2013). Although the reason is unknown, capsid will often migrate as a doublet or triplet by SDS-PAGE (Suomalainen *et al.*, 1990a). The capsid protein contains many positively charged arginine residues particularly in and around the RNA binding region located between residues 28 to 56 near the N-terminus of the protein (Figure 1.3) (Clarke *et al.*, 1987, Liu *et al.*, 1996). Similar to the envelope proteins, capsid is membrane associated and retains the

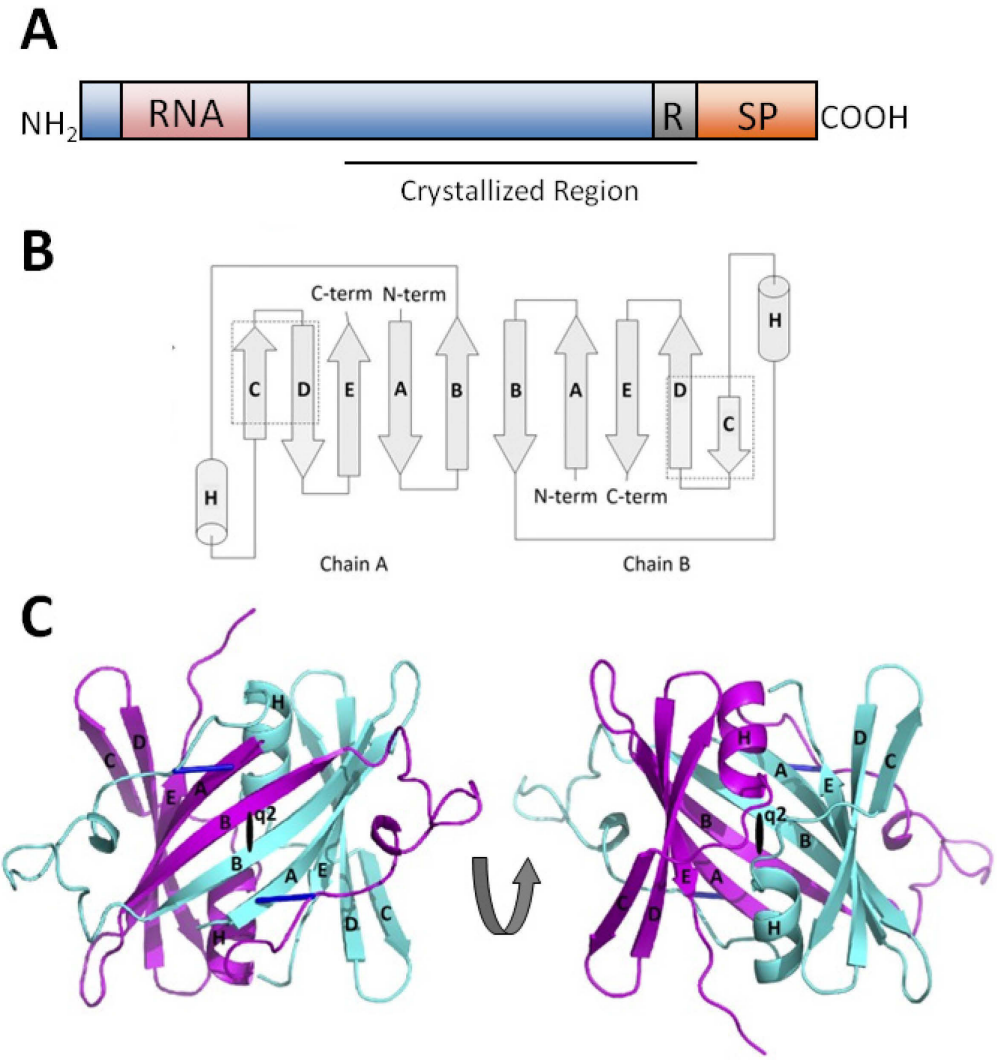

Figure 1.3 Rubella virus capsid structure. (A) Diagram of capsid structure showing the RNA binding region (RNA), C-terminal arginine rich region (R) and transmembrane E2 signal peptide region (SP). The region of capsid used for X-ray crystallography is indicated with a black line. (B) Diagram showing capsid secondary structure in crystallized region. β-strands are marked A-E and the single alpha helix is marked as H. (C) Ribbon diagram of capsid dimers (one monomer in cyan and the other in magenta) as determined by x-ray crystallography. Left and right figures are related by a 180 rotation. A quasi-twofold axis is indicated by black oval (q2). Disulfide bonds are indicated by blue cylinders. Adapted from Mangala Prasad *et al.* (2013)

E2 signal peptide from the original polyprotein for this purpose (Suomalainen *et al.*, 1990b). After it is cleaved from E2, the capsid protein does not appear to undergo subsequent proteolytic processing as evidenced by the fact that the E2 signal peptide is retained by capsid in mature virions (Suomalainen *et al.*, 1990b, McDonald *et al.*, 1991). Unlike the envelope proteins however, for which the bulk of the proteins are in the ER lumen, most of capsid faces the cytoplasm (Hobman, 2013). Capsid's membrane anchorage represents another major way in which RV differs from alphaviruses, whose capsids contain an autoprotease activity that releases them into the cytoplasm (Melancon *et al.*, 1987).

Recently, the crystal structure of a large portion of capsid's C-terminus was determined (Mangala Prasad *et al.*, 2013). Given the lack of sequence similarity between RV and alphaviruses (Clarke *et al.*, 1987), it is perhaps not surprising that the crystal structure of RV capsid bears little resemblance to alphavirus capsids (Choi *et al.*, 1991). Indeed, capsid's structure is unique and does not appear to share any structural similarity to other known protein structures. Capsid, which has already been shown to form disulphide linked dimers in virions (Baron *et al.*, 1991), formed two-fold symmetrical dimers in the crystal structure as well. These dimers form higher order oligomeric rows through hydrogen bonds and hydrophobic contacts, which themselves form even higher order structures through hydrophilic contacts between adjacent rows. Although

disruption of disulfide bonds does not affect virion formation (Lee *et al.*, 1996b), mutations which disrupt the oligomerization of capsid dimers into rows completely abrogate virion release (Mangala Prasad *et al.*, 2013). More recently it was found that another self-interacting region, predicted to be a coiled-coil region, exists in the N-terminus of capsid (Sakata *et al.*, 2014). Although this region was dispensable for virion formation, it was necessary for infectivity.

It has long been known that RV capsid is a phospho-protein (Marr *et al.*, 1991) and phosphorylation seems to occur early after translation and is not dependent on targeting to the Golgi (Garbutt *et al.*, 1999). In fact, capsid is efficiently phosphorylated even when expressed in isolation of other viral proteins (Law *et al.*, 2003). The bulk of phosphorylation occurs on five residues within the RNA binding region of capsid (Law *et al.*, 2003, Law *et al.*, 2006). These phosphorylation events are dependent upon serine 46, as evidenced by the fact that changing this residue to an alanine (S46A) almost completely abrogates phosphorylation of other residues (Law *et al.*, 2003, Law *et al.*, 2006). Phosphorylation appears to control RNA binding, with dephosphorylated capsid binding RNA to a much higher extent than fully phosphorylated capsid (Law *et al.*, 2003). Furthermore, virion-associated capsid contains less phosphate than intracellular capsid, suggesting a dephosphorylation event precedes virion formation (Law *et al.*, 2006). Alternatively, hypophosphorylated capsid may be

selectively incorporated into the virion. Not surprisingly, incorporation of the S46A mutation into an infectious cDNA clone negatively affected viral titers (Law *et al.*, 2006). This was not due to defective virion assembly, but rather was linked to an early infection event such as nucleocapsid disassembly. While capsid does contain potential protein kinase C sites (Garbutt *et al.*, 1999), and can be dephosphorylated by PP1A *in vitro (Law et al., 2003)*, the bona fide kinases and phosphatase responsible for modifying capsid's phosphorylation state have not been determined.

In addition to the ER, where it is synthesized, and the Golgi, where virion assembly takes place, capsid is localized to several other compartments within the cell including replication complexes (Lee *et al.*, 1999). Since capsid appears to play a role in viral genome replication (discussed in detail later), its localization to replication complexes is not unexpected. Second, capsid also associates with the outer mitochondrial membrane in infected cells (Lee *et al.*, 1999), a phenomenon which occurs independently of other viral proteins (Beatch *et al.*, 2005). Moreover, expression of capsid induces mitochondrial clustering and formation of electron dense plaques between apposing mitochondria and ER, both of which are hallmarks of RV infection (Beatch *et al.*, 2005). This process has recently been shown to require microtubules, but not actin (Claus *et al.*, 2011).

1.1.7 Non-structural roles of the capsid protein

Recently, several studies have revealed the non-structural roles of RNA virus capsid proteins (reviewed in Willows *et al.*, 2013). It should come as no surprise that RNA viruses would evolve multifunctional proteins, and capsid proteins are particularly good candidates for multifunctionality. RNA virus genomes range in size from 3kbp to 32kbp and there is a significant selective pressure to keep them as small as possible (Gorbalenya *et al.*, 2006). This selective pressure is due to the low fidelity of the RNA dependent RNA polymerases, which can make as many as 1 mutation per genome per replication cycle, compared with 1/300 for DNA viruses (Drake *et al.*, 1998). With this limited coding capacity, RNA viruses are unable to evolve single purpose accessory genes often seen in DNA viruses. For this reason, conditions are favorable for the evolution of genes that play multiple roles in viral replication particularly genes already required for basic viral replication and virion assembly.

RNA virus capsid proteins are especially suited to multifunctionality for several reasons. First, they are present in large amounts, often significantly exceeding the amount required for virion formation (Scheele *et al.*, 1969). This would make capsid proteins suitable for simple competitive inhibition of host cell factors. Since viral replication functions will innately limit the evolutionary degree of freedom among multifunctional viral proteins, the ability to have an effect

through simple binding rather than a complex enzymatic activity would be highly favorable. For this reason multifunctional capsid proteins would be quicker to evolve and could fulfill more additional functions than the replicase proteins which are usually expressed at lower levels. Other structural proteins, such as the envelope proteins, are less likely to evolve multifunctionality, as RNA virus capsid proteins have greater access to the cytoplasm from which they would normally bind a pool of viral RNA. This cytoplasmic access also allows interaction with a much greater proportion of host cell factors than the extracellular facing envelope proteins. Finally, attaching additional functions to surface antigens would reduce the degree of freedom these proteins would have to sustain mutations that could result in escape from the adaptive immune response.

1.1.7.1 Capsid involvement in viral genome replication

RV capsid is now known to play a significant role in viral genome replication. This was first discovered when it was found that a replicon containing a large deletion in the p150 gene (DeltaNotI) could replicate only in the presence of WT RV helper virus (Tzeng *et al.*, 2001). This was later found to be the result of complementation, both in *cis* and *trans,* by the capsid protein(Tzeng *et al.*, 2003). Further investigation established that an arginine rich region in the RNA-binding region of capsid was required (Tzeng *et al.*, 2009). Interestingly, p150 and capsid share sequence similarity between the p150 region encoded by the NotI-NotI

fragment and the RNA-binding region of capsid (Tzeng *et al.*, 2003) and the authors suggested that the arginine rich motifs in both proteins share a common function. Capsid expression also affected genome replication per se, modulating both the amount of genomic RNA as well as the ratio of subgenomic to genomic RNA produced by RV replicons (Chen *et al.*, 2004b, Tzeng *et al.*, 2005). Capsid seemed to have a balancing effect on genome replication, enhancing it when expressed at low levels while inhibiting it when at high levels (Chen *et al.*, 2004b). Additionally, capsid expression only affected the subgenomic:genomic RNA ratio when supplied in *cis*, even though this effect was dependent on the protein rather than the RNA (Tzeng *et al.*, 2005). The authors hypothesized that translation of capsid in close proximity to viral replication complexes was required for it to affect subgenomic RNA synthesis. Indeed, a pool of capsid localizes to replication complexes in infected cells (Lee *et al.*, 1999, Fontana *et al.*, 2007) and interacts with p150(Tzeng *et al.*, 2006).

The actual function of capsid within the replication complexes is still open for debate, but at least two possibilities have been suggested (Ilkow *et al.*, 2010b). First, capsid could function as an RNA chaperone, stabilizing the newly created genomic RNA and/or altering secondary structure to assist the viral replicase. RNA chaperone activity has been reported for other capsids including those of human immunodeficiency virus (HIV) (Darlix *et al.*, 1993, Peliska *et al.*, 1994, Ji *et*

al., 1996), some flaviviruses (Cristofari *et al.*, 2004, Ivanyi-Nagy *et al.*, 2008), and hantaviruses (Mir *et al.*, 2006). Second, the ability of capsid to modulate ratios between positive strand, negative strand and subgenomic RNA may be required for efficient replication. As mentioned earlier, high levels of capsid protein inhibit genomic RNA replication and subgenomic RNA synthesis, which could possibly liberate genomic RNA for viral assembly once sufficient levels of structural proteins have been reached. Also, capsid may inhibit subgenomic replication thus reducing the subgenomic:genomic RNA ratio in order to prevent more structural proteins from being synthesized when a sufficient concentration has already accrued.

1.1.7.2 Capsid interactions with host factors

In the last fifteen years, several studies reported a cohort of host cell proteins that interact with capsid and a number of these interactions have been studied in greater detail. Initially, a yeast two-hybrid screen detected binding of capsid with the mitochondrial protein p32 and the pro-apoptotic protein Par-4 (Beatch *et al.*, 2000). A GST pulldown in mammalian cells revealed several new interacting proteins, most notably poly-A binding protein (PABP), a translation initiation factor (Ilkow *et al.*, 2008). Other proteins found in this pulldown included many that are involved in mitochondrial metabolism, import and fission as well as the serine/threonine phosphatase protein phosphatase 1 (PP1)

(Carolina Ilkow, unpublished data). A later study showed that capsid also interacts with the pro-apoptotic Bcl-2 protein Bax (Ilkow *et al.*, 2011). Finally, it has also been shown that capsid interacts with cardiolipin, a mitochondrial specific lipid (Ilkow *et al.*, 2010a).

p32, also known as HABP1, MAM33p and gC1q-R, is a 33kDa protein that resides primarily within the mitochondrial matrix (Dedio *et al.*, 1998). It has also been found on the cell surface (Ghebrehiwet *et al.*, 1998) and in the nucleus (Matthews *et al.*, 1998) and has been implicated in a cornucopia of pathways, including oxidative phosphorylation (Muta *et al.*, 1997), messenger RNA (mRNA) splicing (Krainer *et al.*, 1991), mitochondrial morphology (Hu *et al.*, 2013), the innate immune response (Xu *et al.*, 2009) and several different apoptotic pathways (Sunayama *et al.*, 2004, Chowdhury *et al.*, 2008, Itahana *et al.*, 2008). p32 interacts with a variety of pathogen proteins, both bacterial and viral (reviewed in Ghebrehiwet *et al.*, 2001). Besides capsid, p32 also binds the RV p150 protein and associates with replication complexes (Suppiah *et al.*, 2012). The capsid-p32 interaction occurs through the last 69 amino acids of p32's C-terminus and an arginine rich region between amino acids 30 and 69 of capsid (Mohan *et al.*, 2002, Beatch *et al.*, 2005). Mutation of several arginines required for the capsid:p32 interaction to alanines drastically affected viral titers (Beatch *et al.*, 2005), suggesting an important role for p32 in viral replication. This

decrease may be due to impaired mitochondrial clustering, as capsid p32 binding mutants and p32 knockdown both impair capsid's induction of this event (Beatch *et al.*, 2005, Claus *et al.*, 2011). These observations suggest that not only is p32 involved in mitochondrial clustering, but also that capsid induced mitochondrial clustering is important for viral replication.

The canonical role of PABP is initiation of translation in eukaryotic cells (reviewed in Eliseeva *et al.*, 2013). PABP binds to both the poly(A) tail on the 3' end and several proteins on the 5' end of the mRNA, the most notable being eIF4G, consequently forming the mRNA into a looped structure. This interaction stimulates the activity of these initiation factors while the closed loop is thought to assist ribosome recycling. Capsid was found to interact with PABP, both in infected cells or when expressed alone, resulting in relocalization of this host protein to the perinuclear region where capsid resides (Ilkow *et al.*, 2008). Oddly, PABP expression was upregulated in infected cells, something not seen in alphaviruses, possibly due to RV capsid relieving PABP's inhibition of its own translation (Bag *et al.*, 1996). The interaction was through the C-terminal half of PABP, a region that generally mediates interaction with other proteins and oligomerization. Ultimately, capsid was shown to inhibit translation *in vitro* through a stoichiometric, PABP-dependent mechanism, as addition of excess PABP relieved translational inhibition.

Many viruses are known to inhibit host cell translation often by activation of the antiviral factor protein kinase R (PKR), which recognizes double stranded viral RNA and phosphorylates the translation initiation factor eIF2α (reviewed in Garcia *et al.*, 2007). Additionally, several viral proteins also directly inhibit translation. Picornaviruses are the best known, cleaving eIF-4F using virus-encoded proteases to shut down host cell translation (Porter, 1993). Influenza virus also affects eIF-4F but through a different mechanism, instead reducing its phosphorylation (Feigenblum *et al.*, 1993). Some capsid proteins inhibit translation, such as the hepatitis C virus (HCV) core protein, which binds to the capped mRNA unwinding helicase DBX (Mamiya *et al.*, 1999), and the alphavirus Semliki Forest virus capsid protein, which is thought to bind directly to the host mRNA (van Steeg *et al.*, 1984, Elgizoli *et al.*, 1989). PABP is targeted by several viruses (reviewed in Smith *et al.*, 2010), including caliciviruses (Kuyumcu-Martinez *et al.*, 2004) and HIV (Alvarez *et al.*, 2006). Viral inhibition of host cell translation not only frees up cellular resources for translation of viral RNAs, but also prevents expression of anti-viral genes induced by activation of the host innate immune response. Oddly, as mentioned before, RV infection does not usually result in global inhibition of host cell translation, at least not until late in infection in some cases (Hemphill *et al.*, 1988). Because a pool of capsid associates with replication complexes (Lee *et al.*, 1999, Fontana *et al.*, 2007),

locally blocking translation of viral genomic RNAs once a sufficient amount of structural protein has built up may allow genomic RNA to be freed for incorporation into virions, thus increasing the efficiency of replication (Ilkow *et al.*, 2008, Ilkow *et al.*, 2010b).

RV capsid has also been shown to inhibit import of proteins into the mitochondria (Ilkow *et al.*, 2010a). Notably, in both yeast and human cells, capsid expression decreased import of the mitochondrially-targeted substrate Su9-DHFR in a dose-dependent manner. Furthermore, infected cells showed a noticeable decrease of p32 in the mitochondrial matrix. Inhibition of mitochondrial import was independent of both p32 and cardiolipin, as deletion mutants lacking these factors still showed capsid inhibition of mitochondrial import. Treatment of mitochondria with trypsin also failed to limit capsid's inhibition of import, suggesting this activity is independent of outer mitochondrial membrane import receptors. Nevertheless, the import machinery affected by capsid must be highly conserved, given that this viral protein inhibits import in yeast and mammalian cells. A link between the capsid-induced electron dense plaques between mitochondria (Beatch *et al.*, 2005) and inhibition of import has not been investigated, but it is possible that these structures occlude access of translocation substrates to the import machinery on the outer mitochondrial membrane (OMM). Indeed, mitochondria exhibiting electron

dense plaques occasionally exhibit loss of cristae (Lee *et al.*, 2000), an indicator of mitochondrial import inhibition (Perkins *et al.*, 2001). The actual role mitochondrial import plays in RV replication is purely speculative at this point. Since mitochondrial import inhibition requires large quantities of capsid *in vitro* (in the range of several micrograms), this process may only play a role late in infection. It has been previously suggested that inhibition of mitochondrial import could affect RV capsid's anti-apoptotic activity (Ilkow *et al.*, 2010a, Ilkow *et al.*, 2010b, Ilkow *et al.*, 2011). Notably, several apoptotic mediators are reported to interact with components of the translocase of the outer membrane (TOM) complex (reviewed in Petit *et al.*, 2009). Bax, an important target for capsid's anti-apoptotic activity (Ilkow *et al.*, 2011), interacts with TOM22 and this interaction was shown to be important for Bax-dependent apoptosis (Bellot *et al.*, 2007, Ott *et al.*, 2007). Through disrupting mitochondrial import, capsid may impair the ability of Bax to initiate apoptosis at the OMM.

1.2 Rubella virus and apoptosis

Apoptosis is a cellular process that results in the tightly controlled destruction of eukaryotic cells (see Taylor *et al.*, 2008 for an in depth review). All apoptotic pathways eventually lead to activation of a family of cysteine proteases called caspases. Initially present in all cells as inactive zymogens, proteolytic cleavage activates caspases, allowing them to begin a chain reaction of proteolysis events

that result in the destruction of the cell. The executioner caspases 3,6 and 7 mediate most of the events that take place late in apoptosis. Hallmark morphological changes occur in apoptotic cells, including detachment and rounding, nuclear condensation and fragmentation, and membrane blebbing. Several biochemical changes are also characteristic of the late stages of apoptosis, such as DNA degradation, and inhibition of transcription/translation. Exposure of phosphatidylserine on the outer leaflet of the plasma membrane targets cells for phagocytosis by macrophages (Fadok *et al.*, 1992). While the end result is generally the same, several different stimuli and signaling networks can activate apoptosis. These can be divided into two pathways: intrinsic and extrinsic (Figure 1.4).

Extrinsic apoptosis begins when a ligand binds to a death receptor on the cell, activating a signal transduction pathway that ultimately leads to the activation of caspases. One example of an extrinsic apoptotic pathway is activation of the FAS receptor (reviewed in Peter *et al.*, 2003). FAS ligand, a membrane protein expressed on the surface of T-lymphocytes, is involved in inducing apoptosis during cell-mediated cytotoxicity by the adaptive immune response. Interaction between FAS ligand on T-lymphocytes and the FAS receptor on target cells induces the formation of the death-inducing signaling complex (DISC) (Kischkel *et al.*, 1995). The FAS receptor interacts with Fas-associated Death Domain protein

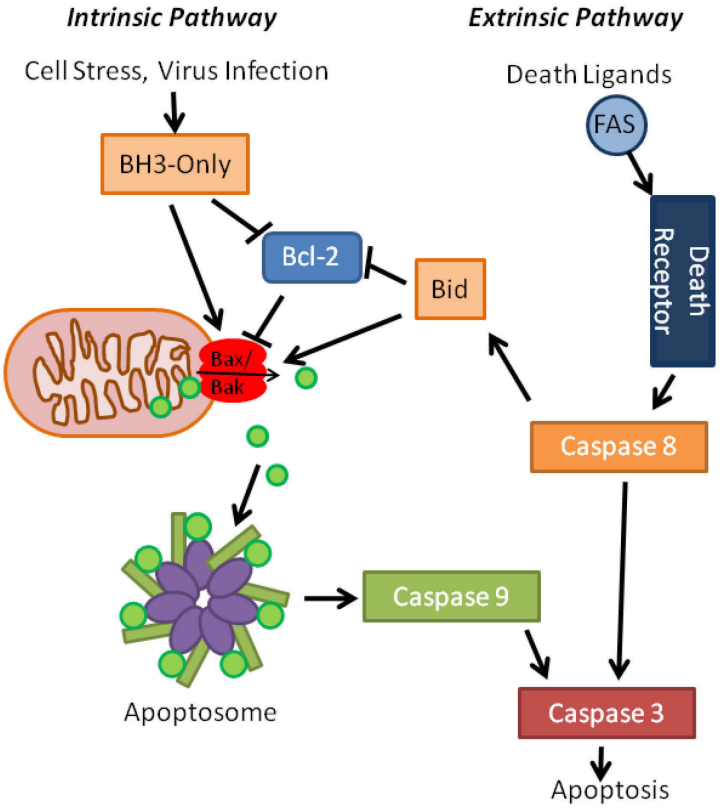

Figure 1.4 Extrinsic and intrinsic apoptotic pathways. In the intrinsic pathway, a stress stimulus leads to the activation or expression of pro-apoptotic BH3-only proteins. These activated proteins sensitize cells to apoptosis by inhibiting anti-apoptotic Bcl-2 proteins or induce apoptosis by activating Bax and Bak. Oligomerization of Bax and Bak on the OMM forms pores that allow the release of cytochrome c (green circles) that, together with APAF1 and caspase 9, forms the apoptosome. Caspase 9 is activated through autoproteolysis and then cleaves and activates the executioner caspase, caspase 3. In extrinsic apoptosis, a ligand binds to a death receptor inducing DISC formation and autoproteolysis of caspase 8. In type I cells, caspase 8 can directly activate caspase 3 through proteolysis. In type II cells, caspase 8 must cleave and activate the BH3-only protein Bid to induce the intrinsic pathway.

(FADD) through a region on its cytoplasmic domain called the death domain (DD) (Chinnaiyan *et al.*, 1995). The death domain is common to many death receptor signaling pathways and is present not only on death receptors, but on their intracellular mediators as well, including FADD. The latter acts as a scaffold for recruitment of various proteins, including the initiator caspase, caspase-8 (also called FLICE and MACH) (Boldin *et al.*, 1996, Muzio *et al.*, 1996). In Type I cells, DISC formation activates caspase-8 efficiently, allowing it to directly activate caspase-3 (Scaffidi *et al.*, 1998). In Type II cells, though, caspase-3 activation requires amplification by the intrinsic apoptotic pathway through cleavage and activation of the BH-3 only protein tBid (Li *et al.*, 1998, Luo *et al.*, 1998).

Unlike the extrinsic pathway, which is triggered by interaction of death ligands with their receptors on the cell surface, intrinsic apoptosis can be initiated by a wide range of apoptotic stimuli. These stimuli include cellular stressors such as growth factor withdrawal, lack of contact with the extracellular matrix (ECM) and other cells, DNA damage, perturbations in mitochondrial metabolism, excessive amounts of unfolded proteins, translational inhibition, and hypoxia. While upstream parts of this pathway are quite diverse, they all activate or induce the expression of the BH-3 only proteins (see Happo *et al.*, 2012 for a short review of these proteins). The activity of these proteins then converge on activation of two Bcl-2 family proteins, Bax and Bak (reviewed in Westphal *et al.*, 2011).

Oligomerization of these proteins forms pores in the OMM, resulting in the release of cytochrome *c* into the cytoplasm. Cytochrome *c* is then incorporated into a complex with APAF-1 and pro-caspase 9, called the apoptosome (Li *et al.*, 1997, Hu *et al.*, 1999, Saleh *et al.*, 1999, Zou *et al.*, 1999). The apoptosome, similar to DISC, results in auto-proteolysis and activation of the initiator caspase 9 that cleaves and activates caspase 3, an executioner type of caspase. There are two prevailing theories to account for how BH3-only proteins activate Bax: the indirect and the direct activation models (Giam *et al.*, 2008). The indirect activation model posits that BH-3 only proteins merely displace the anti-apoptotic Bcl-2 family proteins, such as Bcl-2 and Bcl-XL, preventing them from interacting with Bax and Bak. When free from inhibition, Bax and Bak can oligomerize and induce apoptosis. The direct activation model proposes that a subgroup of BH3-only proteins, termed activators, are required to stimulate the apoptotic activity of Bax and Bak. The non-activator BH3-only proteins bind and inhibit the anti-apoptotic Bcl-2 proteins, but this only sensitizes the cell to the activators. Likely, elements of both models are correct (see Giam *et al.*, 2008 for a more in depth discussion). Notably, in support of the direct activation model, some BH3-only proteins were able to directly activate the pore forming ability of Bax added to liposomes, with Bim and Bid being unambiguously strong activators (Kuwana *et al.*, 2005). The core difference between the models, whether or not Bax and Bak are constitutively active, is a matter of debate.

Bax and Bak are often thought to have redundant functions as evidenced by the fact that knockout of both proteins is required to fully nullify the effects of numerous apoptotic stimuli, including ultraviolet radiation, kinase inhibitors, DNA damaging reagents, serum withdrawal, and BH3-only protein overexpression (Wei *et al.*, 2001, Zong *et al.*, 2001). Several studies have found the situation to be more nuanced though, with Bak and Bax having non-redundant functions for some processes. In HCT116 cells, for example, knockout of Bax alone severely reduces apoptosis caused by many common stimuli (Theodorakis *et al.*, 2002, Gillissen *et al.*, 2003). Furthermore, myc-induced apoptosis was highly suppressed in Bax knockout cells but completely unchanged in Bak knockout cells when compared to wild type (Dansen *et al.*, 2006). Some functions instead require only Bak, for example Vitamin K-induced apoptosis (Karasawa *et al.*, 2013) and long-chain ceramide generation (Siskind *et al.*, 2010). Moreover, some BH3-only proteins showed a preference for Bak or Bax activation (Sarosiek *et al.*, 2013).

While Bak is associated with the mitochondrial membrane under normal conditions, most Bax is in the cytoplasm and only translocates to the mitochondria following induction of apoptosis (Hsu *et al.*, 1997a, Wolter *et al.*, 1997, Griffiths *et al.*, 1999a). During apoptosis activation, a conformational

change exposes the C-terminal hydrophobic alpha helix that is normally buried in a hydrophobic groove in Bax (Suzuki *et al.*, 2000). Apoptosis also causes a change in conformation that reveals the N-termini of both Bax (Hsu *et al.*, 1997b, Nechushtan *et al.*, 1999, Peyerl *et al.*, 2007) and Bak (Griffiths *et al.*, 1999b, Dewson *et al.*, 2009). Exposure of the BH3 domain in these proteins allows dimerization and eventually oligomerization (George *et al.*, 2007, Dewson *et al.*, 2008, Gavathiotis *et al.*, 2010). The resulting oligomers form pores in the OMM that ultimately allows the release of cytochrome *c* from the intermembrane space into the cytosol (Saito *et al.*, 2000, Kuwana *et al.*, 2002, Dejean *et al.*, 2005). The anti-apoptotic Bcl-2 proteins bind to Bax and Bak and inhibit their oligomerization (Ruffolo *et al.*, 2003, Willis *et al.*, 2005, Fletcher *et al.*, 2008), likely through the interaction of the Bax/Bak BH3 region with a hydrophobic groove in the anti-apoptotic Bcl-2 proteins (Sattler *et al.*, 1997).

1.2.1 Viruses and apoptosis

Apoptosis is a major mechanism by which a host can prevent the spread of a viral infection. For example, the FAS pathway is a key mechanism by which cytotoxic T-lymphocytes eliminate cells expressing viral antigens (Depraetere *et al.*, 1997). Interferons, a group of cytokines that induce an antiviral state in neighboring cells, sensitize cells to apoptosis as part of their antiviral program. Furthermore, several interferon-stimulated genes induce apoptosis, the most direct being

through increased expression of the death receptor ligand tumor necrosis factor-related apoptosis inducing ligand (TRAIL) (Kayagaki *et al.*, 1999, Chawla-Sarkar *et al.*, 2001, Chen *et al.*, 2001). RNAse L, an interferon stimulated gene (ISG) that cleaves single stranded RNA in response to viral RNA detection, has also been shown to induce apoptosis (Castelli *et al.*, 1998). Another interferon inducible gene product that directly detects viral dsRNA, protein PKR, induces apoptosis when activated (Der *et al.*, 1997). The RIG-I/MDA5 system, which detects viral RNAs and induces expression of interferon (discussed in more detail in section 1.3), can also activate apoptosis (Rintahaka *et al.*, 2008a, Besch *et al.*, 2009b). A major effector of this pathway, the transcription factor IRF3, directly activates Bax (Chattopadhyay *et al.*, 2010a). Activation of the unfolded protein response (UPR), whose sustained activation leads to apoptosis, occurs in several virus, including Japanese encephalitis virus (Su *et al.*, 2002), West Nile virus (WNV) (Medigeshi *et al.*, 2007), HCV (Asselah *et al.*, 2010), coxsackievirus (Zhang *et al.*, 2010) and African swine fever virus (Galindo *et al.*, 2012). Typically, the UPR is activated through expression of large amounts of viral proteins in association with the host ER, in particular surface glycoproteins.

Not surprisingly, several viruses have evolved mechanisms to inhibit apoptosis in host cells. Many DNA viruses encode proteins dedicated to inhibiting apoptosis, including baculoviruses (Clem, 2015), human papilloma viruses (Mammas *et al.*,

2008), adenoviruses (White, 2006), cytomegaloviruses (Brune, 2011), and poxviruses (Everett *et al.*, 2002). For papilloma virus, the ability to inhibit apoptosis correlates with its oncogenic potential (Thomas *et al.*, 1999). While DNA virus inhibition of apoptosis has been thoroughly researched, RNA virus inhibition of apoptosis is relatively poorly understood. Despite this, several RNA virus anti-viral proteins have been recently characterized. For example, poliovirus 3A protein (Neznanov *et al.*, 2001) inhibits trafficking of the tumor necrosis factor (TNF) receptor to the cell surface, thereby inhibiting TNF-induced apoptosis . Some viruses activate pro-survival pathways, such as the PI3K/AKT and NF-κB pathways by respiratory Syncytial virus NS1/NS2 proteins (Bitko *et al.*, 2007) and HCV NS5A protein (Waris *et al.*, 2003, Street *et al.*, 2004). The Chikungunya nsP4 and nsP2 proteins were found to inhibit the UPR pathway by blocking eIF2α phosphorylation and host cell translational shutoff (Akhrymuk *et al.*, 2012, Rathore *et al.*, 2013, Fros *et al.*, 2015). A number of viral capsid proteins also inhibit apoptosis. For example, WNV capsid inhibits apoptosis through activation of the pro-survival kinase Akt (Urbanowski *et al.*, 2013). The Hantaan virus nucleocapsid protein inhibits apoptosis by both blocking nuclear import of NF-κB and targeting the pro-apoptotic protein p53 for degradation (Ontiveros *et al.*, 2010, Park *et al.*, 2013).

Although inhibition of apoptosis would increase the window of time for viral replication, many viruses instead induce apoptosis. Activation of apoptosis does offer several advantages to viruses, especially those that replicate quickly and don't need to extend the lifespan of their host. Apoptosis can allow the spread of virus through apoptotic bodies, which can disseminate the virus to neighboring cells and phagocytes (Mi *et al.*, 2001, Boehme *et al.*, 2013). The apoptotic bodies would also shield the virions from neutralizing antibodies (Roulston *et al.*, 1999). Furthermore, apoptosis would limit the release of cytokines and viral antigens from the cell, limiting the visibility of the virus infection to the host immune response. Viruses from a variety of families utilize both direct and indirect pathways to induce apoptosis (see Galluzzi *et al.*, 2008 for a more in depth review). The HCV ns4A and ns3 proteins both induce apoptosis, the former through the mitochondrial pathway and the latter through caspase-8 (Prikhod'ko *et al.*, 2004, Nomura-Takigawa *et al.*, 2006). The related flavivirus, WNV, also activates the caspase-8 pathway through its ns3 protein (Ramanathan *et al.*, 2006). Some viral capsid proteins also induce apoptosis. For example, coxsackievirus capsid protein VP2's interaction with the pro-apoptotic host protein siva leads to induction of apoptosis by a currently unknown mechanism (Henke *et al.*, 2000, Henke *et al.*, 2001). Controversially, several flavivirus capsid proteins have been found to both promote and inhibit apoptosis. For example, HCV core binds the transcription factor p53 and has been found to both induce

and repress expression of downstream pro-apoptotic genes (Ray *et al.*, 1997, Lu *et al.*, 1999, Otsuka *et al.*, 2000). It was later found that the level of expression of the core protein changes the effect it has on p53, with lower levels enhancing p53 expression and higher levels inhibiting it (Kao *et al.*, 2004). The WNV capsid protein has also been shown to induce apoptosis by sequestration of the p53 inhibitor HDM2 (Yang *et al.*, 2002, Yang *et al.*, 2008). A more recent study found that WNV capsid instead inhibits apoptosis through activation of the PI3K/AKT survival signaling pathway (Urbanowski *et al.*, 2013). The discrepancy between these studies can be explained by the use of the mature form of capsid in the latter and a longer, membrane-anchored capsid in the former. Since only the mature form of capsid is found in infected cells (Urbanowski *et al.*, 2013), the latter study is more relevant to WNV biology.

1.2.2 Effect of RV infection on apoptosis.

The induction of apoptosis in RV infected cells is controversial. As mentioned earlier, most cell types show little cytopathic effect when infected with RV, at least until late in infection (Hemphill et al., 1988, Duncan et al., 1999). This is in stark contrast to alphaviruses, which tend to induce high levels of apoptosis in infected cells (reviewed in Li et al., 2004). Moreover, RV can establish persistent infections in many cell lines, including RK-13 (Svedmyr, 1965), LLC-MK(2) (Maassab et al., 1966), and BHK21 (Sato et al., 1977). Persistence also occurs in

CRS, with 42% of infants with a maternal history of rubella during pregnancy still shedding virus after birth (Phillips et al., 1965). Low levels of apoptosis would be beneficial for establishing persistence, as it would reduce the loss of infected host cells and attract less attention from immune cells. RV does not simply select for apoptosis resistant cells when establishing persistent infection, as Vero cells that were persistently infected were still sensitive to apoptotic stimuli (Pugachev et al., 1998).

Despite these characteristics, RV has been shown to induce cell death in various cell lines, particularly late in infection. For example, 43% of infected Vero cells were found to have died after three and a half days (Pugachev *et al.*, 1998). This study did not measure apoptosis within the infected cells but rather, cell death was determined by counting the numbers of cells floating in the media at various time points. Notably, different cell types show markedly different rates of cell death. One study found that, 48hrs after infection, 25% of Vero cells and 75% of RK13 cells were detached, while only 2% of BHK21 cells lost contact with the plates (Duncan *et al.*, 1999). In another study, more than 40% of cytotrophoblast cells showed signs of apoptosis four days post-infection, while <1% of human embryonic fibroblasts were apoptotic 10 days post-infection (Adamo *et al.*, 2004). RV-induced apoptosis is also known to be asynchronous, as 40% of Vero cells remain alive five days post infection, despite every cell showing evidence of

infection (Pugachev *et al.*, 1998). Furthermore, up to 10 days after infection almost none of these cells showed signs of death, suggesting that a subpopulation is resistant to RV-induced cytopathology. While one study reported that p53 is important for RV-induced apoptosis (Megyeri *et al.*, 1999), other studies suggest that this is not the case (Hofmann *et al.*, 1999, Domegan *et al.*, 2002). Overall, the use of non-human cell lines and different infection protocols in these studies makes the relevance of virus-induced cell death to RV biology difficult to assess.

While the mechanism remains unknown, genome replication and the replicase proteins are the most likely causes of RV induced cell death. In the related alphavirus Sindbis virus, the viral replicase protein nsP2, the envelope glycoproteins, and even virion entry can all activate apoptosis (Glasgow *et al.*, 1998, Joe *et al.*, 1998, Jan *et al.*, 1999). RV on the other hand does not activate apoptosis by fusion alone and requires viral replication, as UV-inactivated virions do not activate apoptosis (Duncan *et al.*, 1999, Hofmann *et al.*, 1999, Megyeri *et al.*, 1999). Cell death seems to be caused by the non-structural proteins, as more cytopathic RV infectious clones produced more non-structural proteins (Pugachev *et al.*, 1997). This is not surprising, as viral genomic RNA is the primary pathogen product recognized by the innate immune system. Expression of the

structural proteins alone, on the other hand, did not cause significant cell death (Hofmann *et al.*, 1999). In one study, though, the RV capsid protein was found to induce cell death in RK-13 cells (Duncan *et al.*, 2000). This pro-death activity required membrane anchorage and the N-terminal 170 amino acids. These results were contradicted by a more recent study, which showed that RV capsid actually protected from apoptosis in RK-13 cells (Ilkow *et al.*, 2011). This study is likely more accurate, as it measured several markers of apoptosis including caspase 3 activation, release of cytochrome *c* from the mitochondria, and loss of mitochondrial membrane potential. In contrast, Duncan *et al.* (2000) calculated rates of cell death by cotransfecting cells with capsid and a GFP plasmid and measuring the decrease in GFP expressing cells. This did not directly measure apoptosis and could have been confounded by competition between co-expressed plasmids for transcriptional/translational resources. Regardless, RK-13 cells may be a poor model for RV induced apoptosis, as they originate from rabbits, which are not a natural host for RV, and exhibit unusually large amounts of apoptosis when infected with RV.

1.2.3 Bax-dependent inhibition of apoptosis

As mentioned, one of the non-structural functions of RV capsid is preventing apoptosis. This is accomplished through its interaction with the pro-apoptotic Bcl-2 family protein Bax (Ilkow *et al.*, 2011). Unlike previous studies, this recent

study found that RV infection in Vero and A549 cells infected with RV both showed protection from apoptosis induced with the broad spectrum kinase inhibitor staurosporine. Although not previously used as widely as Vero cells, A549 cells, a human lung carcinoma cell line, likely represents a better candidate for studying RV biology as they are from a host and tissue that is naturally infected by RV. The most likely reasons for this novel anti-apoptotic activity is timing; most other studies looked at apoptosis rates 3 or more days after infection, while this study analyzed results generally 48hrs after infection. Further investigation showed that the capsid protein alone could account for this anti-apoptotic activity. When expressed in several different cell lines, including A549, Vero, RK-13 and the primary human cell line HEL-18, capsid expression reduced apoptosis rates by up to 80%. This reduction was seen not only when apoptosis was induced by staurosporine, but also by an anti-FAS antibody that activates the extrinsic apoptosis pathway. Capsid expression in a stable cell line also conferred protection from apoptosis. Unlike previous assays, which measured apoptosis by counting transfected cells that were also stained with an antibody directed towards the active form of caspase-3, this assay looked at depolarization of the mitochondria using the drug Tetramethylrhodamine methyl ester (TMRM). These results show that the anti-apoptotic activity of capsid operates upstream of mitochondrial depolarization and cytochrome *c* release.

One mechanism by which RV capsid functions to block programmed cell death is through its interaction with Bax. A capsid:Bax interaction was shown through reciprocal immunoprecipitations (IPs), and interestingly, induction of apoptosis increased binding between these two proteins. Conversely, capsid did not form a stable complex with the related pro-apoptotic protein Bak. Interaction with Bax required both the N and C-termini of capsid, as neither the C-terminal or N-terminal regions of capsid were sufficient for complex formation. Capsid expression was also found to prevent Bax-induced loss of mitochondrial membrane potential. This protection was not seen upon Bak overexpression though, further supporting the notion that capsid inhibits only Bax. Capsid also prevented cytochrome *c* release in cells over-expressing Bax, indicating that capsid inhibits the pore-forming function of Bax. Counter-intuitively, capsid expression resulted in increased Bax activation as assayed by increased exposure of its N-terminal domain, which is the target of the monoclonal antibody 6A7. Chemical crosslinking of mitochondria revealed that capsid and Bax formed mixed high order oligomers. This occurred even in the absence of apoptotic stimuli. Ultimately, it was suggested that capsid interacts with and activates Bax in order to form non-functional pores that, even while taking on many features of activated Bax, are impaired in their ability to release cytochrome *c*. An alternative explanation could be that capsid activates Bax, but mislocalizes it so as to prevent release of cytochrome *c*. This is supported by the fact that in cells

expressing capsid, activated Bax exhibited a more diffuse localization reminiscent of the ER rather than discrete foci and tubules of the mitochondria.

Ilkow *et al* (2011) also found that an arginine rich region (R-region) in the C-terminus adjacent to the SP was essential for capsid's anti-apoptotic activity. Deletion of the SP from capsid resulted in a slight decrease in protection from αFAS and no protection from staurosporine. Removal of both the SP and the R-region completely abrogated the anti-apoptotic activity of capsid. Indeed a patch of 5 arginines in the R-region where shown to be important for blocking apoptosis. Unexpectedly, mutation of 5 arginines in this region (CR5A) neither disrupted binding to or activation of Bax but did completely disrupt its anti-apoptotic activity suggesting that hetero-oligomerization with Bax is not sufficient for capsid's anti-apoptotic activity. Incorporation of the CR5A mutations into a full-length infectious clone severely affected RV replication, reducing both genomic RNA replication and viral protein production. This was not due to problems with virion formation, as both virus and structural proteins alone formed virions/VLPs and media from infected cells produced plaques in RK-13 cells. Together, these data indicate that inhibition of apoptosis by the RV capsid protein is important for viral replication.

Another Bax inhibiting protein expressed by human cytomegalovirus (HCMV) is viral mitochondrial inhibitor of apoptosis (vMIA) a product of the UL37 gene exon 1. Similar to RV capsid, vMIA binds to Bax and induces its mitochondrial localization and oligomerization (Arnoult *et al.*, 2004, Poncet *et al.*, 2004). vMIA also has a C-terminal, arginine rich region that is required for its anti-apoptotic activity (Hayajneh *et al.*, 2001, Pauleau *et al.*, 2007). This region is very similar to the R-region of RV capsid (Ilkow *et al.*, 2011), and both the arginine-rich region and mitochondrial membrane targeting sequence of vMIA are necessary for interaction with Bax (Arnoult *et al.*, 2004). While it was initially expected to function like anti-apoptotic Bcl-2 proteins, vMIA instead interacts with a previously uncharacterized binding pocket on Bax, in between helices 3 and 4 on one side and helices 5 and 6 on another (Ma *et al.*, 2012). The authors suggest that this prevents a conformational change whereby these helix hairpins separate. Since helices 5 and 6 insert into the mitochondrial membrane and are thought to form the actual pore (Annis *et al.*, 2005), vMIA may lock Bax in a conformation that prevents penetration of the outer mitochondrial membrane. Likewise, the R-region of RV, although dispensable for Bax binding, may bind to this region and lock Bax in a conformation that fails to form a pore. Unlike RV, HCMV can also inhibit Bak induced apoptosis through a separate protein called viral inhibitor of Bak oligomerization (vIBO) (Cam *et al.*, 2010). Interestingly, RV capsid appears to employ a Bax-independent anti-apoptotic mechanism

upstream of Bak. This is evident from the ability of the a C-terminal capsid construct that can efficiently inhibit apoptosis, despite not being able to bind Bax (Ilkow *et al.*, 2011).

1.3 Interaction of RV capsid with PP1

Another host cell-encoded capsid binding protein that was chosen for further study is PP1. As previously mentioned, the alpha isoform of the PP1 catalytic subunit was identified in a capsid pulldown (Carolina Ilkow, unpublished data). PP1 is a serine/threonine phosphatase that is encoded by three different genes: PP1CA, PP1CB and PP1CC. These genes encode the proteins PP1α, PP1β, and PP1γ respectively, each of which has 2-3 isoforms through differential splicing. Almost all of the diversity between PP1 paralogs is present in the N- and C-termini, with the catalytic core being highly conserved (Korrodi-Gregorio *et al.*, 2014). Orthologs of PP1 are also highly conserved, with human PP1 and the yeast homolog Glc7p sharing over 80% sequence identity and human PP1 expression being able to rescue yeast cells from Glc7p deletion (Gibbons *et al.*, 2007). While previously thought to be a promiscuous protein that acts to passively reverse phosphorylation by protein kinases, PP1 is now known to be actively regulated (reviewed in Virshup *et al.*, 2009).

While the human genome encodes over 428 serine/threonine kinases, there are only ~40 genes encoding serine/threonine phosphatases (Moorhead *et al.*, 2007). Not surprisingly, PP1 targets a plethora of proteins and pathways involved in mitosis, transcription, translation, DNA repair, actin rearrangements, and apoptosis (see Korrodi-Gregorio *et al.*, 2014 for a comprehensive list). These functions are regulated by a large number of PP1 interactors, targeting proteins, and inhibitors, with over 180 proteins identified in the PP1 interactome (Heroes *et al.*, 2013). PP1 binding proteins can regulate PP1 by changing its localization, recruiting target proteins or complexes, or by regulating the activity of the catalytic core. Most interactors contained a PP1 binding region called the RVxF motif (Egloff *et al.*, 1997), which has the consensus sequence of [K/R][K/R][V/I][x][F/W] (Peti *et al.*, 2013). Several other docking motifs have also been identified recently, including the SILK motif (consensus [GS]IL[RK]) and the MyPhoNE motif (consensus RxxQ[VIL][KR]x[YW]) (Hendrickx *et al.*, 2009). PP1 binding partners are often intrinsically disordered proteins: a class of proteins that rapidly convert between several conformations (reviewed in Choy *et al.*, 2012).

With respect to interaction with capsid, the most relevant pathways PP1 is involved with are apoptosis and the innate immune response. PP1's role in

apoptosis came to light after it was found in a complex with WAVE-1, glucokinase, and protein kinase A on the OMM (Danial *et al.*, 2003). Notably, a PP1 targeting inhibitor prevented loss of Serine112 phosphorylation on Bad, a pro-apoptotic BH3-only protein, after cytokine deprivation. Dephosphorylation of this residue acts to relieve Bad's inhibition by 14-3-3 proteins, thus allowing it to act pro-apoptotically (Chiang *et al.*, 2003). In this manner, PP1 would seem to be a pro-apoptotic protein. PP1 also plays a role in the innate immune response. The innate immune response to RNA viruses begins by the detection of single and double-stranded RNAs by the RIG-I like receptors, retinoic acid-inducible gene 1 (RIG-I) and melanoma differentiation-associated protein 5 (MDA5) (Figure 1.5) (see Loo *et al.*, 2011 for a review of this pathway). These receptors then signal through a mitochondrial adaptor protein, MAVS, which recruits downstream signaling molecules that result in phosphorylation and activation of interferon regulatory factors (IRF) 3 and 7. These transcription factors are then translocated to the nucleus where they activate transcription of several genes, including type-I interferons. Secreted interferon then activates its cell surface receptor in a paracrine and autocrine manner. The interferon receptor then recruits and activates the tyrosine kinase family Janus Kinase (JAK), which phosphorylates and activates the signal transducer and activator of transcription (STAT) proteins. In the nucleus, activated STAT proteins induce the expression of several ISGs. A recent study has shown that PP1 catalyzes the dephosphorylation

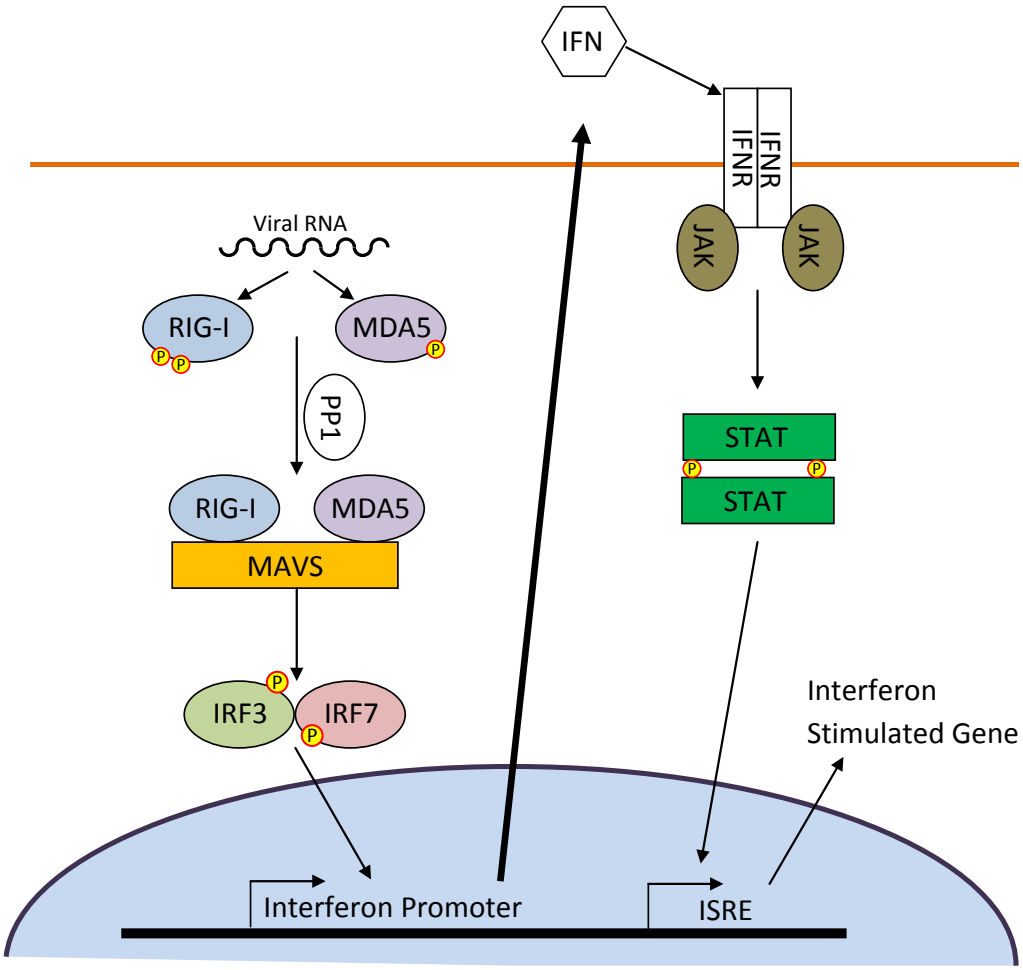

Figure 1.5 Activation of the interferon response by RIG-I like receptors. Viral RNA binds to and activates RIG-I and MDA5. After dephosphorylation by PP1, RIG-I and MDA5 bind to the scaffold protein MAVS, which induces a signal transduction pathway that results in the activation of IRF3/IRF7. IRF3/IRF7 localize to the nucleus and induce the expression and secretion of type-I interferons (IFN). IFN binds to the interferon receptors (IFNR), which recruit and activate JAK kinases. These kinases phosphorylate and activate STAT proteins, which translocate to the nucleus and induce the expression from the interferon stimulated response element (ISRE).

of both RIG-I and MDA5, an event required for downstream signaling to MAVs (Wies *et al.*, 2013). Demonstrating its importance in the innate immune response, measles virus V-protein was reported to inhibit PP1 in order to suppress activation of the innate immune response (Davis *et al.*, 2014, Mesman *et al.*, 2014). Additionally, PP1 has also been implicated in reversing eIF2α phosphorylation, thus relieving translational inhibition induced by the ISG PKR (Brush *et al.*, 2003). Several viruses have been found to utilize PP1 in this pathway, generally by recruiting it into a complex with eIF2α and facilitating its dephosphorylation (Kazemi *et al.*, 2004, Cruz *et al.*, 2011, Li *et al.*, 2011, Van Opdenbosch *et al.*, 2012).

1.4 Rationale and objectives of this thesis

As discussed above, the RV capsid protein plays several non-functional roles to aid viral replication. While capsid's interaction with several of these proteins has been studied, other areas still remain to be investigated. First, while capsid also inhibits apoptosis in a Bax-dependent manner, the mechanism by which it does so is not understood. Moreover, preliminary data suggest that membrane association of capsid and phosphorylation may affect its anti-apoptotic activity. For this reason, I studied the effects of altering these two properties of capsid on apoptosis with the expectation that they could reveal details about capsid's anti-apoptotic mechanism. Second, as has been demonstrated, capsid exhibits a

strong Bax independent anti-apoptotic activity. Given that PP1 is a widely expressed protein with key roles in apoptosis, I investigated whether its interaction with capsid could explain how capsid interferes with apoptosis in multiple cell lines. I also investigated whether capsid's interaction with PP1 affected other aspects of the anti-viral response.

CHAPTER 2
Materials and Methods

2.1 Materials

Table 2.1 Commercial reagents

Reagent	***Source***
10X/6X DNA Gel loading buffer	Invitrogen
16% Paraformaldehyde, electron microscopy grade	Electron Microscopy Sciences
40% Acrylamide/Bis-acrylamide solution, 29:1	Bio-Rad
Agarose, Ultrapure	Invitrogen
Ammonium chloride	EMD Chemicals
Ampicillin	Sigma-Aldrich
Bacto-Agar	BD Biosciences
Benzonase	Novagen
Bovine serum albumin (BSA)	Sigma-Aldrich
Bromophenol blue	Sigma-Aldrich
Complete™ EDTA-free protease inhibitor (CPI)	Roche
Cycloheximide	Sigma-Aldrich
Dextrose	EMD Chemicals
DAPI	Sigma-Aldrich
Diatomaceous Earth	Sigma-Aldrich
Dimethyl sulfoxide (DMSO)	Sigma-Aldrich
Dithiothreitol (DTT)	Sigma-Aldrich
Deoxynucleoside triphosphates (dNTPS)	Invitrogen
Dulbecco's Modified Eagle's medium (DMEM)	GIBCO
Ethanol, 95%	Commercial Alcohols

Table 2.1 Continued...

Reagent	***Source***
Ethidium Bromide (10mg/mL)	Sigma-Aldrich
Ethylenediaminetetraacetic acid (EDTA)	EMD Chemicals
Fetal bovine serum (FBS)	GIBCO
Halt™ Phosphatase Inhibitor	Thermo-Scientific
Luria Broth Base	Invitrogen
Glycerol	Fischer Scientific
HEPES (4-(2-hydroxyethyl)-1-piperazineethanesulfonic acid) 1M Solution	GIBCO
Hydrochloric acid (36.5 to 38% (w/w))	Fischer Scientific
Kanamycin	Sigma-Aldrich
Igepal CA-630	Sigma-Aldrich
Isopropanol	Sigma-Aldrich
Interferon-α	EMD Millipore
L-glutamine	GIBCO
Magnesium chloride hexahydrate	EMD Chemicals
Manganese chloride	Anachemia
Microcystin-Sepharose (MC-Sepharose)	Charles Holmes, UofA
Methanol	Fischer Scientific
Minimal essential medium Eagle (MEM)	Sigma-Aldrich
Mitotracker Red CMXRos	Molecular Probes
Mitotracker Deep Red FM	Molecular Probes

Table 2.1 Continued...

Reagent	***Source***
Non-essential amino acids (NEAA)	GIBCO
N,N,N',N'-Tetramethylethylenediamine (TEMED)	Sigma-Aldrich
OptiMEM	GIBCO
Paraformaldehyde (PFA)	J.T. Baker
Penicillin-streptomycin solution (100X)	GIBCO
Phenol/Chloroform/Isoamyl alcohol (25:24:1)	Sigma-Aldrich
Polybrene	Sigma-Aldrich
Polyinosinic:polycytidylic acid (poly(I:C))	Sigma-Aldrich
Potassium chloride	BDH
Potassium dihydrogen orthophosphate	BDH
ProLong Gold Antifade reagent with DAPI	Invitrogen
Protein-A-Sepharose	GE Healthcare
Protein-G-Sepharose	GE Healthcare
RNaseOUT™	Invitrogen
SlowFade Gold Antifade mountant	Life Technologies
Sodium chloride	Fischer Scientific
Sodium dodecyl sulphate (SDS)	Bio-Rad
Sodium hydroxide	BDH
Staurosporine	Cell Signaling
Tris base	Fischer Scientific
Tris-HCl	Fischer Scientific

Table 2.1 Continued...

Reagent	***Source***
Triton X-100	VWR International
Trypsin-EDTA	Invitrogen
Tween-20	Sigma-Aldrich
β-Mercaptoethanol	Bioshop

Table 2.2 Molecular size standards

Marker	***Source***
0' GeneRuler™ 1kb Ladder	Fermentas
GeneRuler™ 1kb Plus Ladder	Fermentas
PageRuler™ Prestained Protein Ladder	Thermo-scientific

Table 2.3 DNA/RNA modifying enzymes

Enzyme	***Source***
Calf-intestinal alkaline phosphatase	Invitrogen
Restriction Endonucleases	New England Biolabs/Invitrogen
RNase A	Sigma-Aldrich
T4 DNA ligase	Invitrogen

Table 2.4 Immunoblotting reagents

Reagent	***Source***
Nitrocellulose membrane 0.45μM	Bio-Rad
Polyvinylidene difluoride (PVDF) membrane (0.45μM)	Millipore
Polyvinylidene difluoride (PVDF) membrane (0.2μM)	Millipore
Immobilon-FL transfer membrane (0.45μM)	Millipore
Odyssey blocking buffer	LI-COR
Restore™ Western blot stripping buffer	Thermo Scientific

Table 2.5 Multi-component systems

Multi-component system	***Source***
BCA™ Protein assay kit	Thermo Scientific
Dual-Luciferase® Reporter Assay	Promega
ElectroMax Efficiency DH10B Cells	Invitrogen
ElectroMax™ Stbl4™ competent cells	Invitrogen
Lipofectamine 2000	Invitrogen
mMessage mMachine SP6 RNA Transcription Kit	Ambion
PerfeCta SYBR Green Supermix, Low ROX qPCR kit	Quanta Biosciences
Platinum Pfx PCR System	Invitrogen
Platinum Taq HIFI PCR System	Invitrogen
QIAquick Gel extraction kit	QIAGEN

Table 2.5 Continued...

Multi-component system	***Source***
QIAquick PCR purification kit	QIAGEN
QIAGEN plasmid HiSpeed Midi kit	QIAGEN
QIAGEN plasmid Midi kit	QIAGEN
QIAGEN plasmid Maxi kit	QIAGEN
QIAshredder kit	QIAGEN
RNeasy Mini kit	QIAGEN
Subcloning Efficiency DH5alpha Cells	Invitrogen
SuperScript® II Reverse Transcriptase kit	Invitrogen
TNT Coupled Transcription/Translation kit	Promega
Transit-LT1	Mirus Bio

Table 2.6 Buffers and solutions

Name	***Composition***
5X Protein sample buffer	62.5mM Tris-HCl pH 6.8, 25% (v/v) glycerol, 2% (w/v) SDS, 0.01% (w/v) bromophenol blue, 5% (v/v) β-mercaptoethanol
Buffer A	50mM Tris-HCl pH 7.4, 0.1mM EDTA, 0.5mM $MnCl_2$, 0.2% (v/v) β-Mercaptoethanol
Diatomaceous Earth slurry	100mg/mL Diatomaceous Earth, 6M guanidine-HCl, 20mM EDTA, 50mM Tris-HCl pH 7.5

Table 2.6 Continued...

Name	***Composition***
Diatomaceous Earth column wash	200mM NaCl, 20mM Tris-HCl pH 7.4, 5mM EDTA, 50% (w/v) Isopropanol
Gel running buffer (SDS-PAGE)	250mM glycine, 0.1% (w/v) SDS, 100mM Tris base, pH 8.3
Hepes-buffered saline	137mM NaCl, 5mM KCl, 6mM Dextrose, 0.7mM Na_2HPO_4, 20mM HEPES
NP-40 Lysis buffer	1% (v/v) Igepal, 150mM NaCl, 2mM EDTA, 50mM Tris-HCl , pH 7.4
Phosphate-buffered saline (PBS)	137mM NaCl, 2.7mM KCl, 8mM Na_2HPO_4, 0.5mM $CaCl_2$, 1mM $MgCl_2$, pH 7.4
Phosphate-buffered saline plus calcium magnesium (PBSCM)	137mM NaCl, 2.7mM KCl, 8mM Na_2HPO_4, 0.5mM $CaCl_2$, 1mM $MgCl_2$, 0.5mM $CaCl_2$, 1mM $MgCl_2$, pH 7.4
Phosphate-buffered saline plus Tween (PBST)	137mM NaCl, 2.7mM KCl, 8mM Na_2HPO_4, 0.5mM $CaCl_2$, 1mM $MgCl_2$, 0.1% (w/v) Tween-20, pH 7.4
PP1 Co-IP Buffer	1% (w/v) Triton X-100, 10mM HEPES pH 7.5, 10mM KCl, 2mM MgCl, 1mM DTT
4X Resolving gel buffer	1.5M Tris-HCl, 0.1% (w/v) SDS, pH 8.8
4X Stacking gel buffer	1M Tris-HCl, 0.4% (w/v) SDS, pH 6.8

Table 2.6 Continued...

Name	***Composition***
TAE buffer	40mM Tris-Acetate pH 8.0, 1mM EDTA
Transfer buffer	20% (v/v) methanol, 200mM glycine, 25mM Tris base pH 8.3
TE buffer	1mM EDTA, 10mM Tris-HCl pH 7.5

Table 2.7 Primary antibodies

Antigen	***Species***	***Clone/ Identifier***	***Source***	***IF Dilution***	***WB Dilution***
Actin	Mouse		Abcam		4000
Active Caspase-3	Rabbit		Cell Signaling	400	1000
Bax	Mouse	YTH 2D2	Trevigen		2000
Bax	Rabbit		Abcam		1000
Calnexin	Rabbit		Dr. David Williams, U of Toronto	500	

Table 2.7 Continued...

Antigen	*Species*	*Clone/ Identifier*	*Source*	*IF Dilution*	*WB Dilution*
Capsid	Mouse	C-1	Dr. Jerry Wolinsky, U of Texas	800	1000
Capsid	Rabbit	7W7	Hobman lab	500	1000
Decapping protein 1 (DCP1)	Rabbit		Abcam	1000	
GAPDH	Rabbit		Abcam		2000
GFP	Goat		Abcam	1000	1000
HSP60	Mouse		BD Biosciences	500	
Myc	Mouse	4A6	Millipore		4000
Myc	Mouse	9E10	American Type Culture Collection (Hybridoma)	300	
p150	Rabbit		Dr. Tero Ahola, U of Helsinki	300	1000

Table 2.7 Continued...

Antigen	*Species*	*Clone/ Identifier*	*Source*	*IF Dilution*	*WB Dilution*
Protein Phosphatase 1 catalytic subunit α isoform (PP1α)	Goat	C19	Santa Cruz Biotechnology	400	1000
Protein Phosphatase 1 catalytic subunit γ isoform (PP1γ)	Rabbit		Bethyl Laboratories	250	2000
Rubella Virus VLP	Goat		Meridian Life Sciences	800	1000

IF: Immunofluorescence, **IB**: Immunoblot

Table 2.8 Secondary antibodies

Host Species	*Fluorophore*	*Specificity*	*Source*	*IF Dilution*	*WB Dilution*
Goat	Alexa Fluor® 488	Chicken IgG	Invitrogen	400	
Goat	Alexa Fluor® 594	Chicken IgG	Invitrogen	400	
Goat	Alexa Fluor® 647	Chicken IgG	Invitrogen	400	
Goat	Alexa Fluor® 680	Donkey IgG	Invitrogen		2000
Mouse	Alexa Fluor® 488	Donkey IgG	Invitrogen	400	
Mouse	Alexa Fluor® 594	Chicken IgG	Invitrogen	400	
Mouse	Alexa Fluor® 546	Donkey IgG	Invitrogen	400	
Mouse	Alexa Fluor® 647	Donkey IgG	Invitrogen	400	
Mouse	Alexa Fluor® 680	Goat IgG	Invitrogen		2000
Mouse	Alexa Fluor® 750	Goat IgG	Invitrogen		2000
Rabbit	Alexa Fluor® 488	Donkey IgG	Invitrogen	400	
Rabbit	Alexa Fluor® 546	Donkey IgG	Invitrogen	400	
Rabbit	Alexa Fluor® 594	Chicken IgG	Invitrogen	400	
Rabbit	Alexa Fluor® 647	Donkey IgG	Invitrogen	400	
Rabbit	Alexa Fluor® 790	Donkey IgG	Invitrogen		2000
Rabbit	IRDye® 800CW	Donkey IgG	LI-COR		10000

IF: Immunofluorescence, **IB**: Immunoblot

Table 2.9 Oligonucleotides

Name	***Sequence***
5'P-SpeI-SacI-EcoRI-3' Adap	CTA GTG AGC TCA GCG
5'P-EcoRI-SacI-SpeI-3' Adap	AAT TCG CTG AGC TCA
B-ACTIN FW	CCT GGC ACC CAG CAC AAT
B-ACTIN REV	GCC GAT CCA CAC GGA GTA CT
F-Cap-EcoRI	GCC GGA ATT CAC C**AT G**GC TTC CAC TAC CCC C
F-Cap-frag-SalI	GGT CTG GTC GAC CTG CAT TTT ACC AAC CTG G
R-Cap-BamHI	TTG GAT CC**C TA**G GCG CGC GCG GTG
R-Cap-BamHI-NoStop	TAT GGA TCC GGC GCG CGC GGT G
R-Cap-frag-SalI	CGC CGC CAT AGT CGA CGC GGT AGA AGA CC
R-CapΔSP-Stop-BamHI	TTG GAT CC**T TA**G CGG ATG CGC CAA GGA TG
RV-F	AGG TCA TGT CTC CGC ATT TC
RV-R	GTC CCG AGT AGC AAG GGT CT

Underline: Restriction Enzyme Site, **Bold**: Start or stop site

Table 2.10

Cell lines

Cell Line	***Source***	***Cell Type***
A549	ATCC	Human non-small cell lung carcinoma
BHK-21	ATCC	Baby hamster kidney
HEK 293T	ATCC	Human embryonic kidney with SV40 Large T antigen
RK-13	ATCC	Rabbit kidney
Vero	ATCC	African green monkey kidney

Table 2.11 Viruses

Genomic cDNA plasmid	***Source***
pBRM33	Shirley Gilliam, University of British Columbia
pBRM33-S46A	Hobman Lab
pBRM33-S46D	This thesis
pBRM33-RARA	This thesis

Table 2.12 Plasmids

Plasmid Name	***Source***
pcDNA3.1-Capsid-myc/His	This thesis
pCMV5	David Russell, U of Texas
pCMV5-24S	Shirley Gilliam, U of British Columbia
pCMV5-24S-PVWP	Hobman Lab
pCMV5-24S-RARA	This thesis
pCMV5-Capsid	Hobman Lab
pCMV5-Capsid-CT	Hobman Lab
pCMV5-Capsid-NT	Hobman Lab
pCMV5-Capsid-RARA	This thesis
pCMV5-Capsid-S46A	Hobman Lab
pCMV5-Capsid-S46A/ΔSP	This thesis
pCMV5-Capsid-S46D	Hobman Lab
pCMV5-Capsid-S46D/ΔSP	This thesis
pCMV5-Capsid-ΔSP	Hobman Lab

Table 2.12 Continued...

Plasmid Name	***Source***
pCMV5-CR5A	Hobman Lab
pEGFP-C1	Clontech
pEYFP(C1)-PP1α	Addgene
pGag-Pol	Charles Rice, Rockefeller University
pGL3-ISRE-Luc	Rongtuan Lin, McGill University
pHCMV5-VSV-G	Charles Rice, Rockefeller University
pRLTK	Rongtuan Lin, McGill University
pTRIP-Capsid-AcGFP	This thesis
pTRIP-MCS-AcGFP	Hobman Lab
pTRIP-S46A-AcGFP	This thesis
pTRIP-S46A/ΔSP-AcGFP	This thesis
pTRIP-S46D-AcGFP	This thesis
pTRIP-S46D-ΔSP-AcGFP	This thesis
pTRIP-ΔSP-AcGFP	This thesis
pUC57-Cap-RARA	GenScript

2.2 Methods

2.2.1 Cell culture techniques

2.2.1.2 Cell culture maintenance

A549 and 293T cells were maintained in DMEM containing 10% FBS and 20mM HEPES. Vero and BHK-21 cells were maintained in DMEM containing 5% FBS and 20mM HEPES. RK-13 cells were maintained in MEM containing 10% FBS, , 20mM HEPES, 2mM L-Glutamine, 1X NEAA and 1X Pen/Strep. Cells were grown at 37°C incubator with a 5% CO_2 atmosphere unless otherwise specified. Confluent cells were detached from dishes using trypsin-EDTA and either split into new flasks/dishes or used for experiments. A549 cells were chosen for apoptosis assays because they are responsive to several apoptotic stimuli, including αFAS and poly(I:C), and were used prominently in a previous study on capsid's anti-apoptotic activity (Ilkow *et al.*, 2011). HEK 293T cells were used in several pulldown assays because of their ability to express high quantities of protein following transfection. Vero cells and BHK-21 cells have been used extensively by our lab and others, to generate recombinant RV strains following transfection or electroporation of viral genomic RNA. Finally, RK-13 cells were used for plaque assays because they are highly sensitive to RV induced cytopathic effect.

2.2.1.3 Cell transfection

A549 cells were transfected with either Lipofectamine 2000 or Transit-LT1. For Lipofectamine 2000 transfections, cells were seeded the day before at the

following densities: $1x10^6$ cells per 100mm dish, $7.5x10^4$ to $1x10^5$ cells per well in 12 well plates, and $5x10^4$ cells per well in 24 well plates. The next day, cells were transfected with the following amounts of DNA: 8µg per 100mm dish, 1µg per well in 12 well plates, and 0.5µg per well in 24 well plates. A ratio of 1µL of Lipofectamine 2000 per 1µg of DNA was used for all transfections. DNA and Lipofectamine 2000 reagent were initially added to separate tubes containing 25µL of OptiMEM per µg of DNA or µL of Lipofectamine 2000. These reagents were incubated separately for five minutes before being mixed and incubated at room temperature for an additional 20 minutes. The DNA:Lipofectamine mixtures were added onto cells in OptiMEM. Compared to normal culture conditions, half the volume of OptiMEM was used in each well/dish during transfection. After incubating for four hours, OptiMEM was removed and replaced with fresh complete media. Cells were then incubated one to two days before further processing. Vero cells were also transfected with Lipofectamine in a similar manner to A549 cells. Cells were seeded the day before transfection at $1x10^5$ cells per well in six well plates/ 35mm dishes and $5x10^4$ cells per well in 12 well plates. Two µg per well of DNA was used in 35mm dishes, 1-3µg per well of RNA was used in six well plates and 1.5µg per well of RNA was used in 12 well plates. A ratio of 1µL of Lipofectamine 2000 per 1µg of RNA was used in every reaction.

A549 cells were also transfected with Transit-LT1. For immunofluorescence assays, cells (2.5 to $4x10^4$ per well) were seeded onto coverslips in 12 well plates. For Luciferase assays, cells ($5x10^4$ cells per well) were seeded into 24 well plates). The next day, Transit-LT1 was diluted in OptiMEM at a ratio of 1:125 and then incubated at room temperature for five minutes before adding plasmid DNA. Cells in 12 well plates received 0.5µg of DNA and 1µL of Transit-LT1 per well, those in six well plates received 1µg of DNA and 2µL of Transit-LT1 per well and those in 24 well plates received 0.5µg of DNA and 1µL of Transit-LT1. The Transit-LT1:DNA mixtures were incubated for 20 minutes and then added directly to cells in complete media. Unless otherwise indicated, transfected A549 cells were processed 24-48 hours post-transfection. For immunoprecipitation and pulldown experiments HEK293T cells were transfected with Transit-LT1. Cells (1.75 to $2.5x10^6$) were seeded into 100mm dishes one day before transfection. The protocol was the same as for A549 cells except that 13.2µg of DNA and 39.6µL of Transit-LT1 were used for each 100 mm dish.

2.2.2 Molecular biology

2.2.2.1 Isolation of plasmid DNA from Escherichia coli

An in-house developed diatomaceous earth miniprep protocol was used for isolation of small amounts of plasmids. Freshly transformed colonies were used to inoculate 3mL of LB broth containing either 100µg/mL of ampicillin or

30µg/mL of kanamycin (depending on the plasmid). Cultures were incubated overnight at 37°C with shaking at 180-220rpm. Bacteria from the 1.5mL cultures were pelleted by centrifugation in a microfuge at 16,000 *g* for two minutes. Pellets were resuspended in 250µL of cold RNase A (100µg/mL)-containing Buffer P1 from QIAGEN Midi/Maxiprep kits and then lysed by addition of 250µL of room temperature Buffer P2. Lysis reactions were quenched by addition of 300µL cold Buffer P3. Cell debris was pelleted by centrifugation at 16,000 *g* for 10 minutes at room temperature. The resulting supernatants were mixed with 600µL of diatomaceous earth slurry and incubated for at least one minute with rotation at room temperature. The DNA bound to the diatomaceous earth was collected in 1mL micropipette tips with filters fitted onto a vacuum apparatus. When all the liquid had passed through the filter, tips were washed twice with Diatomaceous earth column wash buffer and then the diatomaceous earth resin was dried on the vacuum apparatus for 10 minutes. Residual wash buffer was removed by centrifugation of tips in a microfuge at 16,000 *g* for one minute at room temperature. Plasmid DNA was eluted by adding 30-50µL of MilliQ water to the diatomaceous earth followed by centrifugation at 16, 000 *g* at room temperature for one minute.

Larger amounts of DNA typically used in transfections were isolated using QIAGEN Maxi- or Midi-prep kits. Freshly transformed bacterial colonies were

used to inoculate 3mL LB starter cultures with appropriate antibiotic. This starter cultures were incubated for eight hours at 37°C with shaking after which a 1:1000 dilution of this starter culture was added to 100 or 300 mL of LB with antibiotic for midi- or maxi-preps respectively. Extraction of plasmid was done as per manufacturer's guidelines. Plasmids were resuspended in 50mM Tris-HCl and concentrations were determined using a NanoDrop 1000 Spectrophotometer. All plasmid stocks were adjusted to 1µg/µL and stored at -20°C.

2.2.2.2 Polymerase chain reaction (PCR)

Platinum Taq HIFI PCR or Platinum Pfx PCR Systems were used to amplify DNA. Most reactions (50µL) contained 10-20ng of template DNA, 400nM of each primer, 200nM of each dNTP, and 1U of polymerase. When amplifying high GC content RV cDNAs, 10% DMSO was also added to reactions. Reactions were performed in a Stratagene Robocycler Gradient 40. When PCR reaction products were to be used in restriction endonuclease digestion reactions, the DNA was separated from other reaction buffer components using a QIAquick PCR purification kit.

2.2.2.3 Restriction endonuclease digestion

Restriction endonuclease digests were performed according to manufacturer's guidelines. Ten µL volume reactions were used for diagnostic reactions whereas

20-50µg of DNA in reaction volumes up 100µL was used to prepare DNA fragments for ligation. In some cases, vector fragments were dephosphorylated using one unit of calf intestinal alkaline phosphatase (for 60 minutes at 37°C) prior to ligation.

2.2.2.4 Agarose gel electrophoresis

Ultrapure agarose (0.7-1% (w/v)) was dissolved in TAE buffer by heating in a microwave. Shortly before casting gels, ethidium bromide (0.5µg/mL) was added to the agarose solution. After setting, gels were submerged in electrophoresis tanks containing TAE buffer. DNA samples were mixed with Gel loading buffer before pipetting into wells. Gels were run at 80-120V and then DNA was visualized using a Fischer Scientific Ultraviolet transilluminator or a Bio-Rad Gel Doc™ XR+ imaging system. Gel photos were analyzed using Bio-Rad Image Lab™ software.

2.2.2.5 Extraction of DNA from agarose gel

Desired DNA fragments were excised from agarose gels with clean razor blades. The gel pieces were weighed and the DNA was extracted using QIAquick Gel extraction kit.

2.2.2.6 DNA ligation

Isolated insert and vector were combined at molar ratios of 3:1 and 6:1 and heated for five minutes at 65°C and then cooled on ice followed by a brief low speed spin in a microfuge to collect any condensed liquid at the top of the tubes. If DNA adaptors were used, 1.2ng per added to reactions before the heating step. T4 DNA ligase and buffer were added and reactions were incubated overnight in an ice bucket filled with water initially at 4°C. After incubation, reactions were stored at 4°C until used for bacterial transformation. Reaction mixtures were diluted either 1:3 or 1:5 before transformation of chemically competent or electro-competent bacteria respectively.

2.2.2.7 Transformation of *Escherichia coli*

Three strains of *E. coli* were used for transformation with ligation reaction products and propagation of plasmids: DH5α, DH10β and Stbl4. Most plasmids other than those derived from the large infectious clone plasmid pBRM33 or lentiviral (pTRIP) vectors were propagated in DH5α cells. Ligation reactions involving pTRIP vectors were electroporated into DH10β cells using the Ec1 setting of a Bio-Rad MicroPulser™. All pBRM33-based plasmids were propagated in Stbl4 cells via electroporation with a BTX Electro Cell Manipulator® 600 set at 2.5kV/resistance high voltage (HV) mode with a resistance of 129ohms (R5) and

a voltage of 1.5kV. All electroporations were conducted using Bio-Rad Gene Pulser® 0.1 cm Cuvettes.

2.2.3 Construction of expression plasmids

Oligonucleotides used for plasmid construction are listed in Table 2.9. All recombinant plasmids were subjected to sequencing to confirm their authenticity. pBRM33-based plasmids were sequenced at the Molecular Biology Facility, Department of Biological Sciences (University of Alberta) while all other plasmids were sequenced at The Applied Genomics Center in the Department of Medical Genetics (University of Alberta).

2.2.3.1 pCMV5 based plasmids

To construct the capsid SP truncation mutants pCMV5-S46A/ΔSP and pCMV5-S46D/ΔSP, a 318bp fragment was amplified from pCMV5-capsid by PCR using the primers F-Cap-frag-SalI and R-CapΔSP-Stop-BamHI. The resulting cDNA, which has a stop codon just before the transmembrane region of capsid, was used to replace the 417bp SalI-BamHI fragment in pCMV5-capsid S46A and -S46D. The resulting plasmids encoded amino acid residues 1-277 of capsid with either the S46A or S46D mutation.

pCMV5-24S-RARA was made by using the pCMV5-24S plasmid as a backbone. A 421bp DNA fragment corresponding to the BsrGI-BstEII fragment within the RV 24S cDNA but with valine 276 and phenylalanine 278 to alanine mutations was synthesized by Genscript. This 421bp fragment was isolated from the pUC57-RARA plasmid and used to replace the analogous fragment in pCMV5-24S. The resulting plasmid, pCMV5-24S-RARA, was then subjected to PCR using the primers F-Cap-EcoRI and R-Cap-BamHI and the resulting 924 bp cDNA was digested with EcoRI and BamHI and ligated into the EcoRI and BamHI sites of pCMV5, forming pCMV5-Capsid-RARA.

2.2.3.2 pcDNA 3.1 myc/His plasmids

To construct the pcDNA3.1-Capsid myc/His plasmid, capsid was amplified from pCMV5-Capsid using the primers F-Cap-EcoRI and R-Cap-BamHI-NoStop. The resulting fragment was digested with EcoRI and BamHI and inserted into the EcoRI and BamHI sites of pcDNA3.1/myc-His©(-) A (Invitrogen).

2.2.3.3 pBRM33 based plasmids

The pBRM33-S46D infectious clone was constructed using the pBRM33 RV infectious cDNA (Yao *et al.*, 1999) as a backbone. The 7977 bp NotI-BsrGI and 4937 bp NotI-NotI fragments from pBRM33 and the 466 bp Not1-BsrG1 from pCMV5-Capsid-S46D (Law *et al.*, 2006) were isolated from agarose gels as

described above. The 7977 bp NotI-BsrGI fragment from pBRM33 was ligated to the 466 bp fragment of pCMV5-Capsid-S46D to create an intermediary cloning vector. This shuttle vector was digested with Not1 and then ligated with the 4937 bp Not1-Not1 fragment from pBRM33 to produce pBRM33-S46D. To make the pBRM33-RARA infectious clone, the 2085 bp BsrG1-BamHI fragment from pBRM33 was replaced with the analogous fragment from pCMV5-24S-RARA.

2.2.3.4 pTRIP based plasmids

All pTRIP plasmids used in this study were constructed from pTRIP-MCS-AcGFP (Urbanowski *et al.*, 2013). RV capsid cDNAs that were released from pCMV5-based RV expression constructs by EcoRI and BamHI digestion were ligated into pTRIP-MCS-AcGFP that had been digested with SpeI and BamHI using the adaptors 5'P-SpeI-SacI-EcoRI-3'-Adap and 5'P-EcoRI-SacI-SpeI-3'-Adap.

2.2.4 Lentivirus production and transduction

2.2.4.1 Lentivirus production

To generate recombinant lentivirus stocks, HEK293T cells were seeded the day before transfection at a density of $2.5x10^6$ cells per 100mm dish. The next day, cells were transfected with 5.6µg of pTRIP, 5.6µg of pGag-pol and 1.6µg of pHCMV5 VSV-G plasmids using Transit-LT1. Transfections were performed as described in section 2.2.1.3 except that 800µL of OptiMEM and 25.6µL of Transit-LT1 were used per 100mm dish. Before addition of transfection reagent, the

HEK293T cell growth media in each dish were replaced with 7mL of DMEM + 3%FBS. Six hours after the transfection mixtures and media were replaced with 10mL of DMEM + 3%FBS. After three days, the lentivirus-containing media were collected and filtered through a 0.45µm filter, supplemented to 4µg/mL of polybrene and 20mM HEPES and then stored in 1mL aliquots at -80°C.

2.2.4.2 Lentivirus transduction

A549 cells were seeded the day before transduction at a density of 1-3 $x10^5$ cells/well in six well plates or 0.5-1.5$x10^5$ cells/well in 12 well plates. On the day of transduction, media were changed to DMEM + 3%FBS 20mM HEPES + 4µg/mL polybrene. Sufficient media was added so the final volumes were 4mL per well in six well plates and 2mL per well in 12 well plates respectively after virus addition. Lentivirus stock was mixed into the wells and then plates were spinoculated for 45 minutes at 1200 *g* and 37°C after which the inoculum was replaced with complete media. The transduced cells were used for experiments one to two days later. Unless indicated otherwise, a multiplicity of transduction (MOT) of two was used for all experiments.

2.2.4.3 Determination of lentivirus titer

Six well plates of A549 cells were transduced as described in section 2.2.4.2. Two days post-transduction, cells were washed once in PBS and detached from plates

with trypsin-EDTA. Trypsin was quenched with complete media and the detached cells were collected by centrifugation (800 x *g* for five minutes at room temperature) and then washed twice in PBS + 1%FBS. The washed cells were resuspended in PBS + 1%FBS and then analyzed by flow cytometry using a Becton Dickinson FACScan with CellQuest software or FACSARIA III with FACSDiva software. The proportion of GFP-positive cells was determined after subtracting the false positive background in mock-transduced cells. The equation for determining viral titers was $-\ln(1-p)NV^{-1}$ where ln() is the natural logarithm, p is the corrected proportion of GFP positive cells, N is the estimated number of cells on the day of transduction and V is the volume of virus used. This equation assumes a Poisson distribution can be accurately used to describe the number of cells transduced for a given MOT.

2.2.5 Microscopy techniques

2.2.5.1 Indirect immunofluorescence

Cells ($2\text{-}4x10^4$ per well) were seeded onto coverslips in 12 well plates and the next day were transfected with appropriate expression plasmids using Transit-LT1. Two days post-transfection, cells were washed twice in PBSCM and then fixed with 4% PFA in PBS for 15-30 minutes. Where indicated, cells were stained with Mitotracker CMX ROS (20 nM) or Mitotracker Far Red (100 nM) for 30 minutes before fixation. After fixation, PFA was quenched with 50mM NH_4Cl in

PBS for five minutes and the cells were permeabilized with 0.2% Triton X-100 in PBS for four minutes. After washing twice in PBSCM, cells were then blocked in 1% BSA in PBSCM for 15 minutes. Incubation with primary antibodies diluted in 1%BSA in PBSCM was done overnight at 4°C. The next day, samples were washed three times in 0.1%BSA in PBSCM before incubation with secondary antibodies diluted in 1%BSA in PBSCM for one hour. After two washes in 0.1% BSA in PBSCM and one wash in PBSCM alone, the coverslips were mounted onto microscope slides using ProLong Gold Antifade reagent with DAPI. Images were captured using an Olympus IX-81 microscope base with a Hamamatsu EMCCD (C9100-13) camera. Image acquisition was done using Volocity software (PerkinElmer).

2.2.5.2 Superresolution microscopy

Cells were fixed with 4% electron microscopy grade PFA in PBS as described above. The cells on coverslips were then washed three times in PBS and incubated for one hour at room temperature in Blocking buffer (0.1% Triton X-100, 3%BSA in PBS). Next, samples were incubated with primary antibodies diluted in blocking buffer for 1.5 hours at room temperature, washed twice in Washing buffer (0.01% Triton X-100, 0.3% BSA in PBS) and then incubated with secondary antibodies and 1µg/mL DAPI in Blocking buffer at room temperature for one hour. The coverslips were then washed twice in Washing buffer and once in MilliQ water before mounting onto microscope slides using SlowFade Gold

Antifade reagent. The mounting agent was allowed to set for two hours at room temperature before the coverslips were sealed with nail polish and then stored for at least 16 hours at -20°C. Images were captured using an Applied Precision DeltaVision OMX super resolution microscope. Image acquisition was performed with DeltaVision OMX software and reconstructed using SoftWoRx 6.1 OMX SI Reconstruction tool.

2.2.5.3 Apoptosis assays

To determine how expression of capsid mutants affected apoptosis induction A549 cells were transduced with the appropriate capsid-encoding lentiviruses as described in section 2.2.4.2. The next day, cells were split and seeded at a dilution of 1:2 into 12 well plates with coverslips. Apoptosis was induced on the second day after transduction by treatment with αFAS (0.25µg/mL) and cycloheximide (1µg/mL) for 24 hours. Alternatively, transduced cells were transfected (using Lipofectamine 2000) with poly(I:C) (2µg/mL) or pCMV5 (negative control) 24 hours before fixation. Where indicated, recombinant RV strains with mutations that affect phosphorylation of capsid protein were used to infect A459 cells seeded the day before ($5x10^4$/well) in 12 well dishes at an MOI of 0.5 (see section 2.2.7.3). Apoptosis was induced two days after infection by αFAS (1µg/mL of) and cycloheximide (1µg/mL of) treatment for eight hours.

Cycloheximide was used to prevent upregulation of anti-apoptotic genes by NF-κB, which is activated by the FAS receptor (Wang *et al.*, 1998).

To determine whether expression of the capsid RARA mutant conferred protection against apoptotic stimuli, A549 cells were transfected with relevant pCMV5 constructs using Lipofectamine 2000 as described in section 2.2.1.3. Two days post-transfection, apoptosis was induced with αFAS (0.25μg/mL) and cycloheximide (1μg/mL) for 6 hours. To assay apoptosis induced by viral replication, Vero cells were transfected as described in section 2.2.1.3 with the relevant infectious RNA produced as described in section 2.2.7.1. Two days post-infection, cells were fixed and assayed for apoptosis.

Activated caspase 3 was detected in transduced, transfected or infected cells by indirect immunofluorescence as described in section 2.2.5.1. Transduced cells were detected using a goat antibody to GFP and transfected/infected cells were identified using the mouse αCapsid antibody (C-1). To determine the percentage of apoptotic cells in a sample, caspase 3 reactivity in at least 100 GFP- or capsid-positive cells was assessed as previously described (Ilkow *et al.*, 2011).

2.2.6 Biochemical techniques

2.2.6.1 Preparation of cell lysates

Cells were washed twice in PBS and lysed in 1X Protein sample buffer containing 31.25U/mL Benzonase. For 6 well plates, 200µL of Protein sample buffer /well was used whereas 50 or 100µL/well were used for 24 and 12 well plates respectively. Cell lysates were then immediately boiled and run on gels or stored at -20°C until further use.

To prepare cell lysates with NP-40 or PP1 CoIP lysis buffers, cells were washed twice in cold PBS before lysis buffer was then added. Dishes were incubated on ice for 10 minutes and then cell scrapers were used to dislodge cellular material. The lysates were cleared by centrifugation at 10 000 *g* at 4°C for 10 minutes.

2.2.6.2 Sodium dodecyl sulphate (SDS) polyacrylamide gel electrophoresis (PAGE)

Acrylamide gels were made using 4X Resolving and Stacking gel buffers (Table 2.6). Resolving gels with 10% or 12% acrylamide were used for all experiments. Samples to be analyzed were mixed with 5X Protein sample buffer and then boiled for five minutes, centrifuged at 16,000 *g* briefly, and then loaded onto gels. SDS-PAGE was conducted in Bio-Rad Mini-Protean III systems in Running

buffer at 75-120V. After electrophoresis, proteins were transferred to PVDF or nitrocellulose membranes. Before use, PVDF membranes were activated by washing briefly in methanol. All membranes were equilibrated in Transfer buffer for at least five minutes before use. Transfers were conducted using a Bio-Rad Mini Trans-Blot system at a constant current of 320mA for 1-1.75 hours in an ice water bath.

2.2.6.3 Western blot

After protein transfer, PVDF or nitrocellulose membranes were washed briefly in PBS before incubation for at least one hour in Blocking buffer: a 1:1 mixture of Odyssey Blocking Buffer and PBS. Incubation with primary antibodies was then performed in Blocking buffer for one to three hours at room temperature or overnight at 4°C. Membranes were then washed four times in PBST and incubated with secondary antibodies diluted in Blocking buffer for one hour at room temperature. Before imaging, membranes were washed three times in PBST and one final time in PBS. Image acquisition was done using a LI-COR Odyssey infrared imaging system. If membranes were to be reused, they were washed twice in PBS and incubated with Restore™ Western blot stripping buffer for 15-30 minutes at room temperature. Before re-blocking, membranes were washed twice in PBS.

2.2.6.4 Immunoprecipitation

For immunoprecipitations with rabbit anti-Bax, A549 cells were seeded at $1x10^6$ cells in 100mm dishes and transfected the next day with pCMV5-Capsid, pCMV5-Capsid-S46A or pCMV5-Capsid-S46D using Lipofectamine 2000. Two days post-transfection, cells were lysed in 1.8mL of NP-40 Lysis buffer with 1X CPI and 1XPI. Lysates were precleared by incubation with a Protein-A Sepharose slurry for one hour with rotation at 4°C. After pre-clearing, a small amount of lysate was kept as a loading control. While lysates were preclearing, 15µL of 33% Protein-A Sepharose slurry per sample was incubated with 2µL of Rabbit αBax or pre-immune serum in 1% (w/v) Casein in PBS + 1X CPI for one hour at 4°C with rotation. The antibody-coated beads were then collected by centrifugation (500 x *g* for five minutes) and then mixed with 350µL of pre-cleared lysates together with an additional 2µL of antibody/pre-immune serum. Immune complexes were allowed to form for four hours at 4°C with rotation after which the Sepharose beads were collected by centrifugation and then washed once in NP-40 Lysis buffer and twice in NP-40 Lysis buffer lacking detergent. After the final wash, excess liquid was removed with a gel loading pipette tip and proteins were eluted by boiling in 30µL of 5X Protein sample buffer. The entire immunoprecipitation and 30µL of the saved lysate (8.6% of volume used in IPs) were subjected to SDS-PAGE.

For immunoprecipitations with capsid antibody, HEK293T cells were seeded at $2.25x10^6$ cells per 100mm dish and transfected the next day with Transit-LT1. Cells were then lysed in 1mL of PP1 CoIP buffer + 1XCPI per dish. Lysates were pre-cleared with Protein A Sepharose slurry as described above and 300µL of lysate was incubated with 4µL of rabbit αcapsid (7W7) (Beatch *et al.*, 2000) overnight at 4°C with rotation. In parallel, 33% Protein A Sepharose slurry was blocked in 1% (w/v) Casein in PBS overnight at 4°C with rotation. . The next day, 15µL of 33% bead slurry was incubated with lysates for one hour at 4°C with rotation. Then beads were washed twice in PP1 CoIP buffer and once in PBS before proteins were eluted by boiling in 30µL 5X Protein sample buffer. Twenty µL of the immunoprecipitations and 2µL of lysate saved before pre-clearing were then subjected to SDS-PAGE and immunoblotting.

2.2.6.5 Microcystin-Sepharose pulldown

HEK293T cells ($1.75\text{-}2.5x10^6$) seeded in 100mm dishes were transfected the next day with plasmids using Transit-LT1. Two days post-transfection, cells were lysed in 1mL of NP-40 lysis buffer + 1X CPI per dish. Both Microcystin-Sepharose (MC-Sepharose) and Sepharose beads (33% slurry) were washed twice in cold water and twice in Buffer A. All centrifugations were performed at 8,500rpm in a microfuge at 4°C for three minutes. After washing, where indicated, beads were incubated with 2µg of purified PP1α (courtesy of Dr. Charles Holmes, University

of Alberta) for 1.5 hours at 4°C in 300µL of Buffer A with rotation. Beads were then washed twice in Buffer A + 150mM NaCl + 1% (w/v) Tween-20 before incubating with 500µL of lysate overnight at 4°C with rotation. The next day, the beads were washed four times in Buffer A + NaCl + Tween and bound proteins were eluted by boiling in 45µL of 5X protein Sample buffer for five minutes. Twenty µL of pulldown eluates and 5-20µL of lysate were subjected to SDS-PAGE and immunoblotting.

For pull-downs involving capsid transcribed/translated *in vitro*, reactions were performed as per manufacturer's instructions using 40µL of TnT® Quick Master Mix, 1µL of 1mM Methionine, 7µL of nuclease-free water and 1µg of pcDNA3.1-Capsid-myc/His and incubation for 1.5 hours at 37°C. Pull-downs were conducted as described above except that 7µg of PP1α, PP1γ (courtesy of Dr. Charles Holmes, University of Alberta) or Buffer A alone as a control were used instead of 2µg of PP1α and 40µL of *in vitro* transcription/translation reaction topped up to 800µL with NP-40 lysis buffer + 1% (w/v) BSA + 1XCPI were used instead of 500µL of lysate.

2.2.6.6 Luciferase assays

To assay activation of the ISRE reporter by poly(I:C), A549 cells were seeded in 12 well plates ($1x10^5$ cells per well) and transfected the next day with Lipofectamine

2000 (1µg of DNA/well). To assay activation of the ISRE reporter by interferon-α, A549 cells were seeded into 24 well plates ($5x10^5$ cells per well) and transfected the next day with Transit-LT1 (250ng of DNA/well). Cells were transfected with the indicated pCMV5 plasmid, PGL3-ISRE-Luc and pRLTK at a ratio of 35:3:2 or 30:3:2 in Lipofectamine and Transit-LT1 transfected cells respectively. The next day, cells were transfected with poly(I:C) (2.5µg/mL) or pCMV5 as a control using Transit-LT1 or exposed to 10U/mL of interferon-α. Eighteen hours later, cells were lysed and Luciferase activity was measured with the Promega Dual-Luciferase® Reporter Assay System as per manufacturer's guidelines. Analysis was done using a BioTek Synergy 4 plate reader and accompanying Gen5 software. All data are expressed as a fold induction compared to non-treated cells transfected with vector (pCMV5) alone. All samples were normalized to expression from the control Renilla Luciferase plasmid, pRLTK.

2.2.7 Virology techniques

2.2.7.1 In vitro transcription of infectious RNA

Infectious RNA was transcribed from pBRM33-based plasmids that were linearized by HindIII digestion as described in section 2.2.2.3. The linearized plasmids were subjected to phenol:chloroform extraction followed by ethanol precipitation prior to transcription using Ambion mMessage mMachine SP6 RNA Transcription kits. Xenopus elongation factor 1α RNA transcribed from the pTRI-

Xef plasmid included in this kit was used as a transfection control where indicated. The manufacturer's guidelines were employed with the exception that 1µL of RNAse OUT was added to the 20µL reaction mixtures which were incubated for two hours at 37°C. RNA was then precipitated by addition of LiCl Precipitation Solution (from Ambion kit) and incubated at -20°C for at least 30 minutes. RNA was pelleted by centrifugation at top speed in a microfuge for 15 minutes at 4°C, washed with 70% ethanol and then air-dried and before resuspension in nuclease-free water. RNA concentration was determined using a NanoDrop 1000 Spectrophotometer and quality was assayed through agarose gel electrophoresis. RNA stocks were aliquoted and stored at -70°C until use.

2.2.7.2 Virus stock production

Confluent BHK-21 cells were washed once in PBS before detachment from T75 flasks with trypsin-EDTA. The trypsin was then quenched with media containing 5%FBS after which the detached cells were washed in PBS, pelleted and then resuspended in 400µL of HEPES buffered Saline. Five µL of *in vitro* synthesized infectious RNA (see above) was added to the cell suspension which was then transferred to a Bio-Rad Gene Pulser® 0.2cm Cuvette. Electroporation was done using a BTX Electro Cell Manipulator® 600 with the following settings: 500V/Capacitance and Resistance Low voltage mode, 100µF capacitance, 720ohm (R10) resistance and a charging voltage of 500V. After pulsing, cells

were incubated in HEPES buffered Saline for 10 minutes and then seeded into 150mm plates containing 20mL of complete media. Unless otherwise indicated, all cells infected with RV were cultured at 35°C under 5% CO_2 atmosphere. Three days post-electroporation, the media were then collected, centrifuged at 900 x *g* for five minutes to remove cell debris, aliquoted and stored at -80°C. Before use, virus titers were determined by plaque assay as described in section 2.2.7.4.

2.2.7.3 Virus infection

To infect cells with wild type or mutant RV strains, half of the media from cell cultures was removed before virus stocks were added. Cells were then incubated at 35°C for six hours before media was replaced with the "normal" volume of complete media. Cells were then incubated at 35°C with 5% CO_2 until their use in experiments.

2.2.7.4 Plaque assay

RK-13 cells were seeded at $3x10^5$ cells per well in 6 well plates. The next day, media were replaced with 2mL serial dilutions of virus stock. After a four hour incubation step at 35°C, media were replaced with a warmed, sterile 1:1 mixture of 2X RK-13 media and 1% agarose. The cells were incubated at 35°C for seven days to allow plaque formation after which the agarose was removed. The cells

were fixed and stained with 0.05% (w/v) crystal violet in 17% ethanol for two hours to enable visualization of the plaques.

2.2.7.5 Quantitative polymerase chain reaction (qPCR)

The levels of viral genome in infected cells was determined by qPCR. Vero cells transfected with infectious RNA using Lipofectamine 2000 were cultured for 24 to 72 hours at 35°C, washed in PBS and then lysed using the RNeasy Mini kit. Resulting cell lysates were homogenized using the QIAshredder kit and then stored at -70°C until further use. RNA concentrations in the lysates were measured using a NanoDrop 1000 spectrophotometer and 300ng of total RNA was used for reverse transcription with random primers (200 ng) with the SuperScript® II Reverse Transcriptase kit. qPCR was performed using a PerfeCta SYBR Green Supermix, Low ROX kit in a Stratagene MX3005P instrument. For each experimental condition, qPCR reactions were done in triplicate. Five µL of reverse transcription reactions diluted 1:2 with nuclease free water were used for qPCR. To amplify RV genomes, RV-F and RV-R primers were used at a concentration of 0.2µM each. As an internal control, β-actin mRNA was amplified with B-ACTIN FW and B-ACTIN REV primers (0.1µM each). After an initial denaturing step of 94°C for 3 minutes, 40 cycles of 15 seconds at 95°C, 30 seconds at 58°C and 20 seconds at 72°C were used to amplify RNA. SYBR green and ROX reference dye fluorescence was quantified during the 58°C annealing

step. Viral genome levels are normalized to β-actin and expressed relative to wild type virus at 24 hours using the $2^{-\Delta\Delta CT}$ method.

2.2.7.6 Isolation of Rubella virus-like particles

Vero cells in 35 mm dishes were transfected with pCMV5-24S based constructs or pCMV5 alone as a negative control. Two days post transfection, media were collected and pre-cleared by centrifugation at 10 000 x *g* for 10 minutes at 4°C. The remaining cells were also lysed in 200µL of 1X Protein sample buffer containing Benzonase®. Virus-like particles were pelleted from the pre-cleared media by centrifugation at 53 000 rpm for one hour at 4°C in a Beckman Optima™ TLX Ultracentrifuge equipped with a TLA 100.4 rotor. Media were then aspirated and the pellets were resuspended in 40µL of 5X Protein sample buffer. Twenty µL each of lysate and pellet were then analyzed by SDS-PAGE and immunoblotting.

2.3 Post-acquisition processing

2.3.1 Image processing and presentation

Post-acquisition processing of microscopy images was done by importing images into ImageJ using the Bio-Formats plug-in (Open Microscopy Environment). Images were then either directly processed in ImageJ or Adobe PhotoShop CS6. With the exception of super-resolution microscopy images, all changes were

linear and applied equally across all images for a given channel within the same figure. 3D Superesolution microscopy images were produced with the ImageJ 3D Viewer (Benjamin Schmid, http://imagej.nih.gov/ij/plugins/3d-viewer/). LI-COR TIF files were also opened in ImageJ where brightness and contrast were altered before being final adjustments were made in Photoshop. All changes were linear and applied equally for all samples in a given row within a figure. All quantitative data were processed and graphed in Microsoft Excel before being exported to Photoshop for final adjustments.

2.3.2 Statistical analysis

All quantitative data are the result of at least three but no more than five independent experiments. Asterisks represent a statistically significant difference ($p<0.05$) between the given construct and wild type capsid except where otherwise indicated. All statistical analysis was done using Student's paired t-test or a one-way ANOVA with a Tukey HSD *post-hoc* test (http://statpages.org/anova1sm.html). All error bars represent standard error. Pearson's coefficient was calculated using JACoP (http://rsb.info.nih.gov/ij/plugins/track/jacop.html) in ImageJ.

CHAPTER 3
Importance of phosphorylation and membrane association for the anti-apoptotic activity of Rubella virus capsid protein

Data from this chapter were published previously in Willows *et al.* (2014). Willows, S.D., Ilkow, C.S. and Hobman, T.C. (2014) Phosphorylation and membrane-association of the Rubella virus capsid protein are important for its anti-apoptotic function. *Cell Microbiol*. 16(8): 1201-10.

3.1 Rationale and hypothesis

For many years, viral capsid proteins have been thought to fulfill mostly structural roles, recruiting and protecting the viral genome in the nucleocapsid. Recent research has found that many viral capsid proteins, especially those of RNA viruses, are also able to fulfill non-structural functions. RV capsid is a particularly good example and has been shown, through work in our lab and others, to affect many processes through interaction with several host and viral proteins (Beatch *et al.*, 2000, Tzeng *et al.*, 2003, Beatch *et al.*, 2005, Tzeng *et al.*, 2005, Tzeng *et al.*, 2006, Ilkow *et al.*, 2008, Ilkow *et al.*, 2010a, Ilkow *et al.*, 2011). One of its most important roles is in protecting infected cells from apoptosis, a process that involves the pro-apoptotic Bcl-2 family protein Bax (Ilkow *et al.*, 2011). This protection was observed not only in several different cell lines, including primary cells, but was effective against multiple apoptotic stimuli. It is not surprising that RV would seek to limit apoptosis, as this is a major mechanism by which infected cells are eliminated in host organisms. Furthermore, RV replicates slowly, with titers peaking only after 48hrs (Hemphill *et al.*, 1988), and must extend the window for viral replication for as long as possible. Although one host target has been identified, the mechanism by which RV capsid inhibits apoptosis is still not fully understood.

Although RV capsid expression clearly functions to block apoptosis in a cellular context, recent *in vitro* experiments revealed that RV capsid has effects that may be considered pro-apoptotic in nature. Specifically, exposure of isolated mitochondria to a recombinant capsid protein resulted in characteristic changes to mitochondria that occur during apoptosis. Of significance, the recombinant capsid lacks phosphorylation and is not membrane-associated like bona fide capsid from infected or transfected cells. Therefore, I sought to investigate the role of these two properties in capsid's anti-apoptotic activity.

3.2 Results

3.2.1 Recombinant RV produced in bacteria has pro-apoptotic effects in vitro

Previously, Dr. Carolina Ilkow constructed a system whereby the effects of capsid on mitochondria could be assayed in isolation from other cellular systems (Willows *et al.*, 2014). In these assays, capsid purified from bacteria was incubated with mitochondria isolated from rat liver or A549 cells and two different assays were used to determine the effects on mitochondria. First, the effect of capsid on uptake of Tetramethylrhodamine, methyl ester (TMRM), a fluorescent molecule that collects in mitochondria (Loew, 1994), was determined. Due to its positive charge, an intact mitochondrial membrane potential is required for TMRM to accumulate in this organelle. TMRM can therefore be used to monitor mitochondrial membrane potential both in isolated

mitochondria and intact cells. Loss of mitochondrial membrane potential occurs downstream of cytochrome-*c* release and depends on the action of two pro-apoptotic proteins, Bax and Bak (Goldstein *et al.*, 2000). Although capsid expression inhibits Bax-dependent cytochrome-*c* release *in vivo* (Ilkow et al., 2011), pre-incubation of mitochondria with recombinant capsid severely reduced uptake of TMRM (Figure 3.1A), indicating that this viral protein induces loss of mitochondrial membrane potential. The effect of capsid on TMRM uptake was comparable to a known pro-apoptotic BH3-only protein, tBid. This protein, which is the truncated form of Bid, binds and activates Bax, thus inducing pore formation (Ruffolo *et al.*, 2000). Because loss of mitochondrial membrane potential could also be caused by a Bax-independent event, such as opening of the mitochondrial membrane permeability transition pore (mPTP) (reviewed in Siemen *et al.*, 2013), the effect of recombinant capsid on cytochrome-*c* release directly was investigated (Figure 3.1B). Here, rat liver mitochondria were isolated and exposed to varying levels of the recombinant capsid protein or a similarly sized control protein Sec17, with no known role in apoptosis. The supernatant and mitochondria pellet fractions were then separated by centrifugation and analyzed for the presence of cytochrome-*c*. Immunoblotting for complex II, which resides on the matrix side of the inner mitochondrial membrane, was used as a loading control for mitochondria. Addition of 2µg or more of capsid resulted in a loss of cytochrome-*c* from the mitochondria indicating that the

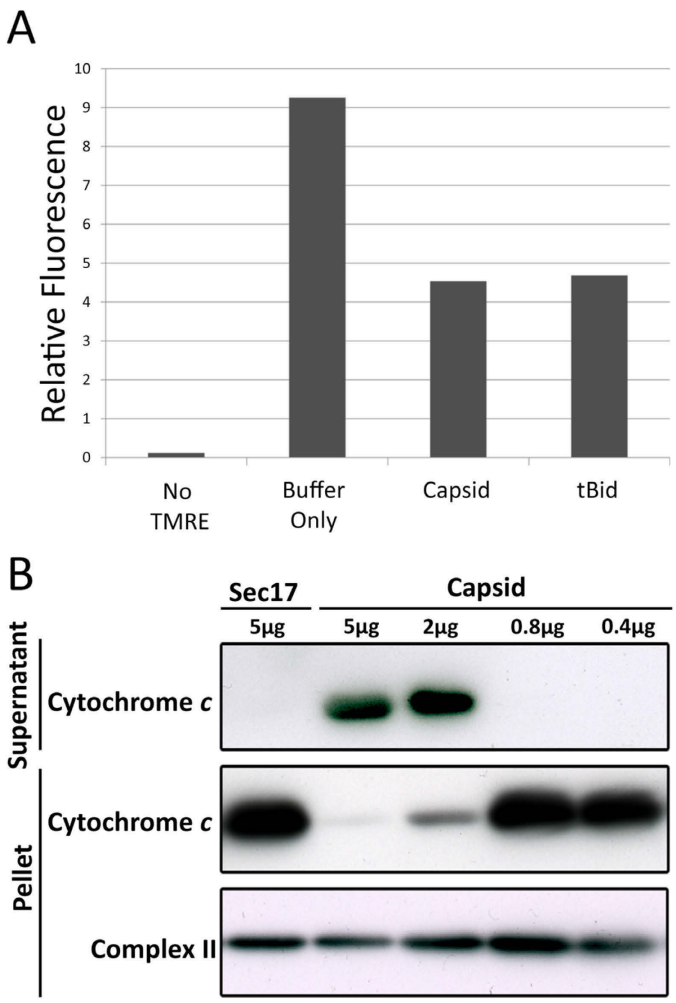

Figure 3.1 Recombinant capsid has pro-apoptotic effects on mitochondria *in vitro.* (A) Mitochondria were isolated from A549 cells and incubated with indicated proteins for 15 minutes at 30°C. TMRE (150nM) was added and mitochondria were incubated for another 30 minutes at 37°C. After washing, mitochondria were subjected to fluorometric analyses. (B) Isolated rat liver mitochondria were first normalized to 1mg/mL of protein and incubated with the indicated protein for 30 minutes at 30°C. Mitochondria were then pelleted by centrifugation and both supernatant and pellet were analyzed by SDS-PAGE and immunoblotting. Data were provided courtesy of Dr. Carolina Ilkow.

pro-apoptotic effects of recombinant capsid were mediated by Bax/Bak pore formation rather than opening of the mPTP.

3.2.2 Phosphorylation of serine 46 in RV capsid is important for protection against Fas-dependent apoptosis

There are several differences between recombinant capsid made in bacteria and *bona fide* capsid made in RV-infected or transfected eukaryotic cells that could explain the opposite effects on apoptosis. One difference is lack of phosphorylation of the recombinant capsid. I next investigated whether capsid mutants lacking known phosphorylation sites were able to protect from cells from apoptotic stimuli. Two previously characterized phosphomutants were used: S46A and S46D (Figure 3.2). As reported previously, mutation of serine 46 to a non-phosphorylatable residue such as alanine results in decreased phosphorylation of multiple residues around the RNA binding region (Law *et al.*, 2003, Law *et al.*, 2006). The S46D mutant, which has a negatively charged residue (aspartate) at position 46, is thought to mimic the negative charge found on the phosphate which is normally added to serine 46 of wild type capsid. Indeed, the S46D mutant shows nearly wild type levels of phosphorylation at other residues, suggesting it is sufficient for recognition by host kinases (Law *et al.*, 2006). In order to understand the effect of these mutations on capsid's anti-apoptotic activity, an immunofluorescence assay (Ilkow *et al.*, 2011) was

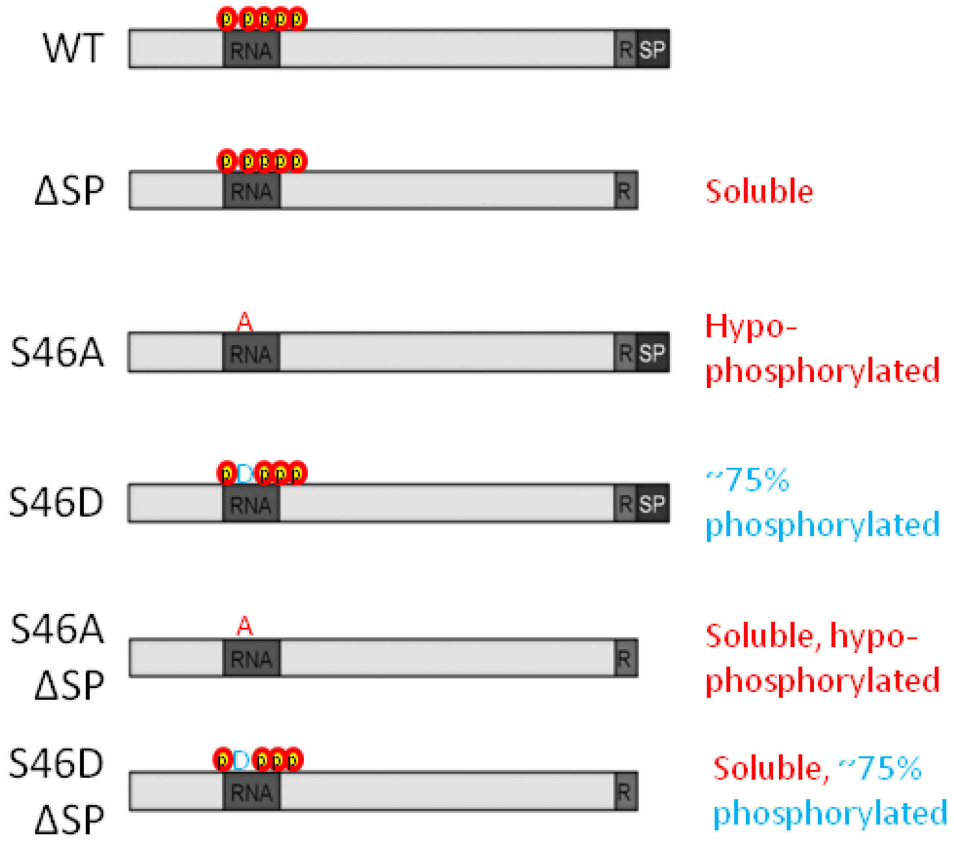

Figure 3.2 Capsid mutants used in this study. The serine 46 to alanine mutation in S46A and S46A ΔSP render capsid almost entirely dephosphorylated. The serine 46 to aspartate mutation in S46D and S46D ΔSP leave capsid nearly fully phosphorylated. Removal of the signal peptide in ΔSP, S46A ΔSP, and S46D ΔSP results in loss of membrane association. RNA-RNA binding region; R- arginine rich R-region; SP-E2 signal peptide, a transmembrane domain that anchors capsid to membranes.

employed to detect apoptosis in transfected cells. A549 cells were transduced with lentiviruses encoding wild type and capsid mutants as well as AcGFP from an internal ribosome entry site (IRES). Transduced cells (AcGFP-positive) identified by fluorescence microscopy were then counted and the percentages that are positive for staining with an α-active Caspase-3 antibody were determined.

Cells expressing phosphomutant capsids were less resistant to the apoptotic stimulus anti-Fas compared to those expressing wild type capsid (Figure 3.3). This was not due to reduced stability of the mutant proteins as previous studies indicated that non-phosphorylated capsid protein is expressed at comparable levels to wild type capsid (Law *et al.*, 2003, Law *et al.*, 2006). Compared to anti-Fas treated cells transduced with lentivirus encoding AcGFP alone, expression of wild type capsid reduced percentage of apoptotic cells by 50%. In contrast, the apoptotic protection conferred by the S46A mutant, while significantly different from AcGFP only expressing cells was less effective compared to wild type capsid. Surprisingly, the S46D mutant that I thought would act similarly to wild type capsid because phosphorylation levels are near normal, exhibited intermediate protection against anti-Fas. These results show that phosphorylation at serine 46 is important for the anti-apoptotic activity of RV capsid.

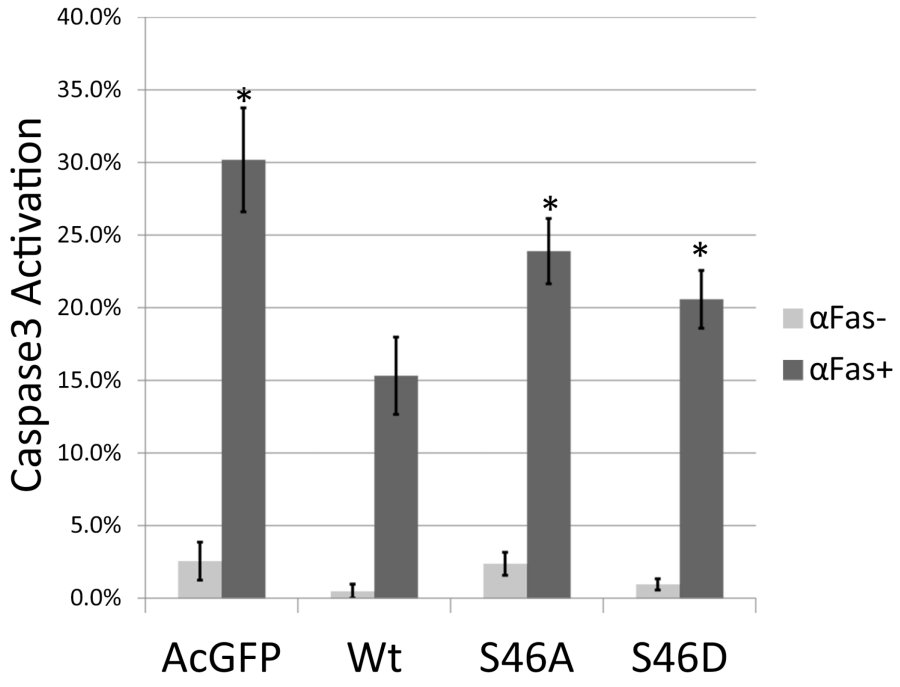

Figure 3.3 Capsid S46A and S46D exhibit reduced protection from αFAS induced apoptosis. A549 cells were transduced (MOT = 2) with lentivirus-encoding the indicated capsid constructs or AcGFP alone. Apoptosis was induced two days later for 24 hours with αFAS (0.25μg/mL) and cycloheximide (1μg/mL). Apoptosis was assayed via immunofluorescence with an antibody directed towards active caspase 3. All error bars indicate standard error from four independent experiments. Asterisks denote a statistically significant difference from wild type capsid ($p<0.05$) as determined by Student's t-test.

3.2.3 Phosphorylation of serine 46 in RV capsid is important for protection against poly(I:C) induced apoptosis

I next examined the importance of capsid phosphorylation in protection from another inducer of apoptosis: Polyinosinic:polycytidylic acid (poly(I:C)). Poly(I:C) is an immunostimulant that is thought to act as an analog to double-stranded RNA, a common viral pattern recognized by the innate immune response. Two types of receptors recognize poly(I:C): the endosome localized toll-like receptor 3 (TLR3) (Alexopoulou *et al.*, 2001) and the intracellular RIG-I like receptors (Yoneyama *et al.*, 2004, Gitlin *et al.*, 2006). Activation of these receptors not only induces the innate immune response, but also causes apoptosis (Salaun *et al.*, 2006, Salaun *et al.*, 2007, Rintahaka *et al.*, 2008b, Besch *et al.*, 2009a). Furthermore, a downstream effector of both pathways, IRF3, has been shown to bind and directly activate Bax, possibly mediating apoptosis in response to innate immune induction (Chattopadhyay *et al.*, 2010b).

The ability of capsid to protect from poly(I:C) induced apoptosis was analyzed in a similar manner to the αFAS assays. Transduced cells were split onto coverslips 1 day post-transduction and transfected with poly(I:C) the next day. Although many studies simply add poly(I:C) to the media, transfection of poly(I:C) was used in these assays, as it better represents activation of intracellular, rather than endosomal receptors of viral dsRNA. Internal receptors are more relevant

for assaying capsid apoptotic protection because RNA replication in the cytoplasm is likely a major stimulus for RV induced apoptosis. Furthermore, addition of poly(I:C) to cell media did not induce significant apoptosis in A549 cells (data not shown), whereas transfection of poly(I:C) strongly induced cell death. Plasmid DNA vector pCMV5 was transfected in parallel to poly(I:C) as a negative control to ensure apoptosis induction was not principally due to the transfection procedure. In these assays, capsid expression conferred moderate protection to poly(I:C) induced apoptosis, reducing the levels by ~40% (Figure 3.4). In contrast, the levels of apoptosis in cells expressing S46A or S46D were no different from the control cells expressing AcGFP alone. This experiment for the first time shows the RV capsid inhibits apoptosis induced by activation of the innate immune response. Furthermore, it shows that the phosphorylation of capsid is critical for protection against apoptosis in contexts that closely resemble infection.

3.2.4 Cells infected with RV with mutations at S46 are highly susceptible to apoptosis

Since poly(I:C) transfection is similar to apoptotic stress encountered during infection, I next sought to investigate how the phosphorylation of serine 46 affected apoptosis in RV-infected cells. To do this, I utilized a previously constructed mutant RV strain containing the S46A mutation in the capsid gene

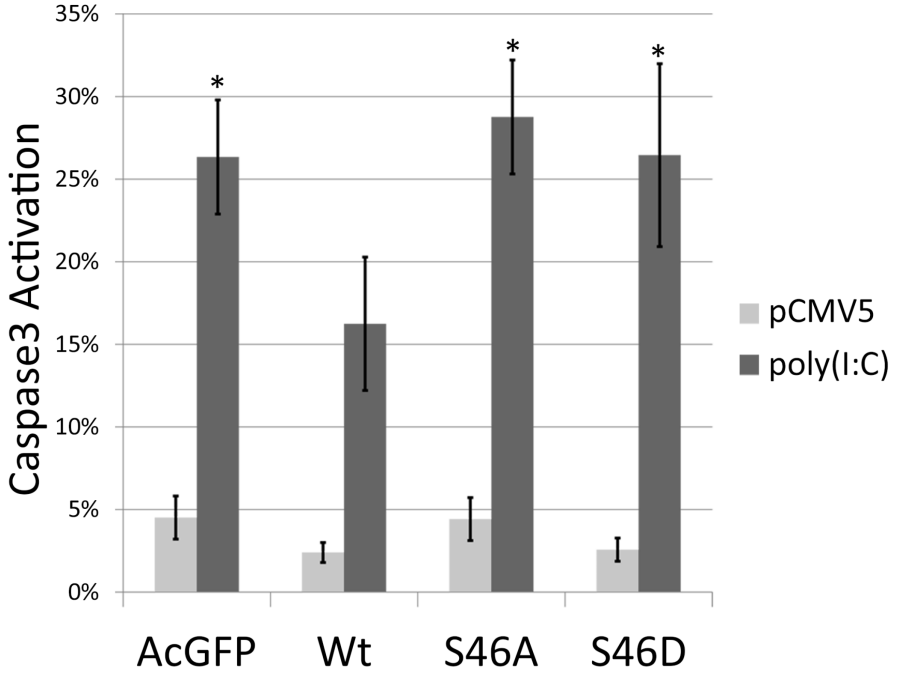

Figure 3.4 Wild type capsid, but not S46A and S46D, protect from poly(I:C) induced apoptosis. A549 cells were transduced (MOT = 2) with lentivirus encoding wild type (Wt), S46A or S46D capsid mutants or AcGFP alone. Two days post-transduction, cells were transfected with poly(I:C) (1µg/mL) or pCMV5 plasmid DNA as a control. Apoptosis was assessed 24 hours after transfection via immunofluorescence with an antibody towards active caspase 3. All error bars indicate standard error among five independent experiments. Asterisks denote a statistically significant difference from wild type capsid ($p<0.05$) as determined by Student's t-test.

(Law *et al.*, 2006). I also generated an infectious RV clone containing the S46D mutation. Infectious RNAs produced by *in vitro* transcription of the linearized infectious clone plasmids were electroporated into BHK-21 cells to produce RV stocks that were used to infect A549 cells on coverslips. Infected cells were then treated with αFAS two days later. Here, the cells were treated with higher amounts of αFAS (1μg/mL) for a shorter duration (eight hours) to prevent significant RV induced apoptosis that occurs 72hrs post-infection from affecting results. Similar to the data from the lentivirus transduction experiments, cells infected with RV strains encoding S46A and S46D phosphomutants were not resistant to Fas-dependent apoptosis (Figure 3.5). Background death rates were relatively low, but were lowest for the S46A mutant.

3.2.5 Loss of phosphorylation does not decrease binding of capsid to Bax

Since Bax has been previously shown to be involved in one mechanism by which RV capsid blocks apoptosis, I next investigated how phosphorylation affects the interaction between capsid and Bax through immunoprecipitation. I initially hypothesized that capsid S46A and S46D would bind less well to Bax thereby explaining the loss of anti-apoptotic activity in serine 46 mutants. To test this, transfected cells were subjected to co-immunoprecipitation with anti-Bax, SDS-PAGE and immunoblotting with antibodies to capsid. Surprisingly, neither the S46A nor S46D mutants were defective for Bax binding (Figure 3.6). In fact,

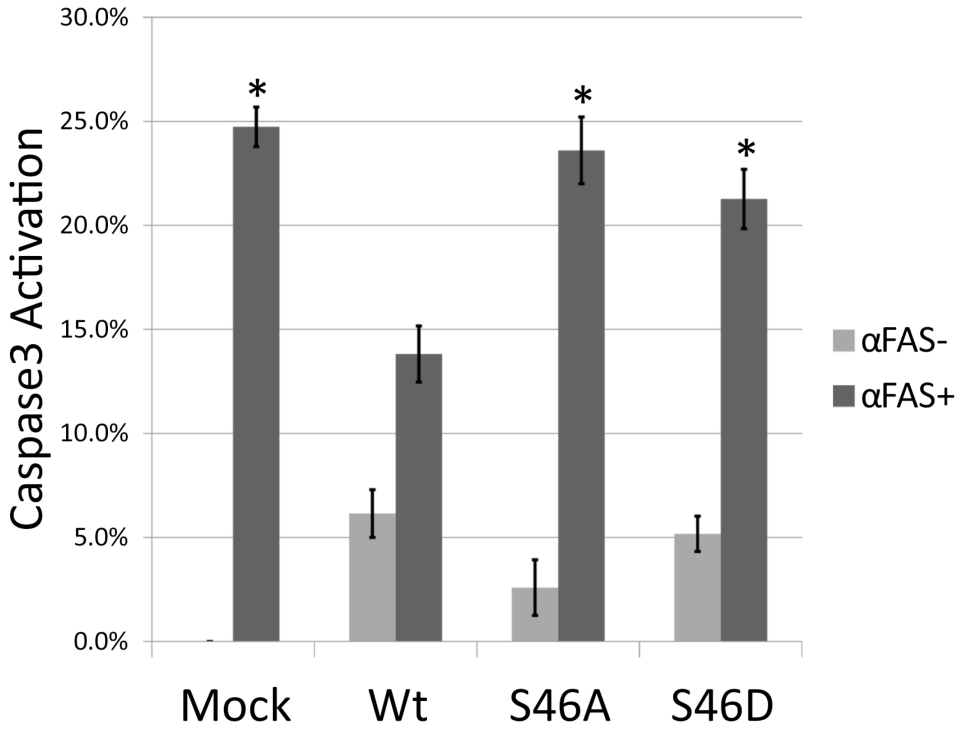

Figure 3.5 RV strains harboring S46A and S46D mutations are not resistant to treatment with αFAS. A549 cells were infected (MOI = 0.5) with indicated RV strain. Two days post-infection, apoptosis was induced with αFAS (1μg/mL) and cycloheximide (1μg/mL) for eight hours. Apoptosis was assayed via immunofluorescence with an antibody directed towards active caspase 3. All error bars indicate standard error from five independent experiments. Asterisks denote a statistically significant difference from wild type capsid ($p<0.05$) as determined by Student's t-test.

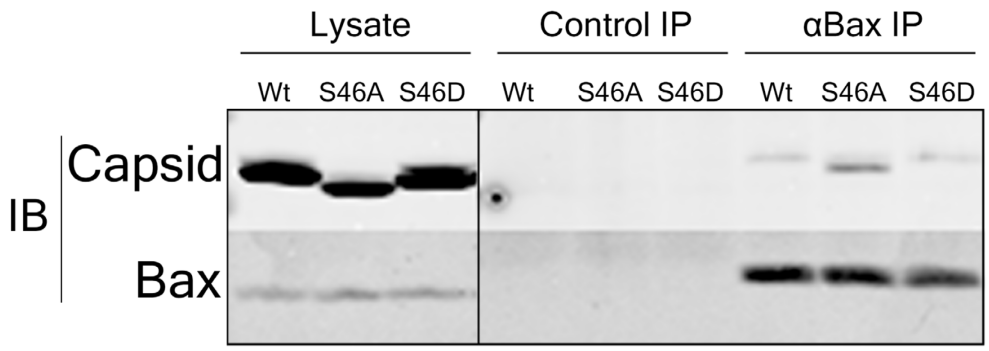

Figure 3.6 Capsid S46A and S46D bind Bax. A549 cells were transfected with indicated pCMV5-capsid constructs and lysates were harvested two days later. Endogenous Bax was bound to rabbit anti-Bax antibody or rabbit serum as a control and precipitated with Protein A Sepharose beads. Proteins were eluted with Protein sample buffer and assayed by SDS-PAGE and immunoblotting with 8.6% volume of the original lysates.

higher levels of S46A were consistently pulled down with anti-Bax than wild type capsid. This clearly indicates that phosphorylation of capsid is not required for stable interaction with Bax. Furthermore, it is unlikely that the apparent increased affinity of S46A for Bax contributes to its reduced anti-apoptotic activity, as the S46D mutant (which also has reduced anti-apoptotic activity) is indistinguishable from wild type capsid with respect to Bax interaction.

3.2.6 High level expression of S46A and S46D mutants confers protection from Fas-dependent apoptosis

Compared to our standard lentiviral transduction protocols (MOT = 2), I consistently observed higher resistance to apoptosis in transfected cells expressing capsid (data not shown). This discrepancy may be related to the differences in number of transgenes in transfected vs transduced cells. Specifically, in transfected cells, there can be as many as 10^4 and 10^6 copies of plasmid per cell (Fliedl *et al.*, 2015). In contrast, lentiviral transduction generally delivers less than 10 vector copies per cell (Charrier *et al.*, 2011). I asked whether, when expressed at higher levels, could the capsid phosphomutants confer significant resistance to apoptotic stimuli. Higher MOTs would increase the amount of cells transduced multiple times, thus increasing the amount of capsid expressed in individual cells. As hypothesized, higher MOTs increased the anti-apoptotic activity in cells expressing capsid S46A or S46D (Figure 3.7). When

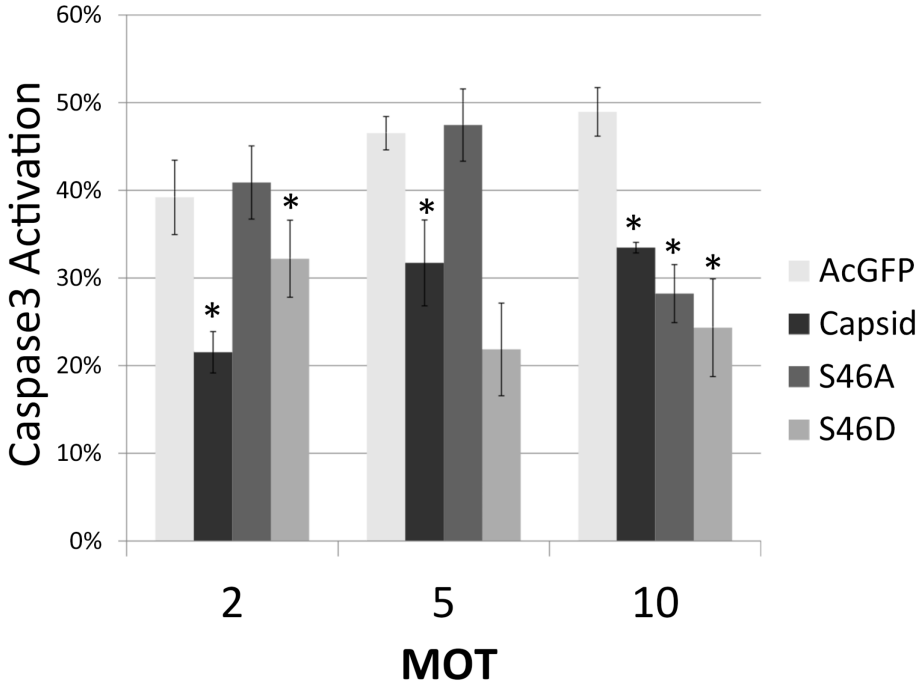

Figure 3.7 High level expression of S46A and S46D confers resistance to apoptosis. A549 cells were transduced at give MOT with lentivirus expressing indicated capsid construct or AcGFP alone. Two days post-transduction, apoptosis was induced with αFAS (0.25μg/mL) and cycloheximide (1μg/mL) for 24 hours. Apoptosis was assayed via immunofluorescence with an antibody directed towards active caspase 3. All error bars indicate standard error from three independent experiments. Asterisks denote a statistically significant difference from AcGFP alone at the given MOT ($p<0.05$) as determined by Student's t-test.

cells were transduced with lentiviruses using an MOT of 10, similar levels of protection from anti-Fas were observed with S46A, S46D and wild type capsid. Interestingly, at an MOT of five, S46A expressing cells were not protected at all compared to the AcGFP control. This suggests that a certain threshold of this capsid mutant is required for apoptotic protection. Higher MOTs also resulted in slightly higher rates of apoptosis in cells transduced with wild type capsid or AcGFP only, suggesting a greater sensitivity to apoptosis is induced by high MOTs. Overall these results show that capsid S46A and S46D do in fact retain some anti-apoptotic activity.

3.2.7 Membrane association of capsid is important for its anti-apoptotic activity

In addition to lacking phosphorylation, the recombinant capsid used in the initial *in vitro* assays (Figure 3.1) also lacked the E2 SP which serves to anchor the capsid to membranes. When full-length capsid was expressed in bacteria, the hydrophobic E2 SP resulted in the formation of aggregates in the bacteria. I questioned whether the lack of membrane association could affect the ability of capsid to protect against apoptotic stimuli. To investigate this possibility, I utilized a previously characterized capsid truncation mutant, CapΔSP, in which the E2 signal peptide (SP) was removed (Law *et al.*, 2001). I also constructed versions of the S46A and S46D mutants that lack the membrane association

domain (Figure 3.2). Because expression of the S46A, S46D, or ΔSP mutants did not induce apoptosis *in vivo* (Figure 3.3 and Ilkow *et al.*, 2011), I reasoned that only "soluble" capsid constructs that lacked phosphorylation would exhibit the pro-apoptotic activity seen with recombinant capsid *in vitro*.

Using assays identical to those seen in Figure 3.3, A549 cells were transduced with the above-mentioned capsid mutants and apoptosis was induced with αFAS. All capsid truncation mutants showed a significant reduction in anti-apoptotic activity (Figure 3.8), with the S46AΔSP mutant being the least protective. This reduction in anti-apoptotic activity was not due to instability of the mutant capsid as it has been reported by this laboratory that removal of the E2 signal peptide does not significantly affect the stability of capsid (Law *et al.*, 2001). These data indicate that indeed membrane association and phosphorylation are both important for the ability of capsid to protect cells from apoptotic stimuli. Notably, none of the capsid mutants tested induced apoptosis, suggesting that loss of membrane association and phosphorylation are not sufficient to produce the pro-apoptotic effects of recombinant capsid *in vitro*.

3.2.8 Subcellular localization of capsid mutants

Earlier studies from this laboratory established that loss of the membrane association domain (E2 SP) affects the localization of capsid

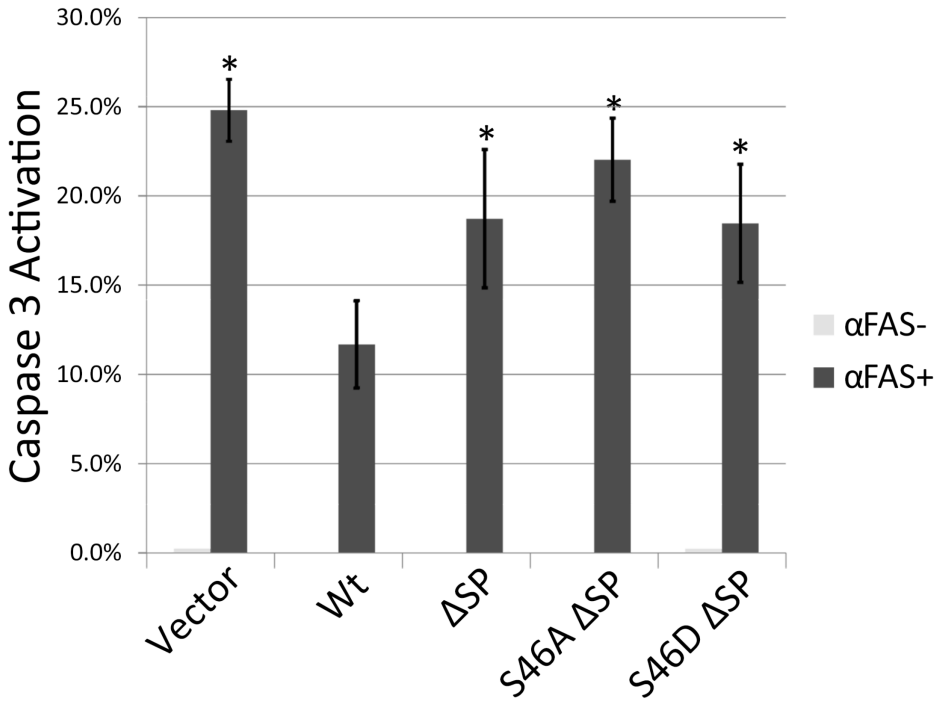

Figure 3.8 Membrane association is important for the anti-apoptotic activity of capsid. A549 cells were transduced (MOT = 2) with lentivirus expressing the given capsid constructs or AcGFP alone. Apoptosis was induced two days later for 24 hours with αFAS (0.25μg/mL) and cycloheximide (1μg/mL). Apoptosis was assayed via immunofluorescence with an antibody directed towards active caspase 3. All error bars indicate standard error from four independent experiments. Asterisks denote a statistically significant difference from wild type capsid ($p<0.05$) as determined by Student's t-test.

(Law *et al.*, 2001, Ilkow *et al.*, 2011). I next investigated whether loss of phosphorylation influences the subcellular localization of capsid. The rationale for these experiments is that a change in localization could affect the pool of host proteins that a particular capsid mutant is exposed to, and may therefore shed light onto why some mutants are less protective against apoptosis. A549 cells were transfected with the different capsid constructs and localization was determined using a monoclonal antibody to the N-terminus of capsid. ER and mitochondria were detected using an antibody to calnexin and Mitotracker, respectively. While a large pool of capsid has previously been shown to localize to the mitochondria in Vero cells (Beatch *et al.*, 2000), it exhibits a much more diffuse localization in A549 cells with less apparent mitochondrial association (Figure 3.9). The phosphomutants S46A and S46D exhibited a similar distribution, suggesting that changes to phosphorylation alone do not dramatically affect localization. However, compared to wild type capsid, it did appear that a larger pool of the phosphomutants were associated with mitochondria. Moreover, the mitochondria-associated cohort had a more punctate appearance. Similar punctae were occasionally observed in cells expressing wild type capsid, but they were more common in the cells expressing S46A or S46D, particularly the former. Notably, both the S46A and S46D mutants appeared to have reduced mitochondrial clustering, although this too was highly heterogeneous and was not quantified.

Figure 3.9 Subcellular localization of capsid mutants. A549 cells were transfected with indicated pCMV5-capsid construct or eGFP as a control. Two days after transfection, cells were treated with Mitotracker and processed for indirect immunofluorescence. ER was labeled with an antibody towards calnexin and capsid was labeled with a monoclonal mouse antibody. Scale bar represents a length of eight micrometers.

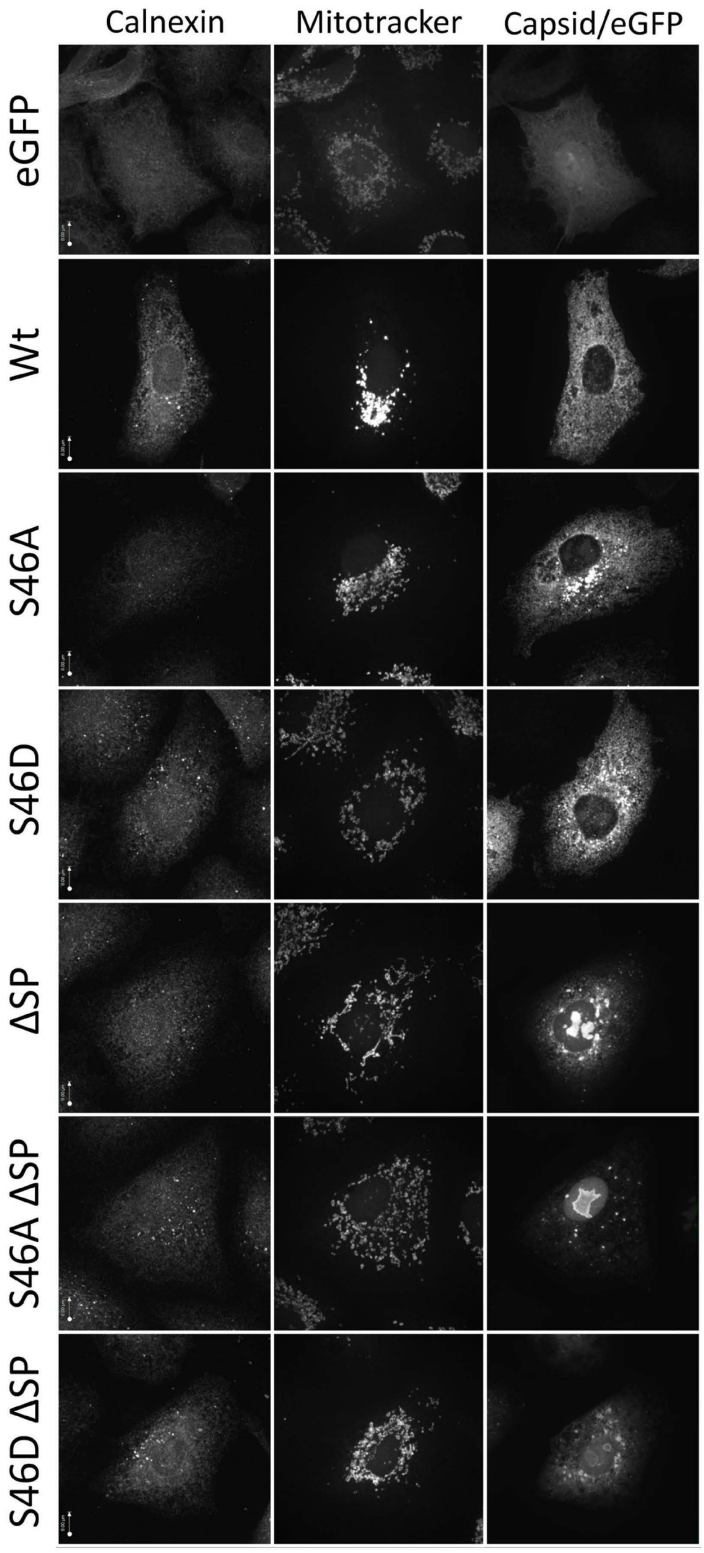
Calnexin
Mitotracker
Capsid/eGFP
eGFP
Wt
S46A
S46D
ΔSP
S46A ΔSP
S46D ΔSP

Loss of membrane association had a much more dramatic affect on capsid localization. All of the ΔSP capsid mutants localized to large cytoplasmic clusters and nuclei and/or nucleoli. The S46A/ΔSP was localized almost entirely to these regions, whereas a larger portion of ΔSP and S46D/ΔSP were detected in the cytoplasm. Notably, none of these constructs induced clustering of mitochondria as was seen in cells expressing wild type capsid. This suggests that membrane association of capsid is important for this process. Together, these data show that membrane association of capsid and, to a lesser extent, its phosphorylation state are important for localization.

3.2.9 Membrane association is important to prevent capsid from accumulating in RNA rich regions of the cell that have no obvious role in virus replication or assembly

Given that some capsid mutants localize to RNA-rich regions of the nucleus (nucleoli), I next investigated whether these mutants also accumulate in RNA-rich granules in the cytoplasm. The rationale for these experiments is as follows: First, capsid is highly positively charged and binds to RNA, a process that is negatively regulated by phosphorylation. As such, loss of phosphorylation may allow capsid to promiscuously localize to structures rich in cellular RNAs. Second, truncation mutants of capsid localized to subnuclear structures, likely nucleoli which are the primary sites of ribosome synthesis (see Pederson, 2011 for a

historical review). When not anchored to membranes, capsid may freely diffuse to these sites only to become sequestered through interaction with the high concentrations of ribosomal RNA. In the cytoplasm, processing bodies (P-bodies) are cytoplasmic granules that function in various aspects of RNA metabolism including mRNA repression and degradation (reviewed in Erickson *et al.*, 2011). Because P-bodies are dense RNA-rich structures it is possible that they could sequester unanchored capsid proteins through RNA-protein interaction. To study this, immunofluorescence assays were used to examine the distributions of the capsid mutants relative to the P-body marker decapping protein 1 (DCP1) (Erickson *et al.*, 2011).

Very little if any of the membrane-anchored wild type and S46D capsid localized to DCP1-positive punctae (Figure 3.10), however some S46A overlapped with P-bodies (Figure 3.10 arrowheads). In contrast, the capsid mutants lacking the membrane anchor domain (ΔSP, S46A-ΔSP and S46D-ΔSP) showed extensive localization to DCP1-positive structures in the cytoplasm (Figure 3.10 arrowheads). As best illustrated in the S46A-ΔSP sample, these structures were often very large and misshapen, an atypical morphology for P-bodies. In some cells expressing S46A, S46AΔSP and S46DΔSP mutants, DCP1 staining was inexplicably dim or absent. Whether this was due to expression of these mutants

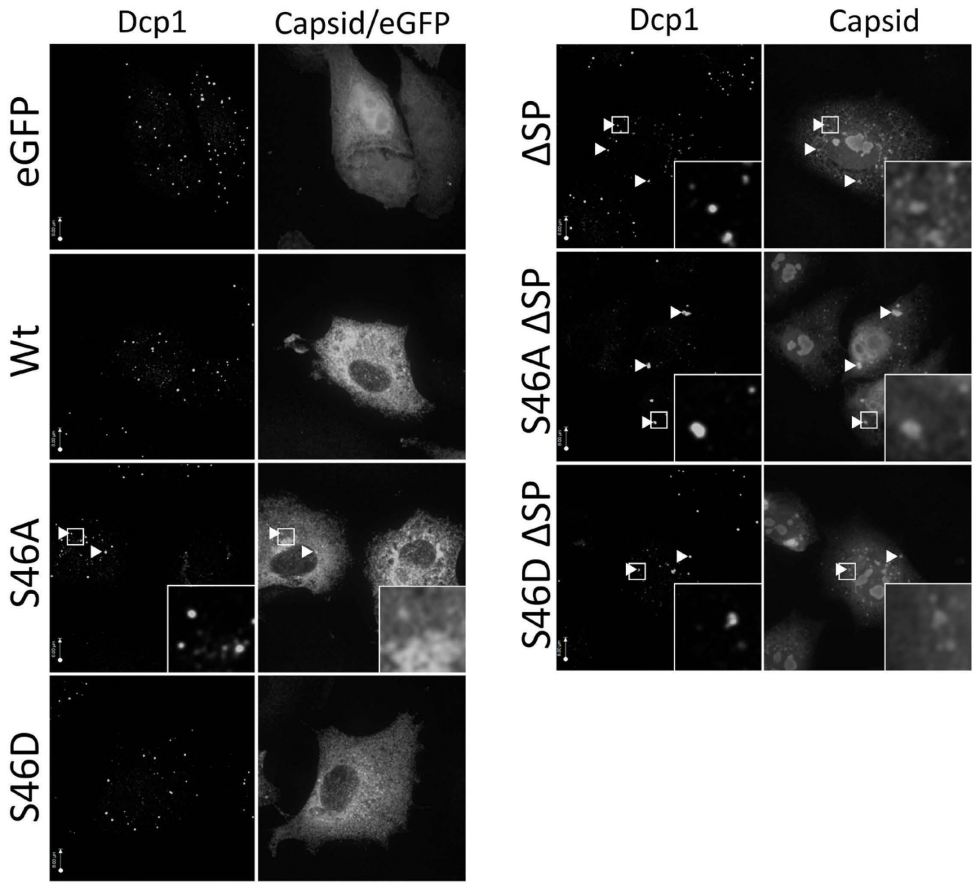

Figure 3.10 Capsid membrane truncation mutants localize to areas of high RNA content. A549 cells were transfected with indicated pCMV5-capsid construct or eGFP as a control. Two days after transfection, cells were processed for indirect immunofluorescence using a mouse monoclonal antibody to detect capsid and a rabbit antibody towards DCP1 to detect P-bodies. Arrowheads indicate punctae positive for both capsid and DCP1. White rectangles represent area enlarged fivefold in inset. Scale bar represents a length of eight micrometers.

or simply due to heterogeneity of DCP1 structures in different cells is not known. Together, these data support the idea that phosphorylation and membrane association of capsid are important for reducing promiscuous and presumably non-productive interaction of RV capsid with RNA-rich structures in host cells.

3.3 Summary

Previous studies have shown that RV capsid inhibits apoptosis through its interaction with the pro-apoptotic protein Bax. While this interaction has been thoroughly characterized, the actual mechanism by which capsid blocks Bax-mediated pore formation is still unknown. Unexpectedly, addition of recombinant capsid produced in bacteria to isolated mitochondria resulted in pro-apoptotic effects. Since this recombinant capsid lacked both membrane association and phosphorylation, I investigated the role of these two properties on capsid's anti-apoptotic ability. Alterations to the phosphorylated residue serine 46 caused a reduction in apoptotic protection from this protein. The lack of protection from apoptosis was even more apparent in the context of infection, as these capsid mutants showed no protection from the apoptotic stimulus poly(I:C) nor were recombinant viruses harboring these mutations resistant to apoptosis. The reduction in anti-apoptotic activity was unlikely to be due to loss of Bax binding, as both mutants co-precipitated with Bax to a similar or greater extent than wild type capsid. However, since immunoprecipitations

were performed using lysates from transfected cells (as opposed to transduced cells), I could not rule out the possibility that these mutants do not bind Bax when expressed at lower levels. Further investigation revealed that when expressed at very high levels, the mutant capsid proteins were able to protect cells from αFAS induced apoptosis. Membrane association was also important for anti-apoptotic activity, as deletion of the E2 signal peptide resulted in loss of anti-apoptotic activity, an effect that was even more pronounced when combined with lack of phosphorylation. Membrane association of capsid was found to be important for its subcellular localization, as the ΔSP mutants all localized to the nucleus/nucleolus and cytoplasmic granules, which further testing revealed to be P-bodies. For these reasons I propose that membrane association and phosphorylation prevent capsid from being sequestered to locations in the cell with high RNA content. This would ensure capsid is concentrated at other locations where it could fulfill non-structural and structural roles.

CHAPTER 4
A PP1 binding motif in capsid is important for viral replication

4.1 Rationale and hypothesis

Work in our lab and others identified several RV capsid interacting proteins. Although a handful have been explored in depth, most capsid:host protein interactions remain unstudied. I decided to focus on a novel capsid-binding protein identified in a large scale co-immunoprecipitation (Dr. Carolina Ilkow, unpublished): the alpha isoform of protein phosphatase I (PP1). For several reasons, PP1 is of significant interest to justify further study. First, capsid contains a putative PP1-binding site in the R-region near the C-terminus (Figure 4.1). A mutant (CR5A) containing several arginine to alanine mutations in this region has reduced anti-apoptotic activity and an RV strain with these mutations incorporated into the capsid gene has severe replication defects (Ilkow *et al.*, 2011). Two of these arginines are within the PP1 binding motif, and as such the CR5A mutant phenotype may be caused by disruption of capsid's interaction with PP1. Indeed, this mutant binds and activates Bax similar to wild type, suggesting a Bax-independent mechanism may be involved. Second, PP1 was previously shown to have pro-apoptotic activity (Danial *et al.*, 2003), so the interaction between capsid and PP1 may play a role in capsid's anti-apoptotic function. As already discussed in section 1.2.3, a truncation mutant containing only the capsid C-terminus confers significant apoptotic protection, but does not bind Bax, suggesting a Bax independent capsid anti-apoptotic mechanism. Since the putative PP1 binding site is in capsid's C-terminus, interaction with PP1 may

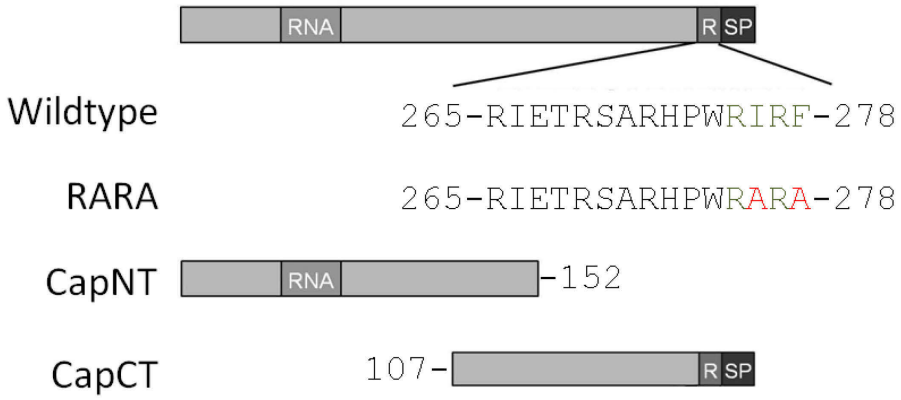

Figure 4.1 Capsid mutants used in this chapter. The capsid RARA mutant contains two mutations in the RVXF motif located in the C-terminal R-region. Mutations at these positions within the RVXF are known to disrupt binding to PP1 when introduced in other PP1 interacting proteins. The CapNT construct encodes amino acids 1-152 of wild type capsid. The CapCT construct encodes amino acids 107-300. Adapted from Ilkow *et al* 2011.

be important for the Bax-independent anti-apoptotic activity of this viral protein. After confirming the interaction between capsid and PP1 using different assays, I investigated whether interaction between capsid and PP1 affected apoptosis and/or viral replication.

4.2 Results

4.2.1 Capsid binds to PP1

To confirm the interaction between capsid and PP1, reciprocal pulldowns were conducted. First, capsid from transfected HEK293T lysates was immunoprecipitated with a rabbit polyclonal capsid antibody and immune complexes were subjected to SDS-PAGE and immunoblotting with a PP1α specific antibody. It was found that endogenous PP1 co-precipitated with capsid (Figure 4.2 A). The reciprocal pulldown used microcystin-Sepharose (MC-Sepharose) to precipitate PP1. Microcystins are a group of cyanobacterial toxins that potently inhibit both PP1 and PP2A (Dawson *et al.*, 1999). These cyclic heptapeptides bind very strongly to the catalytic center of PP1 (Goldberg *et al.*, 1995), but do not disrupt RVXF motif-dependent interactions. Sepharose beads crosslinked to this toxin were provided by Dr. Charles Holmes (University of Alberta, Canada). Capsid transfected HEK293T lysates were incubated with MC-Sepharose and after washing proteins were eluted and analyzed by SDS-PAGE. Capsid co-precipitated with PP1 (Figure 4.2 B), and when lysates were

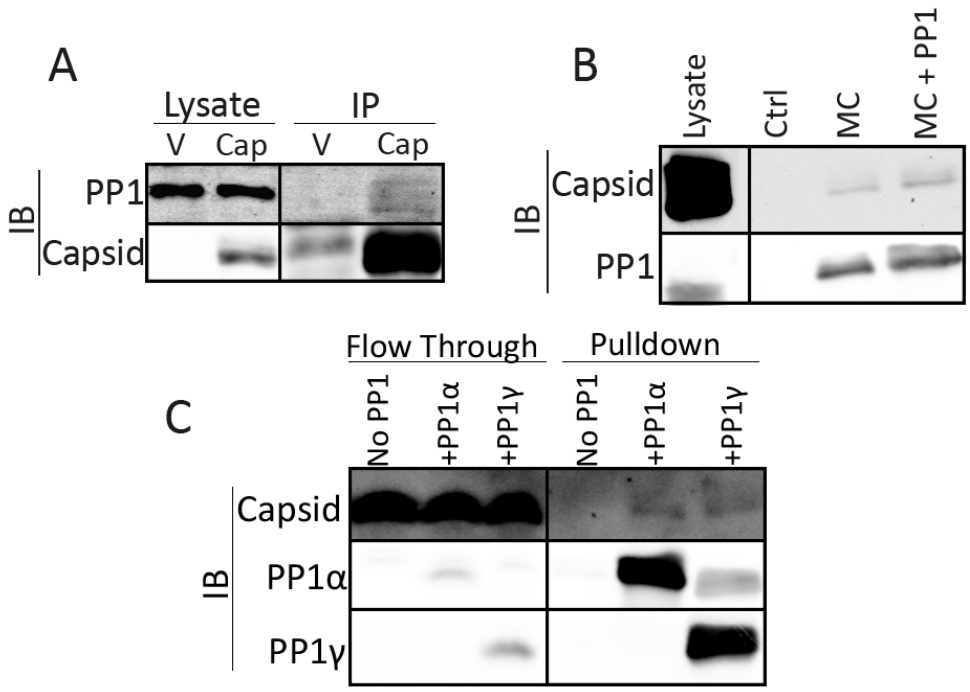

Figure 4.2 Capsid binds to PP1α. (A) HEK293T cells were transfected with pCMV5 or pCMV5-capsid. Two days later, cells were lysed and immunoprecipitated (IP) with a rabbit antibody to capsid and protein A Sepharose beads. Bound proteins were analyzed by SDS-PAGE and Immunoblotting (IB). (B) Transfected HEK293T cell lysates were incubated with MC-Sepharose beads or beads alone as a control. Where indicated, MC-Sepharose beads were pre-incubated with purified PP1α. Bound proteins were analyzed by SDS-PAGE and immunoblotting. (C) Capsid synthesized in vitro was combined with MC-Sepharose beads pre-bound to PP1α or PP1γ. After overnight incubation beads were washed and proteins were eluted then subjected to SDS-PAGE and immunoblotting.

supplemented with exogenous PP1α (provided by Charles Holmes, University of Alberta, Canada) even more capsid was recovered. This suggested that capsid specifically interacts with PP1α. Binding was further confirmed using isolated PP1 and capsid. Capsid was produced *in vitro* from the pcDNA3.1 Capsid myc/His plasmid using an *in vitro* transcription/translation system. After binding to PP1α or PP1γ, MC-Sepharose beads were incubated with capsid overnight, washed and proteins were eluted and analyzed by SDS-PAGE. Both PP1α and PP1γ co-precipitated capsid indicating that capsid interaction was not specific to PP1α, which was the only isoform identified in the initial pulldown.

4.2.2 Neither the N- nor C-terminus of capsid is sufficient for PP1 binding

Since the putative PP1 binding region is in the C-terminus of capsid, I next assessed whether the C-terminus alone was sufficient to bind PP1. I transfected HEK293T cells with pCMV5 capsid, pCMV5-capsid-CT, or pCMV5-capsid-NT and the lysates from these cells were subjected to an MC-Sepharose pulldown as described above. Neither the capsid C- nor the N-terminus alone was sufficient for PP1 pulldown, and only full-length capsid co-precipitated with PP1 (Figure 4.3).

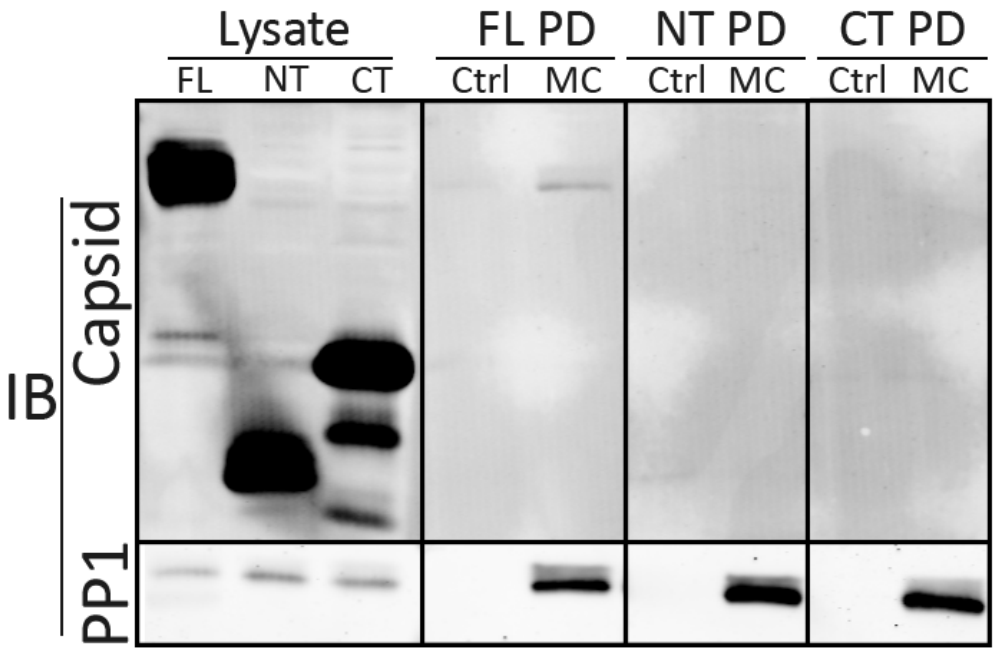

Figure 4.3 Neither the N- nor C-termini of capsid are sufficient for PP1 binding. HEK293T cells were transfected with pCMV5-capsid (FL), pCMV5-capsid-NT (NT), or pCMV5-capsid-CT (CT) and lysed two days later. Lysates were then incubated with MC-Sepharose beads (MC) or beads alone (Ctrl) as a control. After incubation, beads were washed and proteins were eluted by boiling in Protein sample buffer. Pulldowns (PD) and lysates (1.7% volume) were then subjected to SDS-PAGE and immunoblotting.

4.2.3 Capsid expression does not alter localization of PP1

I next investigated whether capsid and PP1 localize to the same intracellular compartments in transfected cells. Although PP1 and capsid interact in pulldown assays, the relevance of this interaction is questionable if capsid cannot access PP1 *in vivo.* Capsid expression is known to alter the subcellular localization of several of its binding partners including PABP, Bax, and p32 (Beatch *et al.*, 2005, Ilkow *et al.*, 2008, Ilkow *et al.*, 2011). Relocalization of PP1 in capsid expressing cells would not only provide additional evidence that these proteins interact, but may also shed light onto how capsid could affect the function of PP1. pCMV5-capsid, pEYFP PP1α, or both plasmids together were transfected into A549 cells and two days later immunofluorescence was conducted using a mouse monoclonal antibody to capsid and EYFP fluorescence to visualize PP1. YFP-PP1 was localized primarily to the nucleus in cells, although a small pool was present in the cytoplasm (Figure 4.4). When expressed at high concentrations, more YFP-PP1 was detected in the cytoplasm as large punctae or membranous structures. Capsid exhibited a diffuse distribution in the cytoplasm with occasional perinuclear punctae. When expressed together, both proteins exhibited similar distribution but, unlike other capsid-binding partners, capsid expression did not dramatically alter the localization PP1. Overlap between capsid and PP1 was modest (Pearson's coefficient r=0.456), and increased when PP1 was expressed

Figure 4.4 Capsid expression does not significantly alter the localization of PP1α. A549 cells were transfected with pCMV5-capsid, pEYFP-PP1, or co-transfected with both plasmids. Two days after transfection, cells were processed for indirect immunofluorescence. A mouse monoclonal antibody was used to visualize capsid and YFP fluorescence was used to visualize PP1. Pearson's coefficients for YFP and capsid are indicated in lower right hand corner of composite images.

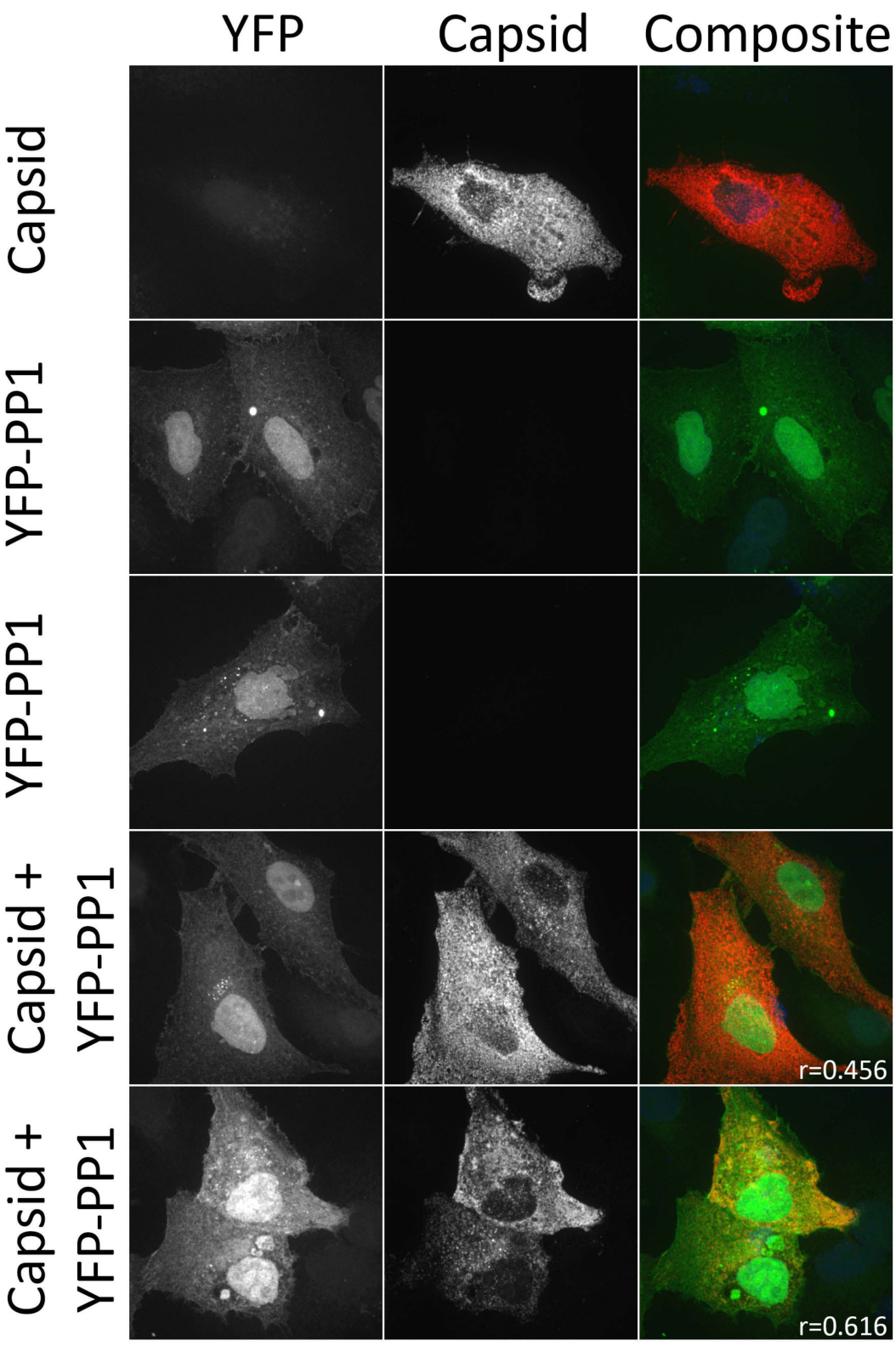
YFP
Capsid
Composite
Capsid
YFP-PP1
YFP-PP1
Capsid +
YFP-PP1
Capsid +
YFP-PP1
r=0.456
r=0.616

at higher levels (Pearson's coefficient r=0.616).

4.2.4 The capsid RARA mutant is deficient in anti-apoptotic activity

In order to understand the significance of the capsid:PP1 interaction, I next sought to disrupt complex formation between these two proteins. To do this, I constructed a capsid mutant where two residues in the putative PP1 binding site were changed to alanines (Figure 4.1). The Valine/Isoleucine and Phenylalanine/Tryptophan residues in the RVXF motif are critical for PP1 binding, and mutation of these residues to alanines has been used before to disrupt PP1 binding to other interactors (Trinkle-Mulcahy *et al.*, 1999, Llorian *et al.*, 2004). These mutations were incorporated into a synthetic DNA construct which was then used to make three the expression plasmids pCMV5-capsid-RARA, pCMV5-24S-RARA and pBRM33-RARA.

Since PP1 plays a role in apoptosis by dephosphorylating the pro-apoptotic BH3-only protein Bad, I first investigated the effect of the RARA mutation on capsid's anti-apoptotic activity. To do this, A549 cells were transfected with pCMV5-capsid wild type, pCMV5-capsid RARA, pCMV5-CR5A or pEGFP as a control. After two days, cells were treated with anti-FAS and cycloheximide and apoptosis was measured via indirect immunofluorescence with an antibody against active caspase 3. While expression of wild type capsid reduced apoptosis by nearly

50%, RARA mutant expression did not provide any protection from anti-FAS (Figure 4.5). This result matches the previously characterized capsid R-region mutant CR5A, which also had no measurable anti-apoptotic activity. In fact, expression of RARA or CR5A mutants induced significant apoptosis in cells that were not treated with anti-FAS (Fig. 4.5).

4.2.5 The capsid RARA mutant exhibits an unusual subcellular localization

During previous experiments, I noticed that the RARA mutant had a different localization than wild type capsid. Since capsid's localization is important for its structural and non-structural functions, I next determined the subcellular distribution of the RARA mutant. After transfecting A549 cells, capsid was visualized with a rabbit polyclonal antibody and mitochondria were visualized with an antibody specific for heat shock protein 60 (HSP60), a mitochondrial matrix protein. Mitochondria were chosen as a marker for subcellular distribution because many of capsid's binding partners localize to this organelle. RARA localization was dramatically different from wild type capsid, which showed a diffuse distribution with a small pool near the mitochondria (Figure 4.6). In cells expressing the RARA mutant, the majority of capsid was present near the mitochondria, although a diffuse cytoplasmic/ER localization was often seen. At low expression levels, the RARA mutant localized primarily to small punctae on mitochondria. At higher expression levels, it instead formed a

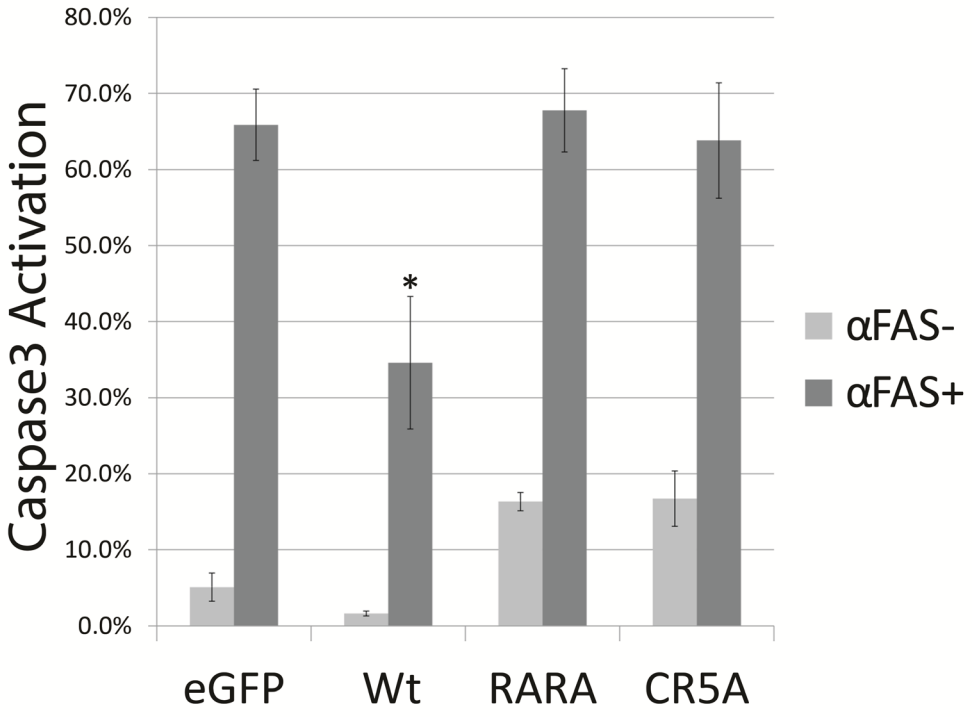

Figure 4.5 Capsid RARA mutant does not protect from apoptosis. A549 cells were transfected with indicated pCMV5-capsid constructs or pEGFP. Two days later, apoptosis was induced with αFAS (0.25μg/mL) and cycloheximide (1μg/mL) for six hours. Apoptosis was assayed via immunofluorescence with an antibody directed towards active caspase 3. All error bars indicate standard error from three independent experiments. Asterisk indicates a statistically significant difference from αFAS treated, EGFP transfected cells as determined by Tukey's HSD test.

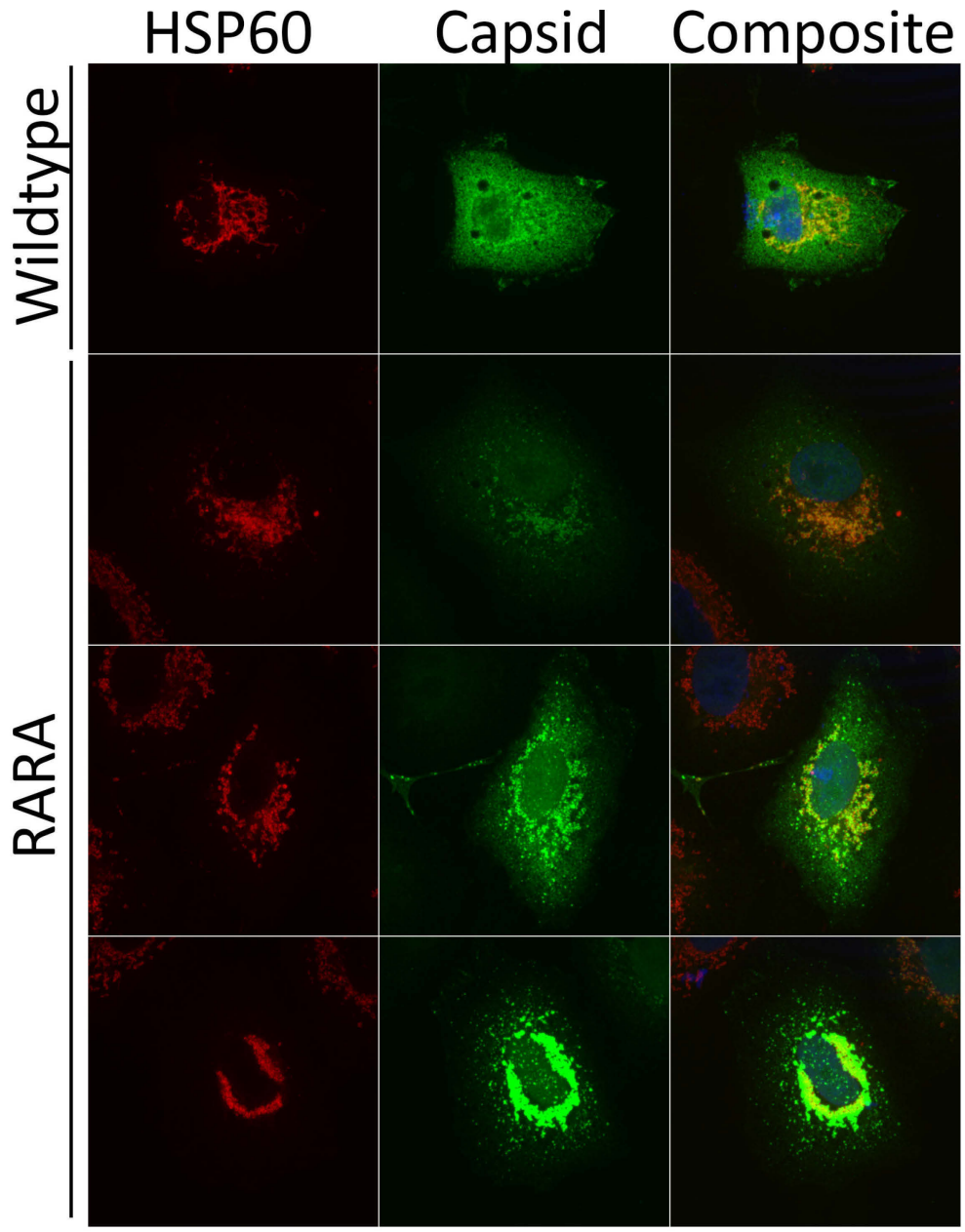

Figure 4.6 Capsid RARA exhibits altered localization compared to wild type. A549 cells were transfected with pCMV5-capsid or pCMV5-capsid-RARA. Two days later, an indirect immunofluorescence was conducted with a rabbit polyclonal antibody to capsid and a mouse antibody to HSP60 to visualize the mitochondrial matrix.

continuous cluster both at and between mitochondria and at very high levels, these clusters were dense and compacted near the nucleus. Mitochondria were also highly clustered under these conditions, showing that the RARA mutant exhibits exaggerated mitochondrial clustering compared to wild type capsid.

The nature of the RARA capsid:mitochondria clusters in transfected cells was not clear, as they were not sufficiently resolved by confocal microscopy. Therefore, I elected to use structured illumination microscopy (SIM) (Coltharp *et al.*, 2012) to examine these structures at higher resolution. SIM uses interference produced from overlaying known illumination patterns over fluorescent samples to produce images with up to twice the resolution of conventional microscopes in all dimensions, which corresponds to an eightfold improvement in volume resolution. SIM images were produced from A549 cells transfected with pCMV5-capsid and pCMV5-capsid-RARA. Wild type capsid had a diffuse localization throughout the cell (Figure 4.7 A). It appeared as many small punctae and was most concentrated in the perinuclear region between apposing mitochondria (Figure 4.7 C). In contrast, the RARA mutant was largely concentrated in reticular structures around the nucleus (Figure 4.7 B & D). Small, spherical mitochondria were found both interlaced in these structures and free in the cytoplasm. Although the RARA mutant localized to, or at least contacts, the OMM, it was also present in places where mitochondria are absent. This implies that the RARA

Figure 4.7 Superresolution microscopy with the capsid RARA mutant. A549 cells were transfected with pCMV5-capsid (A and C) or pCMV5-capsid-RARA (B or C) and processed for indirect immunofluorescence two days later. A rabbit polyclonal antibody was used to visualize capsid (green) and a mouse antibody to HSP60 to visualize the mitochondrial matrix (red). Images are presented either as a single slice (A and B) or a 3D reconstruction (C and D).

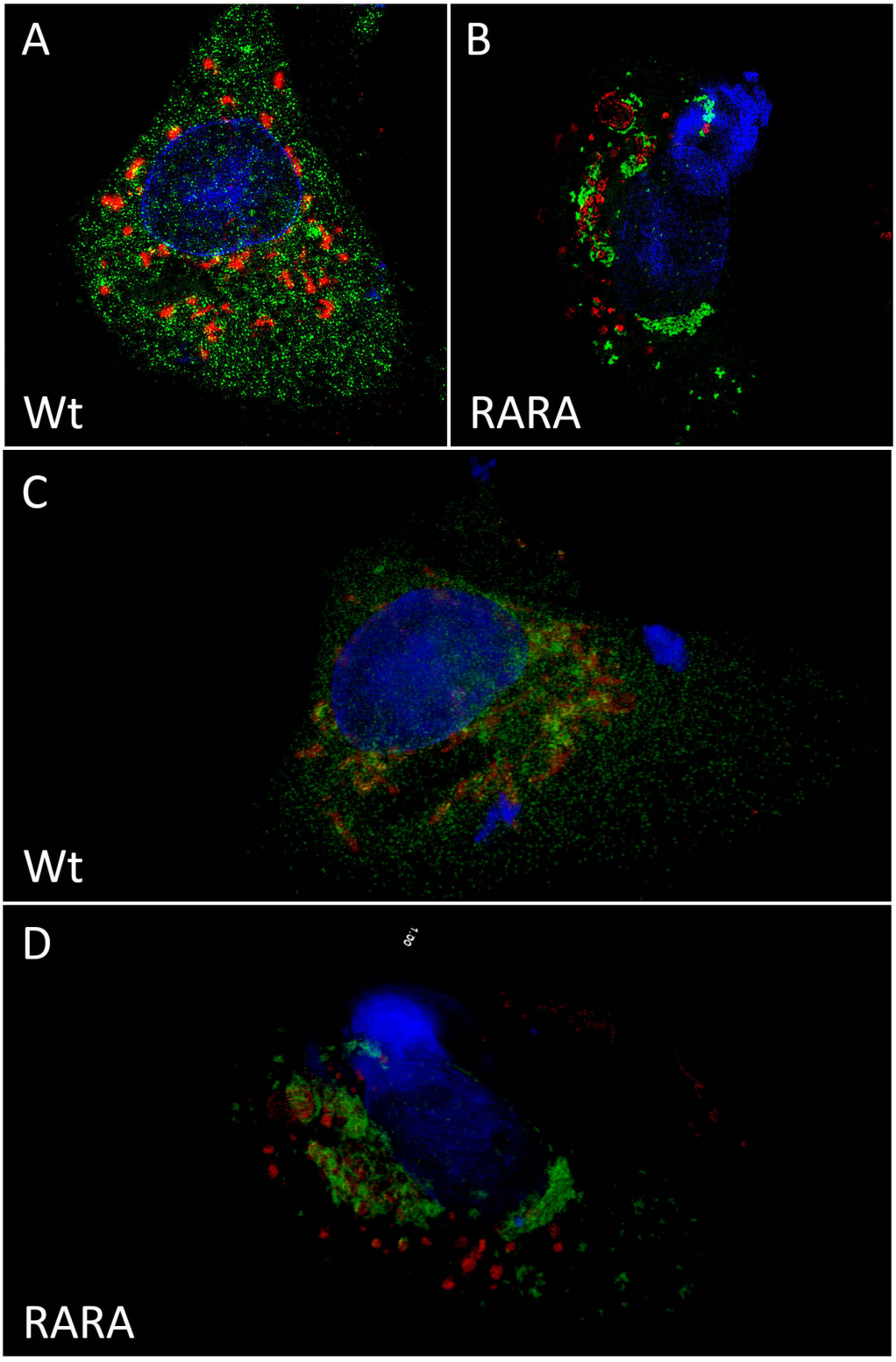
A
Wt
B
RARA
C
Wt
D
RARA

mutant is not simply targeted to the OMM but instead may be associated with other membranes that become closely apposed to mitochondria in capsid RARA expressing cells.

4.2.6 The RV RARA mutant has severe replication defects

Disrupting capsid's anti-apoptotic activity is known to affect viral replication (Ilkow *et al.*, 2011), so I next investigated replication of a RV strain with the RARA mutation incorporated into the capsid gene. Vero cells transfected with infectious RNA were incubated one, two or three days before media were collected and cells were lysed. Media were used to perform plaque and specific infectivity assays. At every time point, the specific activity of infectious RNA from wild type RV exceeded that of the RARA mutant strain by 1000 to 10 000 fold (Figure 4.8 A). Under most conditions, only a few plaques were evident in the lowest dilution (-1) of media from RARA infected cells. Similarly, viral protein production was drastically reduced in RARA mutant transfected cells (Figure 4.8 B). At two and three days post-transfection, p150 levels in cells transfected with the RARA mutant RNA were much lower than in wild type RV RNA transfected cells. Capsid was not detected at any time point in the RARA mutant transfected cells, despite its antigenicity and stability being similar to wild type (data not shown). It is unlikely that these differences were caused by variation in transfection efficiencies or viral replicase activity, as genomic RNA levels in wild

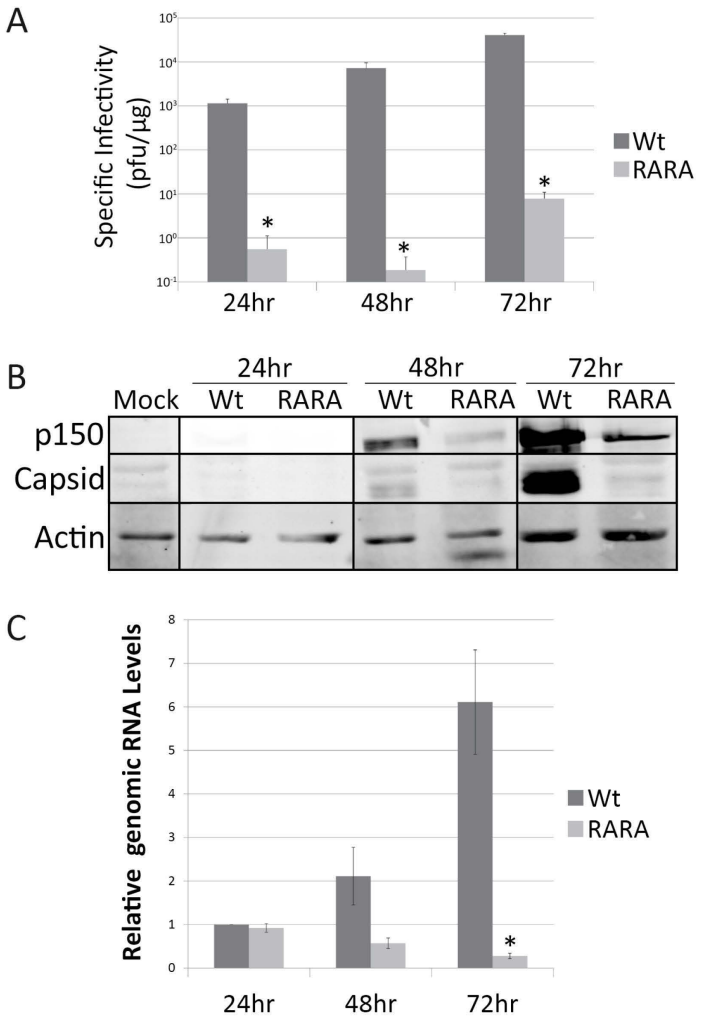

Figure 4.8 The RARA mutant virus exhibits severe replication defects. Vero cells were transfected with infectious RNA transcribed from pBRM33 or pBRM33-RARA. At indicated times after transfection, cells were lysed or media was collected. Viral titers were determined by plaque assay (A) and viral protein levels were measured by SDS-PAGE and immunoblotting (B). RNA was also extracted in cells transfected as in (A) & (B). (C) After extraction, RNA was reverse transcribed and relative genomic RNA levels were determined by qPCR. All error bars denote standard error from three independent experiments. Asterisks indicate a statistically significant difference ($p<0.05$) from wild type transfected cells at the same time point as determined by Student's t-test

type and RARA transfected cells were nearly identical at 24 hours post-transfection (Figure 4.8 C). However, at later time points, levels of wild type genomic RNA were much higher than RARA genomic RNA presumably due to more efficient replication. Together, these experiments show that the PP1-binding motif in the capsid protein is important for replication or another critical aspect of the virus life cycle.

4.2.7 The RARA mutation negatively affects virion formation/release

Given that the capsid RARA mutant does not inhibit apoptosis, I next explored the possibility that virus replication is impeded by the inability of this mutant to protect from virus-induced apoptosis in infected cells. After transfection with infectious RNA, Vero cells were incubated for two days and caspase 3 activation rates were assayed by indirect immunofluorescence. Compared to wild type virus, there were more apoptotic cells in the population transfected with the RARA mutant (Figure 4.9 A), however this was less than 5%. As such, it seems unlikely that increased apoptosis accounts for the severe reduction in replication of RARA mutant genomic RNA.

For several reasons, I next investigated whether the RARA mutation affected virion formation. First, mutations in capsid can affect its structural role, which could explain the decrease in viral titers. Second, the RARA mutation has a

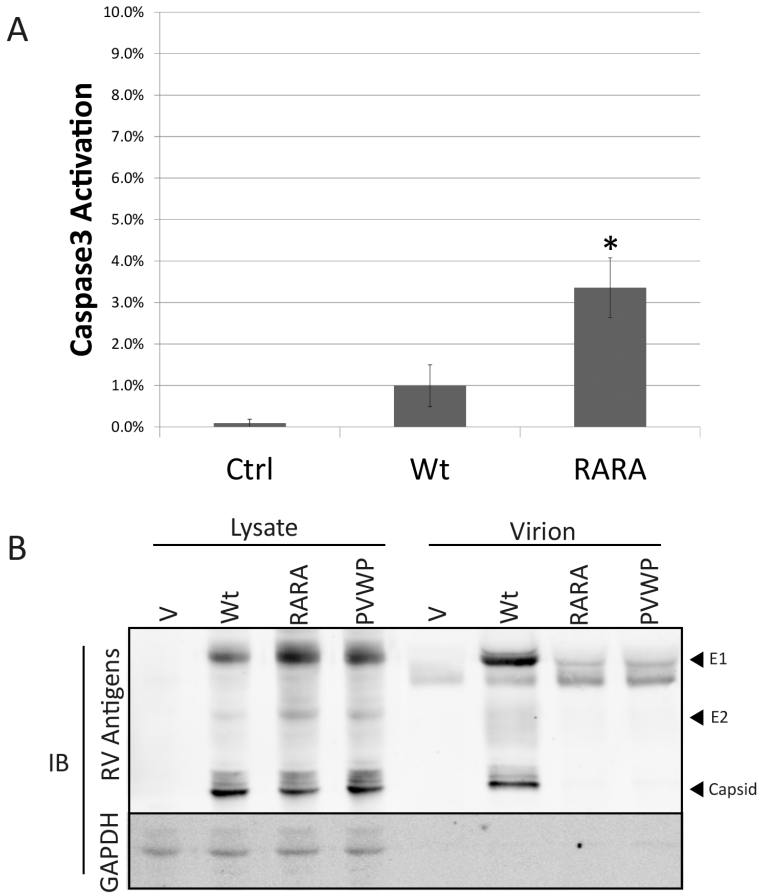

Figure 4.9 The effects of the RARA mutation on viral replication is due to defective virion formation. (A) Vero cells were transfected with infectious RNA transcribed in vitro from indicated pBRM33 plasmid. Xenopus elongation factor 1α RNA transcribed from the pTRI Xef plasmid was used as a control (Ctrl). Two days later, apoptosis was assayed via immunofluorescence with an antibody directed towards active caspase 3. All error bars indicate standard error from three independent experiments. Asterisk denotes a statistically significant difference ($p<0.05$) from control RNA transfected (Ctrl) as determined by Tukey's HSD test. (B) Vero cells were transfected with given pCMV5-24S construct or vector alone (V) and incubated two days. Media was then collected and virions were precipitated via ultracentrifugation. Levels of RV antigens from virions and cell lysates were determined by SDS-PAGE and immunoblotting.

severe effect on capsid localization, which may prevent capsid from accumulating at the Golgi where virion assembly takes place. Finally, capsid is a substrate for PP1 *in* vitro (Law *et al.*, 2003) and is dephosphorylated before being incorporated into virions (Law *et al.*, 2006). The RARA mutation may therefore affect dephosphorylation of capsid, which in turn may impair its ability to form virions. A surrogate assay for RV virion formation is based on the observation that the structural proteins are able to form VLPs in the absence of viral RNA (Hobman *et al.*, 1994, Qiu *et al.*, 1994). I utilized the pCMV5-24S-RARA plasmid to assay for defects in virion formation. Vero cells were transfected with pCMV5-24S, pCMV5-24S-RARA, pCMV5-24S-PVWP or pCMV5 alone and incubated for two days before media were collected and lysates were made. After preclearing, virions were pelleted by subjecting media to ultracentrifugation. VLP-containing pellets were resuspended in Protein sample buffer and analyzed by SDS-PAGE and immunoblotting. The pCMV5-24S-PVWP plasmid, which encodes a capsid unable to form virions due to point mutations in capsid-capsid contact regions (Mangala Prasad *et al.*, 2013), was used as a negative control for virion formation. While pCMV5-24S wild type, RARA, and PVWP constructs expressed comparable amounts of all structural proteins, only wild type was able to form VLPs (Figure 4.9 B). This suggests that the RARA mutation disrupts capsid's structural role in addition to its anti-apoptotic activity.

4.2.8 Wild type capsid, but not the RARA mutant, prevents activation of interferon-stimulated response element (ISRE)

Since apoptosis is only one of many processes PP1 is involved in, I next explored the possibility that capsid could affect other functions of PP1. One function of particular relevance to RV replication is activation of the RIG-I like receptors. After detection of viral RNA, these receptors must be dephosphorylated by PP1 in order for downstream signaling to occur (Wies *et al.*, 2013). If capsid inhibits or sequesters PP1 it may prevent dephosphorylation and inhibit the host innate immune response. A549 cells were transfected with pCMV5, pCMV5-capsid or pCMV5-capsid-RARA and two Luciferase reporter vectors: PGL3-ISRE-Luc and pRLTK. PGL3-ISRE-Luc expresses *Photinus pyralis* (firefly) Luciferase under the control of the ISRE: a short sequence located upstream of several ISGs that allows upregulation in response to interferon α/β (Cohen *et al.*, 1988, Levy *et al.*, 1988, Porter *et al.*, 1988, Rutherford *et al.*, 1988). pRLTK expresses *Renilla reniformis* luciferase from a constitutive promoter and acts as a control for transfection and basal expression. The day after transfection, ISRE was induced by transfecting cells with poly(I:C) or control DNA (pCMV5) and incubating for 18hrs. The activity of firefly luciferase was then measured, normalized to *Renilla* luciferase activity and the fold induction relative to non-induced, vector-transfected control was determined. Co-transfection of reporter plasmids with wild type capsid reduced induction of the ISRE by 50% (Figure 4.10 A). In

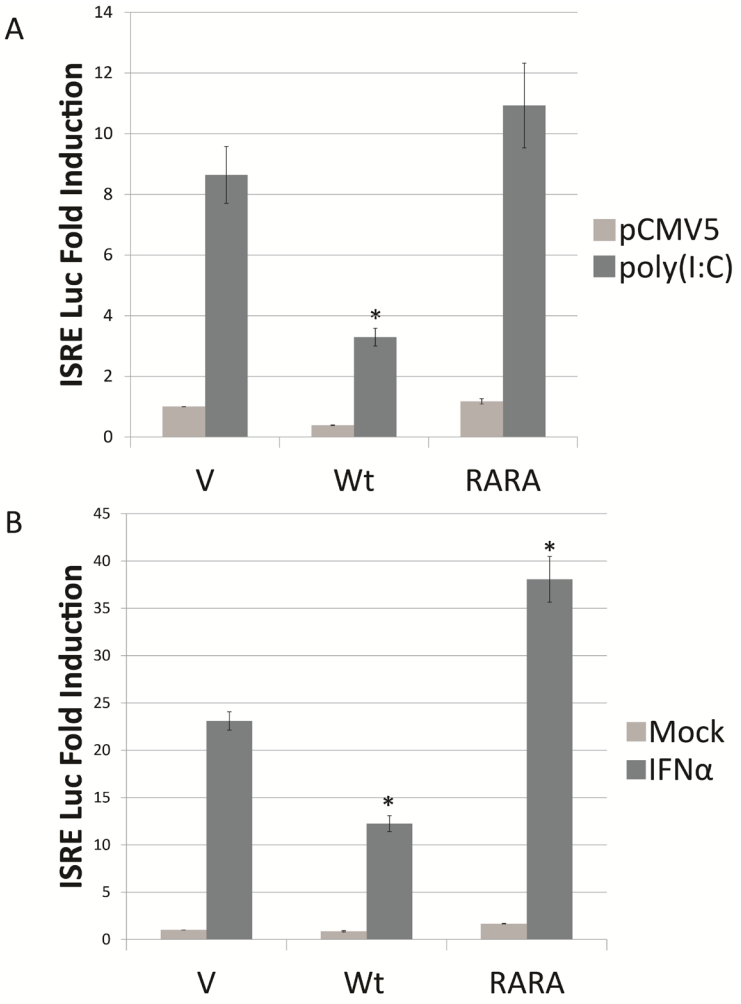

Figure 4.10 Capsid expression inhibits activation of the ISRE by poly(I:C) and interferon-α. A549 cells were co-transfected with indicated pCMV5-capsid construct or pCMV5 alone (V), PGL3-ISRE-Luc, and pRLTK. The next day, cells were either transfected with poly(I:C)/pCMV5 (2.5μg/mL) (A) or exposed to interferon-α (10U/mL) (B) and lysed after 18 hours. Luciferase activity was measured, normalized to pRLTK expression, and expressed as a fold increase compared to uninduced, vector transfected samples. Error bars denote standard error from three independent experiments. Asterisks indicate a statistically significant difference ($p<0.05$) from induced, vector transfected (V) as determined by Tukey's HSD test.

contrast, expression of the capsid RARA mutant increased ISRE induction slightly compared to vector expressing cells.

To identify what part of the interferon induction pathway capsid inhibits, the ability of capsid to protect from interferon-α induction of the ISRE was also assayed. Capsid inhibition of PP1 was not expected to affect this process, as PP1 acts on the RIG-I like receptors, which operate upstream of interferon. ISRE induction was measured using the same assay mentioned above, except instead of poly(I:C) transfection, interferon-α was added directly to media. Surprisingly, wild type capsid protected from interferon-α, reducing activation of the ISRE by almost 50% (Figure 4.10 B). Again, the capsid RARA mutant showed no protection and instead showed a nearly 50% increase in ISRE induction in response to interferon-α. Together, these data indicate that wild type capsid, but not the RARA mutant reduce activation from the innate immune response. Furthermore, inhibition occurs downstream of interferon rather than at activation of RIG-I like receptors.

4.3 Summary

While several interactions between RV capsid and host proteins have already been characterized, many intriguing capsid-host protein complexes have not been thoroughly characterized, including the capsid-PP1 interaction. After

confirming binding between capsid and PP1, it was determined that both the N- and C-termini of capsid were necessary for stable interaction with PP1. A mutant version of capsid (RARA), in which the C-terminal PP1 binding site was disrupted, was constructed and although, due to technical difficulties (reduced extraction by non-ionic detergent and increased background during pull-downs), I was unable to determine whether this mutant was deficient in binding PP1, it was found to have profound effects on capsid's function. First, the RARA mutation eliminated the ability of capsid to protect from αFAS-induced apoptosis. Second, this mutation significantly affected localization, of capsid. Third, incorporation of the RARA mutation into a RV infectious clone resulted in severely reduced replication, likely by affecting the ability of capsid to support formation and/or release of nascent virions. Finally, whereas wild type capsid was found to block ISRE induction by poly(I:C) and interferon-α, the RARA mutant was unable to do so. For these reasons I propose that the PP1 binding site in capsid and, by extension, its interaction with this phosphatase is important for its localization and functions, both structural and non-structural.

CHAPTER 5
Discussion

5.1 Overview

Until relatively recently, viral capsid proteins were largely considered to have only structural roles in virion formation, egress and entry. However, it is now clear that these proteins are often multifunctional and are required for "non-structural" roles that are unrelated to virus assembly or entry. For the RV capsid protein, several non-structural roles have already been described, including modulation of viral genome replication (Chen *et al.*, 2004b), inhibition of translation (Ilkow *et al.*, 2008), interfering with mitochondrial import (Ilkow *et al.*, 2010a), and blocking apoptosis (Ilkow *et al.*, 2011). Given that apoptosis is a primary means by which multicellular organisms clear themselves of viral pathogens, it is not surprising that many viruses encode anti-apoptotic proteins. For RV, inhibition of apoptosis induced by the innate and adaptive immune responses is particularly important, because it has a long eclipse period and replicates slowly. As such, the virus must expand the window of time for viral replication as long as possible. While it has already been shown that RV capsid interferes with programmed cell death by binding the pro-apoptotic Bcl-2 family protein Bax, the underlying mechanism is still unclear. Moreover, evidence suggests that capsid can also block apoptosis through a Bax-independent pathway. In order to gain a more complete understanding of the mechanisms by which capsid inhibits apoptosis, I pursued two different avenues of investigation. First, I examined how phosphorylation and membrane association affect the

ability of capsid to modulate apoptosis. Then, I investigated the role of the host cell-encoded capsid binding protein PP1 in blocking cell death pathways.

5.1.1 Capsid phosphorylation and membrane association are important for its anti-apoptotic activity.

With few exceptions, the phosphorylation states of viral proteins are controlled by host kinases and phosphatases. One example is the vesicular stomatitis virus (VSV) phosphoprotein (P), an important component of the viral replicase. By modulating the phosphorylation state of the P protein, the virus is able to control the switch from transcription to replication. Phosphorylation of the P protein in the N-terminal region by casein kinase II promotes transcription of the viral genome (Barik *et al.*, 1992a, Gupta *et al.*, 1995). Conversely, phosphorylation in the C-terminal region by the VSV L protein is required for viral genome replication (Chattopadhyay *et al.*, 1987, Barik *et al.*, 1992b, Pattnaik *et al.*, 1997, Hwang *et al.*, 1999). The PB1-F2 protein of influenza A virus, an accessory protein that induces apoptosis through activation of the mPTP, is another example of a viral phospho-protein (Zamarin *et al.*, 2005). Phosphorylation of PB1-F2 by protein kinase C is necessary for its pro-apoptotic activity, and mutations that prevent phosphorylation of this protein significantly reduce apoptosis in infected cells (Mitzner *et al.*, 2009).

As with RV, many virus capsid proteins are phosphorylated, including HIV-1 (Cartier *et al.*, 1997), hepatitis B virus (HBV) (Deroubaix *et al.*, 2015), HCV (Lu *et al.*, 2002), and severe respiratory syndrome coronavirus (SARS-CoV) (Surjit *et al.*, 2005). Phosphorylation of these proteins is important for function, and can affect uncoating and genome release (Misumi *et al.*, 2010), oligomerization (Mondal *et al.*, 2015), trafficking (Lu *et al.*, 2002, Kock *et al.*, 2003, Surjit *et al.*, 2005) chaperone activity (Chu *et al.*, 2014), and RNA binding (Chen *et al.*, 2005, Cheong *et al.*, 2011).

Phosphorylation of RV capsid is known to affect its function in virus assembly; specifically, phosphorylation of serine and threonine residues in the RNA binding region reduces its affinity for genomic RNA (Law *et al.*, 2003). In this thesis research, I have shown that phosphorylation is also important for the anti-apoptotic activity of capsid. Surprisingly, mutation of serine 46 to an aspartate, which is expected to mimic the negative charge on a phosphoserine, decreased capsid's anti-apoptotic ability as much as a mutation to a non-phosphorylatable amino acid (alanine). While having aspartate at position 46 was sufficient to recruit the host kinase machinery to phosphorylate other amino acid residues in capsid, we cannot rule out the possibility that interactions with other cellular proteins are affected; particularly those required to block apoptosis. Indeed, there are cases where changing phosphoresidues to alanine or aspartate does

not fully mimic the unphosphorylated or phosphorylated states, respectively. For example, oligomerization of the influenza virus nucleocapsid *in vitro* fails to occur when either of the two phosphoserine residues are mutated to alanine or aspartate (Mondal *et al.*, 2015). Similarly, changes in phosphorylation of the Duck HBV capsid significantly affect the structure of nucleocapsids. When serine 245 in the capsid protein, which is normally phosphorylated, is changed to alanine or aspartate, resulting nucleocapsids can no longer protect viral nucleic acid from nucleases (Kock *et al.*, 2003). Finally, phosphorylation of multiple residues in the N-terminus prevent the RV capsid from binding genomic RNA; however when three of these residues are mutated to aspartate or alanine, the mutant capsids resemble non-phosphorylated capsid in that they bind RNA with high affinity (Law *et al.*, 2006).

Notably, whereas expression of capsid mutants S46A and S46D exhibited a modest level of protection from αFAS in transduced cells, they showed no protection from poly(I:C) or apoptosis induced by virus replication. Poly(I:C), which is thought to mimic dsRNA produced during virus replication, stimulates apoptosis via different upstream pathways than FAS activation and is a more physiologically relevant apoptotic stimulus than αFAS, at least early in infection. Unlike in lentivirus-transduced cells, infection with S46A or S46D RV strains did not protect cells from apoptosis induced by αFAS. Viral dsRNA produced during

replication likely triggers apoptotic pathways, which would further sensitize cells to other apoptotic stimuli such as αFAS. Because the S46A and S46D mutants cannot protect cells when apoptosis is induced by the innate immune response (dsRNA detection), they are in turn more sensitive to αFAS in infected cells than transduced cells, which do not endure the added apoptotic stress induced by dsRNA production.

Truncation of the membrane anchoring SP domain of capsid also impaired its anti-apoptotic activity and, when combined with loss of phosphorylation (i.e. S46A/ΔSP mutant), the lowest level of anti-apoptotic activity among capsid constructs was observed. This does not appear to be the result of a simple additive effect of these mutations, because a combination of SP truncation with the S46D mutation, which reduces the anti-apoptotic activity of capsid to a similar extent as S46A, protected as well as ΔSP. Instead, the low level of anti-apoptotic activity associated with S46A/ΔSP compared to ΔSP may be due to lower levels of free capsid in the cytoplasm in the former (see section 5.1.1.2). Although it was previously reported that deletion of the SP domain only caused a mild-reduction in apoptotic protection from αFAS (Ilkow *et al.*, 2011), those assays utilized transfection instead of transduction. Since transfection results in higher protein expression levels per cell, the ΔSP mutant may, similar to S46A

and S46D capsid, retain some anti-apoptotic activity that becomes evident at higher expression levels.

5.1.1.1 Effect of capsid phosphorylation on Bax binding

Phosphorylation has been shown to modulate the activities of several Bax binding proteins. For example, phosphorylation of the BH3-only protein Puma, which binds to and activates Bax, reduces its pro-apoptotic activity by decreasing its stability (Fricker *et al.*, 2010). Another Bax activating BH3-only protein, Bim, is also phosphorylated (Lei *et al.*, 2003, Putcha *et al.*, 2003). Phosphorylation of Bim prevents its sequestration by dynein and myosin V motor complexes, allowing it to target and activate Bax. Phosphorylation of the retinoblastoma protein (Rb) has also been reported to affect its interaction with Bax (Antonucci *et al.*, 2014). Dephosphorylation of Rb at residues 807/811 prevents stable interaction with Bax, resulting in increased apoptosis.

Unlike the proteins described above, loss of phosphorylation does not reduce binding of capsid to Bax. In fact, the S46A mutant co-immunoprecipitated with Bax at higher levels than wild type capsid, while the S46D mutant behaved similarly to wild type capsid. This observation rules out the simplest explanation for how capsid could inhibit Bax: that capsid binding to Bax occludes an intra/intermolecular interaction necessary for pore formation. Although capsid

S46A and S46D both bind Bax, the phosphoserine at residue 46 of wild type capsid may be positioned in a specific configuration in capsid:Bax oligomers that cannot be mimicked by an alanine or aspartate residue. There are at least three possibilities to account for how a phospho-serine at position 46 is required for blocking apoptosis: i) It blocks inter/intramolecular interactions at a site removed from the primary capsid:Bax binding surface; ii) It is positioned so as to induce a conformation in Bax or capsid that prevents pore formation; or iii) It is positioned so as to block the pore formed by oligomerized Bax. Ultimately, determining the crystal structure of the capsid:Bax oligomer would allow us to distinguish between these possibilities, although the third scenario could be tested using an *in vitro* assay where the ability of Bax to release a fluorescent dye from liposomes is measured (Antonsson *et al.*, 1997). If wild type capsid, but not S46A or S46D, prevents Bax-mediated dye release from liposomes, it would indicate that the phosphomutants are unable to block the Bax pore.

It is also possible that the lower anti-apoptotic activities of the capsid phosphomutants are unrelated to Bax inhibition. As previously mentioned, some capsid mutants that don't bind Bax are still able to protect from apoptosis (Ilkow *et al.*, 2011). Therefore, phosphorylation at serine 46 may instead affect a Bax-independent anti-apoptotic activity of capsid. This could be tested by

determining whether S46A or S46D can protect cells from apoptosis induced by Bax over-expression.

5.1.1.2 Importance of membrane association and phosphorylation on localization of capsid

The most likely reason for the reduced anti-apoptotic activity of the SP truncation mutants is that their localizations are different from wild type capsid (Figure 5.1). When not anchored to membranes, capsid localizes to structures with high RNA content: P-bodies and nuclei/nucleoli. Because capsid is an RNA binding protein, loss of the membrane anchor may allow non-productive sequestration of this viral protein at these locations by binding to host RNA. Even though phosphorylated capsid does not bind RNA strongly *in vitro* (Law *et al.*, 2003), it may retain a low level RNA binding activity that is sufficient to affect its localization *in vivo*. I hypothesize that when sequestered in RNA granules or the nucleus/nucleoi, the Capsid-ΔSP mutant is unable to access host factors necessary for the anti-apoptotic function of capsid. Two observations suggest that phosphorylation may also affect capsid's localization: the cytoplasmic pool of hypophosphorylated, soluble capsid mutant (S46A/ΔSP) is smaller than other truncation mutants and the membrane-associated S46A mutant showed limited overlap with P-bodies that was not observed in cells expressing wild type.

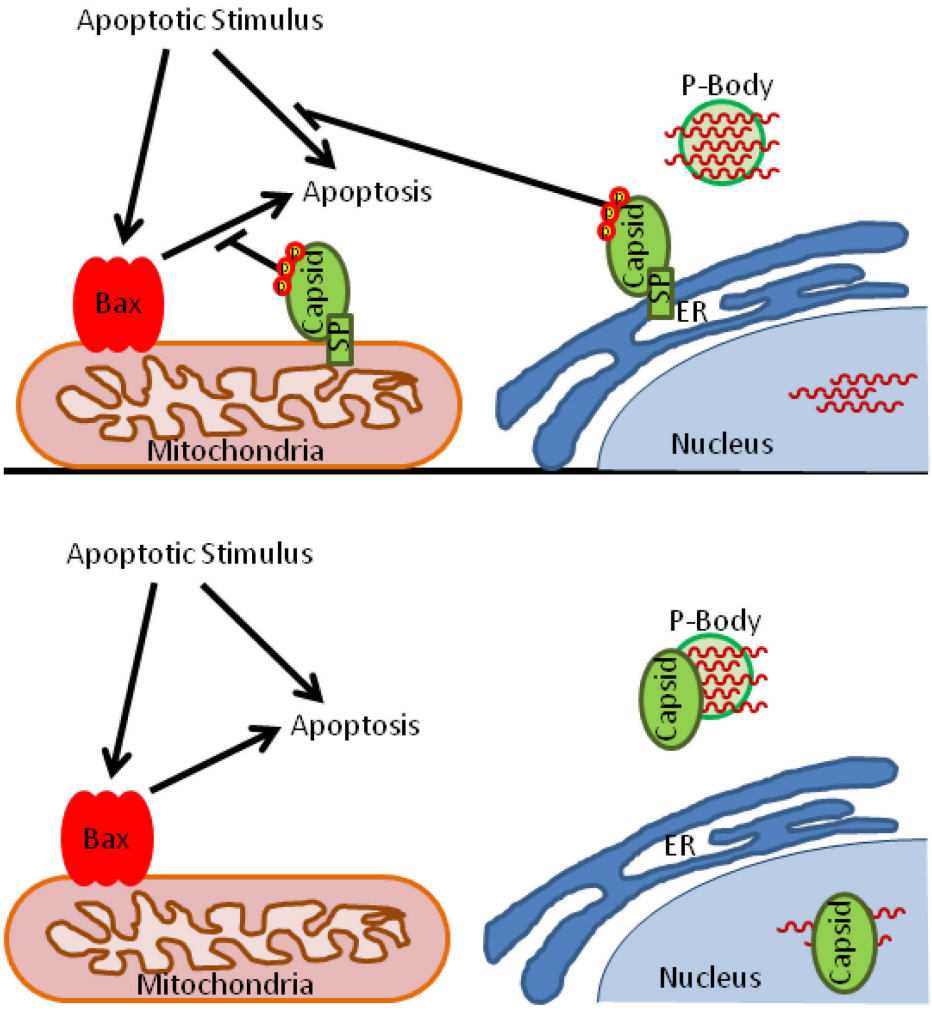

Figure 5.1 Model for how membrane association and phosphorylation affect the anti-apoptotic activity of capsid. Schematics of wild type capsid (Top) and hypo-phosphorylated capsid without the signal peptide (SP) (bottom) are shown. The SP and phosphorylation together prevent capsid from localizing to areas of the cell rich in RNA (curly red lines). The S46A/ΔSP mutant, which is both soluble and hypophosphorylated, localizes to P-bodies and the nucleus/nucleolus, preventing it from accessing factors necessary to inhibit apoptosis.

Membrane association is one feature that differentiates RV capsid from alphavirus capsids. Although most alphavirus capsids are soluble, the majority of these proteins are diffusely localized throughout the cytoplasm, although, in some cases, they have been reported to associate with cytoplasmic granules and the nucleus/nucleolus. One example is the Sindbis virus capsid, which associates with large cytoplasmic granules that contain Ras-GAP SH3 domain binding protein (G3BP), a stress granule marker (Zheng *et al.*, 2013). Localization of alphavirus capsids to the nuclei and nucleoli is an active process mediated by nuclear import sequences (Favre *et al.*, 1994, Atasheva *et al.*, 2010, Thomas *et al.*, 2013). Because it does not contain a known nuclear localization signal and is small enough to pass through nuclear pores, it is likely that anchorless RV capsid enters the nucleus by passive diffusion. RV and alphavirus capsids show little sequence similarity and it is possible that the latter evolved alternative mechanisms to limit sequestration of the capsid to RNA-rich regions of the cell.

The effect of phosphorylation on capsid localization is not unique to RV as trafficking of several other viral capsids between the nucleus and cytoplasm is reportedly controlled by phosphorylation. For example, phosphorylation of WNV capsid and influenza A virus nucleoprotein both affect nuclear/cytoplasmic shuttling by modulating binding to importin-α, a protein involved in nuclear

import (Bhuvanakantham *et al.*, 2010, Zheng *et al.*, 2015). Another example, the SARS-CoV nucleocapsid protein, is exported from the nucleus and retained in the cytoplasm by phosphorylation dependent binding to 14-3-3 proteins (Surjit *et al.*, 2005). Like RV, VSV utilizes phosphorylation to prevent interactions between capsid proteins and host RNAs (Chen *et al.*, 2013). Phosphorylation of the VSV phosphoprotein is necessary to prevent the nucleocapsid from binding host RNAs and forming nucleocapsid-like structures in the cytoplasm that interrupt this protein's mediation of viral genome transcription and replication.

5.1.2 Capsid interacts with the host protein PP1

Using reciprocal co-purification assays, I confirmed the interaction between capsid and PP1, first discovered in a large-scale pulldown experiment (Dr. Carolina Ilkow, unpublished data). A canonical PP1-binding site was identified in the C-terminus of capsid, however this region of capsid is not sufficient for binding to PP1. This situation is not unique as several other proteins that interact with PP1 employ two or more motifs to stably bind this phosphatase (Hurley *et al.*, 2007, Carmody *et al.*, 2008). Although capsid does not contain any other canonical PP1-binding motifs, new motifs that mediate interaction with PP1 are still being discovered and therefore it is possible that capsid contains an as yet unidentified PP1-binding motif in its N-terminus. Many PP1 interacting proteins contain large disordered regions that only adopt a stable conformation after

binding to PP1 (Bollen *et al.*, 2010, Choy *et al.*, 2012). These disordered regions allow large interaction surfaces to form between the protein and its binding partner, and their flexibility facilitates interaction with many different target proteins. As with other capsid proteins with highly basic N-termini (Rossmann *et al.*, 1989), the N-terminus of RV capsid is predicted to be highly disordered (Beatch *et al.*, 2005, IUPred unstructured protein prediction algorithm (http://iupred.enzim.hu/)). As such, it is possible that the capsid N-terminus binds to PP1 in a similar manner to other disordered regions that mediate interaction with this phosphatase.

The interaction between PP1 and capsid may not be stable, as only a small portion of capsid or PP1 co-purify in pulldown experiments. Furthermore, over-expression of YFP-PP1 or capsid does not noticeably affect the other's intracellular localization. However, given the large pool of PP1 inhibitors and targeting proteins within a cell, it is not necessarily surprising that only a small pool of PP1 is available to interact with capsid. Another potential explanation is that capsid's interaction with PP1 is transient and that only a small proportion of the total capsid pool interacts with PP1 at any one time.

A number of other viral proteins have been shown to interact with PP1 in a functional manner. Measles virus utilizes at least two different mechanisms to inhibit PP1 activity in order to dampen activation of the RIG-I like receptors. Early in infection, virions interact with the C-type lectin receptor DC-SIGN on dendritic cells. This activates a signaling cascade that leads to the incorporation of the PP1 inhibitor, I-1, into the PP1 holoenzyme complex, which normally dephosphorylates RIG-I like receptors (Mesman *et al.*, 2014). Binding of I-1 to the PP1 complex blocks dephosphorylation of these receptors, thereby preventing activation of the host innate immune system in response to detected viral RNA. The activation of DC-SIGN is only transient, though, and the measles virus V protein later inhibits activation of RIG-I like receptors (Davis *et al.*, 2014). V protein binds to PP1α and PP1γ through an RVXF motif, preventing their interaction with and dephosphorylation of RIG-I and MDA5. Other viral proteins bind PP1 to prevent eIF2α-mediated host translational shutdown in response to infection, including human papilloma virus type E6 oncoprotein (Kazemi *et al.*, 2004), herpes simplex virus ICP34.5 (Zhang *et al.*, 2008, Li *et al.*, 2011), pseudorabies virus IE180 (Van Opdenbosch *et al.*, 2012), and transmissible gastroenteritis virus gene 7 (Cruz *et al.*, 2011). Most of these viral proteins bind to PP1 holoenzyme complexes and target them to eIF2α, reversing the phosphorylation of this host protein thereby relieving translational inhibition. The HIV-1 Tat protein also binds to PP1 and targets it to the nucleus where it is

required for transcription of HIV-1 genes (Ammosova *et al.*, 2003). Tat is thought to activate transcription by using PP1 to alter phosphorylation of the RNA polymerase II C-terminal domain (CTD) directly or through dephosphorylation of the CTD kinase cyclin-dependent kinase-9 (Washington *et al.*, 2002, Ammosova *et al.*, 2005, Ammosova *et al.*, 2011). The interaction between the HBV protein X regulatory protein and PP1 is necessary to induce viral DNA transcription but not host gene transcription (Cougot *et al.*, 2012). By binding and inhibiting PP1, HBV protein X regulatory protein preserves phosphorylation of the transcription factor cyclic adenosine monophosphate response element-binding protein, thereby maintaining its interaction with co-activators and promoting transcription.

5.1.2.1 The RVXF motif in capsid is important for localization.

To understand the role of the PP1:capsid interaction in RV replication, I constructed a mutant (RARA) in which the PP1 binding site in the C-terminus was disrupted. Although I was not able to determine whether this mutation actually disrupted PP1 binding, I found it did have several effects on capsid, the most striking of which was a dramatic change in localization. Unlike wild type capsid, which localizes primarily to the ER and, to a lesser extent, the mitochondria, the RARA mutant localized almost exclusively to and around mitochondria. Moreover, the mitochondria in RARA expressing cells were highly clustered and

fragmented, not unlike mitochondria in cells over-expressing components of the fission/fusion machinery (Santel *et al.*, 2001, Stojanovski *et al.*, 2004) or mitophagy pathway (Vives-Bauza *et al.*, 2010). The effect of the RARA mutation on capsid's localization may also underlie its inability to block apoptosis and anti-viral signaling through a loss of interaction with host factors involved in these processes (discussed in more detail in sections 5.1.2.2 and 5.1.2.3). While it is known that viral glycoproteins E2 and E1 are required for transport of the capsid to the Golgi (Hobman *et al.*, 1990, Baron *et al.*, 1992), little else is known about how capsid traffics between the ER and other subcellular membranes. Accordingly, the mechanism by which the PP1-binding motif (RVXF) affects capsid localization is not clear. Similar to RV capsid, a number of eukaryotic proteins, known as tail-anchored (TA) proteins, contain a single pass, C-terminal transmembrane domain (Borgese *et al.*, 2003). Several TA proteins target to the mitochondria using a short transmembrane domain flanked on both ends by positively charged amino acids as a signal sequence (Nguyen *et al.*, 1993, Isenmann *et al.*, 1998, Kuroda *et al.*, 1998, Nemoto *et al.*, 1999). Since it too is flanked by positively charged amino acids, capsid's SP may act as the signal that targets it to the outer mitochondrial membrane, and mutations in the R-region may therefore affect the localization of capsid by disrupting this signal. Surprisingly, both the RARA and CR5A mutations increased the amount of capsid associated with the mitochondria (Ilkow *et al.*, 2011), while disruption of basic

residues surrounding the transmembrane domain of TA proteins tend to disrupt targeting to the mitochondria (Isenmann *et al.*, 1998, Kuroda *et al.*, 1998, Borgese *et al.*, 2001, Kaufmann *et al.*, 2003). Though the capsid SP and C-terminus could still act as the mitochondrial targeting sequence, the RIRF motif instead may serve to retain capsid on the ER. Another area where capsid and TA proteins differ is import; TA proteins are inserted directly into the OMM (Borgese *et al.*, 2001), while capsid is first inserted into the ER membrane as a polyprotein (Suomalainen *et al.*, 1990b, Marr *et al.*, 1991). This suggests that capsid utilizes a different subcellular trafficking system than host TA proteins.

The HCMV protein vMIA, like RV capsid, localizes to both the ER and mitochondria (Mavinakere *et al.*, 2004) and is initially inserted into the ER membrane before being post-translationally targeted to the OMM (Mavinakere *et al.*, 2006). A bipartite leader sequence in the N-terminus determines localization, with a short hydrophobic leader sequence directing import into the ER and an adjacent basic sequence mediating mitochondrial trafficking (Mavinakere *et al.*, 2004). Although capsid's SP is at the C-terminus, it may utilize a similar pathway as vMIA to traffic to the OMM. The mechanisms by which membrane proteins traffic from the ER to the mitochondria are not known, but a recent study of the mitochondrial protein apoptosis inducing factor (AIF) suggests that a vesicular trafficking system may be involved (Chiang *et al.*,

2012)(Chiang 2011). Both AIF and vMIA are present on the MAM (Bozidis *et al.*, 2008, Bozidis *et al.*, 2010, Chiang *et al.*, 2012), which may indicate that targeting to the MAM precedes their transport to mitochondria. Similarly, it is possible that capsid transits through the MAM *en route* to the mitochondria. Under this scenario, high levels of expression of the RARA mutant, which is almost exclusively associated with the mitochondria, may saturate the ER to mitochondria trafficking machinery resulting in buildup on the MAM and formation of the large, reticular, mitochondria-apposed structures observed in transfected cells. This could be further investigated by determining whether there is any overlap between wild type/RARA capsid and MAM markers.

Since the RARA mutation does not change the overall charge of capsid or significantly alter the hydrophobicity or length of the transmembrane region (SP), it is unlikely that it affects a canonical mitochondrial targeting signal. Whether the altered localization of the RARA mutant is due to loss of PP1 binding or a signal sequence that acts independently of PP1 is not clear. Interestingly, expression of the CapCT protein, which also does not bind PP1, results in its accumulation near mitochondria similar to the RARA capsid mutant (Ilkow *et al.*, 2011). It is unlikely that binding to a PP1 holoenzyme complex anchors capsid to the ER because the interaction between capsid and PP1 is either not very stable and/or only involves a small proportion of capsid. Instead,

PP1 may alter the interaction between capsid and ER anchoring factors by dephosphorylating capsid. Unlike the S46A mutant, whose electrophoretic mobility on SDS-PAGE is significantly different than wild type capsid, the RARA mutant's apparent molecular mass is not different from wild type. This suggests that the RARA mutation does not affect the phosphorylation of multiple amino acid residues in capsid.

Like the RARA mutant, CapCT expression causes extensive mitochondrial clustering and collapse (Ilkow *et al.*, 2011). Moreover, since CapCT does not bind PP1, this suggests that binding to PP1 prevents capsid-induced collapse of the mitochondrial network. Although PP1 has not been shown to directly dephosphorylate any components of the mitochondrial motility or fission/fusion machinery, it has been implicated in these processes. In one study, PP1 was reported to compete with RNA for binding to the A-kinase-anchoring protein (AKAP) 149 (Rogne *et al.*, 2009), and expression of a phosphomutant of AKAP149 that binds PP1 (but not RNA) collapsed the mitochondria in a manner similar to the capsid RARA mutant. Another study found that targeting the PP1 inhibitor inhibitor-2 to the OMM resulted in increased mitochondrial fusion and/or decreased mitochondrial fission (Merrill *et al.*, 2011). It is tempting to speculate that capsid-induced clustering of mitochondria involves disruption of the mitochondrial motility machinery, which is known to result in collapse of the

mitochondrial network and apoptosis induction (Fransson *et al.*, 2003, Fransson *et al.*, 2006, Cho *et al.*, 2007). The interaction between capsid and PP1 may therefore be necessary to limit collapse and fragmentation of the mitochondrial network that would otherwise occur from inhibiting components of the mitochondrial motility machinery. This hypothesis could be tested by determining whether co-expression of the RARA mutant and an OMM-targeted PP1 inhibitor can prevent capsid RARA-induced collapse of the mitochondrial network.

5.1.2.2 Effect of the RARA mutation on non-structural functions of capsid

The RARA mutation was found to affect two non-structural functions of capsid: protection from apoptosis and inhibition of innate immune signaling. The best characterized pathway in which PP1 affects apoptosis is through dephosphorylation of the BH3-only protein Bad (Ayllon *et al.*, 2000, Danial *et al.*, 2003). However, I did not find any evidence that capsid expression affects Bad dephosphorylation (data not shown). Instead, capsid may affect one of the other apoptotic pathways in which PP1 has been implicated. One such pathway is dephosphorylation of AKT, a serine/threonine kinase that acts in a pro-survival/anti-apoptotic manner. PP1 dephosphorylates this kinase in response to sphingosine treatment and growth factor receptor antagonism/depletion, resulting in the onset of apoptosis (Xu *et al.*, 2003, Thayyullathil *et al.*, 2011). In

this regard, capsid may inhibit or sequester PP1 to prevent dephosphorylation and inactivation of AKT, thereby promoting cell survival. PP1 also interacts with the Inhibitory Member of the Apoptosis-stimulating Proteins of the p53 Family (iASPP) protein (Llanos *et al.*, 2011). This protein inhibits apoptosis induced by the pro-apoptotic transcription factor p53 in a PP1-dependent manner. When the PP1 binding site in iASPP is ablated, the protein can no longer block apoptosis induced by p53 overexpression. PP1 dephosphorylates and inhibits p53 activity (Takenaka *et al.*, 1995, Haneda *et al.*, 2004) and iASPP2 likely functions by apposing p53 and PP1, resulting in dephosphorylation of the transcription factor. In theory, the RV capsid protein could act in an analogous manner to stabilize or bridge the interaction between PP1 and p53. Finally, it is also possible that the effects of PP1 on capsid phosphorylation and/or localization may affect its Bax-associated activity in blocking apoptosis. Although I have not tested it directly, it is unlikely that the RARA mutation affects Bax binding, because previously our lab showed that another capsid mutant, CR5A (in which the RIRF motif is ablated) still binds to, oligomerizes with, and activates Bax (Ilkow *et al.*, 2011). Similar to the S46A mutant, binding of the RARA mutant to Bax may not impair its function in apoptosis. Alternatively, targeting of capsid to ER may be important for Bax-dependent inhibition of apoptosis, possibly by sequestering Bax away from the mitochondria. Future studies will be necessary to discern the host pathways affected by the RARA mutation.

For the first time, I have shown that RV capsid inhibits activation of the innate immune response by poly(I:C) and interferon-α treatment. Inhibition of this response is a strategy used by many viruses with nearly every component in this system being inhibited by at least one or more viral proteins (Devasthanam, 2014). Though PP1 plays an important role in anti-viral defense through activation of RIG-I like receptors, data from this thesis research show that capsid acts downstream of this step. Specifically, capsid expression inhibits ISRE induction not only in response to poly(I:C), which directly activates RIG-I family members, but also when interferon-α is added to cells to activate interferon receptors. One possibility is that capsid inhibits JAK kinases and STAT transcription factors, both of which are common viral targets. While it is clear that the activity of these proteins is affected by phosphorylation (Yokota *et al.*, 2003, Lin *et al.*, 2006), the role of capsid's interaction with PP1 in this pathway, if any, remains to be determined. PP1 is not known to function in the JAK/STAT pathway, and in any case most phospho-amino acid residues involved in activating this pathway are tyrosines, which are not normally substrates of PP1. The capsid RARA mutant does not reduce ISRE activation, and instead seems to exacerbate activation of the ISRE by interferon-α, suggesting a possible role for PP1 in this process. Future studies should be aimed at determining the other host factors involved by examining the effect of capsid expression on individual

events in the interferon pathway; including phosphorylation of JAK, phosphorylation and/or nuclear localization of STAT, and expression of endogenous interferon stimulated genes.

The effects of the RARA mutation on the non-structural functions of capsid may be caused in part (or wholly) by mis-localization (Figure 5.2). Since the RARA mutant is almost entirely localized to and around mitochondria, it may not be able to access key host proteins at other membranes where wild type capsid is present. Furthermore, the tight packing of the reticular structures seen in RARA mutant expressing cells may hinder access of capsid to target proteins in the cytoplasm. The ability of CapCT to protect from apoptosis despite not binding PP1 further supports this hypothesis. Even though CapCT localizes to the mitochondria in a manner similar to the RARA mutant, a substantial fraction of CapCT also resides at the ER and other areas of the cytoplasm (data not shown, Ilkow *et al.*, 2011). The pro-apoptotic activity of the capsid RARA mutant could also be explained by its altered localization. *In vitro*, addition of capsid to mitochondria was found to induce cytochrome *c* release, but only above a certain threshold. Capsid may act pro-apoptotically *in vivo* when it is present in very high concentrations near the mitochondria. As such, the pro-apoptotic effect of the RARA and CR5A mutants may be due to their extensive buildup in the vicinity of the mitochondria. Capsid's inhibition of mitochondrial import,

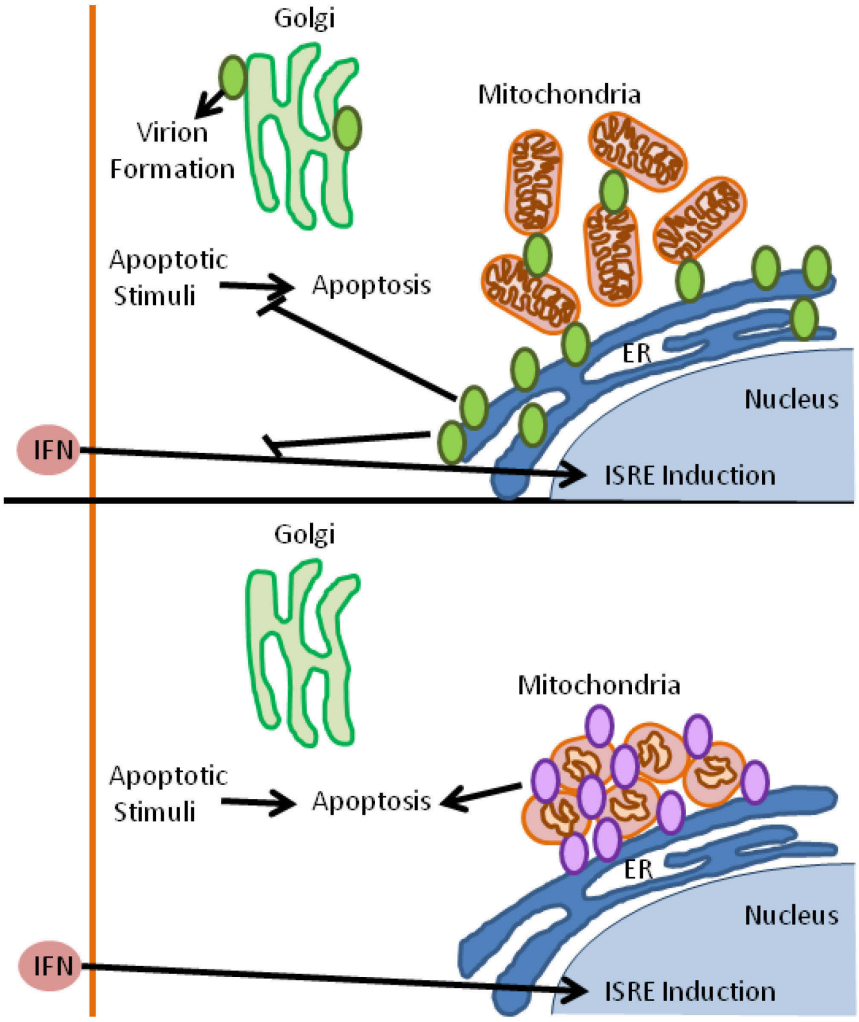

Figure 5.2 Effect of the RARA mutation on the localization and function of capsid. Wild type capsid (green ovals, top panel) localizes primarily to the ER and Golgi with only a small pool on the OMM. The RARA mutant (purple ovals, bottom panel) localizes primarily on and around mitochondria. As a result, the RARA mutant may not be able to access host factors necessary to block apoptosis and ISRE activation by interferon (IFN). The RARA mutant also cannot traffic to the Golgi, where virion assembly occurs. The buildup of RARA on the mitochondria also leads to mitochondrial collapse and apoptosis.

which is likely a concentration dependent effect, provides a possible mechanism for this, as inhibition of mitochondrial import leads to loss of cristae (Perkins *et al.*, 2001), a change in mitochondrial morphology that is associated with apoptosis (Cipolat *et al.*, 2006). This is further supported by the observation that the CapCT truncation mutant, which is missing a cluster of N-terminal arginines required for inhibition of mitochondrial import (Ilkow *et al.*, 2010a), localizes mainly to the mitochondria but does not induce apoptosis like CR5A or RARA (Ilkow *et al.*, 2011). In this respect, it would be of interest to investigate whether expression of Capsid-RARA or CapCT affects import of abundant matrix proteins such as p32. Specifically, using electron microscopy, this laboratory was able to show that RV infection significantly reduced import of p32 (Ilkow *et al.*, 2010a). It would also be of interest to determine if/how expression of RARA and CapCT mutants correlated with the appearance of apoptotic features, such as mitochondrial fragmentation and loss of cristae.

5.1.2.3 Effect of the RARA mutation on RV replication

Mutation of the PP1-binding site in capsid had a considerable effect on viral replication, as both viral protein levels and titers were significantly reduced in a RV strain with the RARA mutation. Since viral genome levels in wild type and RARA RV infected cells were comparable 24 hours after transfection, it is unlikely that this mutation perturbs genome replication *per se*. Rather, there is evidence

to suggest that this mutant is unable to assemble infectious virions. In cells transfected with infectious RV genomic RNA containing the RARA mutation only a small portion of cells exhibited signs of apoptosis, suggesting that loss of infected cells to apoptosis does not significantly alter viral titers. Conversely, expression of a 24S cDNA with the RARA mutation resulted in production of very few virus-like particles. Extrapolating the data from this surrogate virion assembly assay suggest that the low viral titers from cells expressing RARA genomic RNA are due to a defect in virus assembly. Although capsid-RARA does not support virion assembly very well, cells transfected with RV-RARA infectious RNA did produce a small number of infectious virions that could be detected in plaque assays. This may be due to the high rate of reversion in R-region mutants (Carolina Ilkow, unpublished data).

Since capsid is dephosphorylated by PP1 *in vitro* (Law *et al.*, 2003), and dephosphorylation occurs before virion release (Law *et al.*, 2006), it is tempting to speculate that the RARA mutation disrupts the ability of capsid to be dephosphorylated before virion assembly. If true, this would imply that dephosphorylation of capsid is an essential step in virion formation. Alternatively, since the RARA mutant has a severe effect on capsid localization, it may prevent capsid from trafficking to the Golgi where virion assembly takes place. Future studies could differentiate these possibilities in two ways. First,

indirect immunofluorescence could be used to determine the relative localizations of capsid mutants and glycoproteins E1/E2 in infected cells. If capsid does not co-localize with the envelope proteins in the Golgi region, the inability to form virions is likely due to a localization defect. Second, the S46A mutation, which results in capsid being hypophosphorylated, and the RARA mutation could be combined and if the resulting mutant was still able to form virions, it would suggest that dephosphorylation is necessary for virion formation and that a lack of dephosphorylation underlies the inability of the RARA mutant to form virions. It is important to note that the CR5A mutant does form virions when co-transfected with the envelope proteins in Vero cells (Ilkow *et al.*, 2011). Given that the amino acid residues altered in the RARA mutant are thought to be more critical for PP1 binding than those altered in CR5A, it is possible that the CR5A mutant may retain sufficient PP1 binding activity for virion assembly.

5.2 Concluding remarks

During the course of infection, it is critical for viruses to alter host pathways to enhance viral replication and cell survival. Of particular importance are evasion of the host immune response and inhibition of apoptosis, both of which are used to clear the host of viral infection. RNA viruses, because of their limited genome size, must make use of multifunctional proteins to accomplish these functions. Recently, work in our lab and others has characterized the interactions between

RV capsid and several host proteins and investigated the non-structural functions of the capsid protein. The work in this thesis furthers our understanding of how RV capsid inhibits apoptosis and reveals another activity of this protein: inhibition of the innate immune response. Additionally, the effects of the SP truncation and RARA mutants illustrate the importance of localization for both structural and non-structural functions of this protein. Ultimately, future studies will be needed to fully elucidate the mechanisms by which the RV capsid protein modulates host functions to facilitate viral replication. Given that viral persistence is thought to play an important role in CRS and RV-associated arthropathy, further study of capsid's anti-apoptotic activity could be the key to understanding the underlying pathophysiology of these diseases. Further study of the non-structural roles of the capsid protein is essential not only for understanding the biology of RV, but may also provide important clues as to how other RNA viruses manipulate host cell pathways.

References

[No_Authors_Listed] (2005). Standardization of the nomenclature for genetic characteristics of wild-type rubella viruses. *Releve epidemiologique hebdomadaire / Section d'hygiene du Secretariat de la Societe des Nations = Weekly epidemiological record / Health Section of the Secretariat of the League of Nations* **80,** 126-132.

Adamo, P., Asis, L., Silveyra, P., Cuffini, C., Pedranti, M. and Zapata, M. (2004). Rubella virus does not induce apoptosis in primary human embryo fibroblast cultures: a possible way of viral persistence in congenital infection. *Viral immunology* **17,** 87-100.

Akhrymuk, I., Kulemzin, S.V. and Frolova, E.I. (2012). Evasion of the innate immune response: the Old World alphavirus nsP2 protein induces rapid degradation of Rpb1, a catalytic subunit of RNA polymerase II. *Journal of virology* **86,** 7180-7191.

Alexopoulou, L., Holt, A.C., Medzhitov, R. and Flavell, R.A. (2001). Recognition of double-stranded RNA and activation of NF-kappaB by Toll-like receptor 3. *Nature* **413,** 732-738.

Alvarez, E., Castello, A., Menendez-Arias, L. and Carrasco, L. (2006). HIV protease cleaves poly(A)-binding protein. *The Biochemical journal* **396,** 219-226.

Ammosova, T., Jerebtsova, M., Beullens, M., Lesage, B., Jackson, A., Kashanchi, F.*, et al.* (2005). Nuclear targeting of protein phosphatase-1 by HIV-1 Tat protein. *The Journal of biological chemistry* **280,** 36364-36371.

Ammosova, T., Jerebtsova, M., Beullens, M., Voloshin, Y., Ray, P.E., Kumar, A.*, et al.* (2003). Nuclear protein phosphatase-1 regulates HIV-1 transcription. *The Journal of biological chemistry* **278,** 32189-32194.

Ammosova, T., Yedavalli, V.R., Niu, X., Jerebtsova, M., Van Eynde, A., Beullens, M.*, et al.* (2011). Expression of a protein phosphatase 1 inhibitor, cdNIPP1, increases CDK9 threonine 186 phosphorylation and inhibits HIV-1 transcription. *The Journal of biological chemistry* **286,** 3798-3804.

Annis, M.G., Soucie, E.L., Dlugosz, P.J., Cruz-Aguado, J.A., Penn, L.Z., Leber, B. and Andrews, D.W. (2005). Bax forms multispanning monomers that

oligomerize to permeabilize membranes during apoptosis. *The EMBO journal* **24,** 2096-2103.

Antonsson, B., Conti, F., Ciavatta, A., Montessuit, S., Lewis, S., Martinou, I.*, et al.* (1997). Inhibition of Bax channel-forming activity by Bcl-2. *Science* **277,** 370-372.

Antonucci, L.A., Egger, J.V. and Krucher, N.A. (2014). Phosphorylation of the Retinoblastoma protein (Rb) on serine-807 is required for association with Bax. *Cell cycle* **13,** 3611-3617.

Arnoult, D., Bartle, L.M., Skaletskaya, A., Poncet, D., Zamzami, N., Park, P.U.*, et al.* (2004). Cytomegalovirus cell death suppressor vMIA blocks Bax- but not Bak-mediated apoptosis by binding and sequestering Bax at mitochondria. *Proceedings of the National Academy of Sciences of the United States of America* **101,** 7988-7993.

Asselah, T., Bieche, I., Mansouri, A., Laurendeau, I., Cazals-Hatem, D., Feldmann, G.*, et al.* (2010). In vivo hepatic endoplasmic reticulum stress in patients with chronic hepatitis C. *The Journal of pathology* **221,** 264-274.

Atasheva, S., Fish, A., Fornerod, M. and Frolova, E.I. (2010). Venezuelan equine Encephalitis virus capsid protein forms a tetrameric complex with CRM1 and importin alpha/beta that obstructs nuclear pore complex function. *Journal of virology* **84,** 4158-4171.

Atreya, C.D., Kulkarni, S. and Mohan, K.V. (2004). Rubella virus P90 associates with the cytokinesis regulatory protein Citron-K kinase and the viral infection and constitutive expression of P90 protein both induce cell cycle arrest following S phase in cell culture. *Archives of virology* **149,** 779-789.

Atreya, C.D., Lee, N.S., Forng, R.Y., Hofmann, J., Washington, G., Marti, G. and Nakhasi, H.L. (1998). The rubella virus putative replicase interacts with the retinoblastoma tumor suppressor protein. *Virus genes* **16,** 177-183.

Ayllon, V., Martinez, A.C., Garcia, A., Cayla, X. and Rebollo, A. (2000). Protein phosphatase 1alpha is a Ras-activated Bad phosphatase that regulates interleukin-2 deprivation-induced apoptosis. *The EMBO journal* **19,** 2237-2246.

Bag, J. and Wu, J. (1996). Translational control of poly(A)-binding protein expression. *European journal of biochemistry / FEBS* **237,** 143-152.

Baltimore, D. (1971). Expression of animal virus genomes. *Bacteriological reviews* **35,** 235-241.

Banatvala, J.E. and Brown, D.W. (2004). Rubella. *Lancet* **363,** 1127-1137.

Bardeletti, G. (1977). Respiration and ATP level in BHK21/13S cells during the earlist stages of rubella virus replication. *Intervirology* **8,** 100-109.

Bardeletti, G. and Gautheron, D.C. (1976). Phospholipid and cholesterol composition of rubella virus and its host cell BHK 21 grown in suspension cultures. *Archives of virology* **52,** 19-27.

Bardeletti, G., Tektoff, J. and Gautheron, D. (1979). Rubella virus maturation and production in two host cell systems. *Intervirology* **11,** 97-103.

Barik, S. and Banerjee, A.K. (1992a). Phosphorylation by Cellular Casein Kinase-Ii Is Essential for Transcriptional Activity of Vesicular Stomatitis-Virus Phosphoprotein-P. *Proceedings of the National Academy of Sciences of the United States of America* **89,** 6570-6574.

Barik, S. and Banerjee, A.K. (1992b). Sequential phosphorylation of the phosphoprotein of vesicular stomatitis virus by cellular and viral protein kinases is essential for transcription activation. *Journal of virology* **66,** 1109-1118.

Baron, M.D., Ebel, T. and Suomalainen, M. (1992). Intracellular transport of rubella virus structural proteins expressed from cloned cDNA. *The Journal of general virology* **73 (Pt 5),** 1073-1086.

Baron, M.D. and Forsell, K. (1991). Oligomerization of the structural proteins of rubella virus. *Virology* **185,** 811-819.

Battisti, A.J., Yoder, J.D., Plevka, P., Winkler, D.C., Prasad, V.M., Kuhn, R.J.*, et al.* (2012). Cryo-electron tomography of rubella virus. *Journal of virology* **86,** 11078-11085.

Beatch, M.D., Everitt, J.C., Law, L.J. and Hobman, T.C. (2005). Interactions between rubella virus capsid and host protein p32 are important for virus replication. *Journal of virology* **79,** 10807-10820.

Beatch, M.D. and Hobman, T.C. (2000). Rubella virus capsid associates with host cell protein p32 and localizes to mitochondria. *Journal of virology* **74,** 5569-5576.

Bellot, G., Cartron, P.F., Er, E., Oliver, L., Juin, P., Armstrong, L.C.*, et al.* (2007). TOM22, a core component of the mitochondria outer membrane protein translocation pore, is a mitochondrial receptor for the proapoptotic protein Bax. *Cell death and differentiation* **14,** 785-794.

Besch, R., Poeck, H., Hohenauer, T., Senft, D., Hacker, G., Berking, C.*, et al.* (2009a). Proapoptotic signaling induced by RIG-I and MDA-5 results in type I interferon-independent apoptosis in human melanoma cells. *J Clin Invest* **119,** 2399-2411.

Besch, R., Poeck, H., Hohenauer, T., Senft, D., Hacker, G., Berking, C.*, et al.* (2009b). Proapoptotic signaling induced by RIG-I and MDA-5 results in type I interferon-independent apoptosis in human melanoma cells. *J Clin Invest* **119,** 2399-2411.

Bhuvanakantham, R., Cheong, Y.K. and Ng, M.L. (2010). West Nile virus capsid protein interaction with importin and HDM2 protein is regulated by protein kinase C-mediated phosphorylation. *Microbes and infection / Institut Pasteur* **12,** 615-625.

Bitko, V., Shulyayeva, O., Mazumder, B., Musiyenko, A., Ramaswamy, M., Look, D.C. and Barik, S. (2007). Nonstructural proteins of respiratory syncytial virus suppress premature apoptosis by an NF-kappaB-dependent, interferon-independent mechanism and facilitate virus growth. *Journal of virology* **81,** 1786-1795.

Boehme, K.W., Lai, C.M. and Dermody, T.S. (2013). Mechanisms of reovirus bloodstream dissemination. *Adv Virus Res* **87,** 1-35.

Boldin, M.P., Goncharov, T.M., Goltsev, Y.V. and Wallach, D. (1996). Involvement of MACH, a novel MORT1/FADD-interacting protease, in Fas/APO-1- and TNF receptor-induced cell death. *Cell* **85,** 803-815.

Bollen, M., Peti, W., Ragusa, M.J. and Beullens, M. (2010). The extended PP1 toolkit: designed to create specificity. *Trends in biochemical sciences* **35,** 450-458.

Borgese, N., Colombo, S. and Pedrazzini, E. (2003). The tale of tail-anchored proteins: coming from the cytosol and looking for a membrane. *The Journal of cell biology* **161,** 1013-1019.

Borgese, N., Gazzoni, I., Barberi, M., Colombo, S. and Pedrazzini, E. (2001). Targeting of a tail-anchored protein to endoplasmic reticulum and

mitochondrial outer membrane by independent but competing pathways. *Molecular biology of the cell* **12,** 2482-2496.

Boue, J.G. and Boue, A. (1969). Effects of rubella virus infection on the division of human cells. *American journal of diseases of children* **118,** 45-48.

Bozidis, P., Williamson, C.D. and Colberg-Poley, A.M. (2008). Mitochondrial and secretory human cytomegalovirus UL37 proteins traffic into mitochondrion-associated membranes of human cells. *Journal of virology* **82,** 2715-2726.

Bozidis, P., Williamson, C.D., Wong, D.S. and Colberg-Poley, A.M. (2010). Trafficking of UL37 proteins into mitochondrion-associated membranes during permissive human cytomegalovirus infection. *Journal of virology* **84,** 7898-7903.

Brune, W. (2011). Inhibition of programmed cell death by cytomegaloviruses. *Virus Res* **157,** 144-150.

Brush, M.H., Weiser, D.C. and Shenolikar, S. (2003). Growth arrest and DNA damage-inducible protein GADD34 targets protein phosphatase 1 alpha to the endoplasmic reticulum and promotes dephosphorylation of the alpha subunit of eukaryotic translation initiation factor 2. *Molecular and cellular biology* **23,** 1292-1303.

Cam, M., Handke, W., Picard-Maureau, M. and Brune, W. (2010). Cytomegaloviruses inhibit Bak- and Bax-mediated apoptosis with two separate viral proteins. *Cell death and differentiation* **17,** 655-665.

Carmody, L.C., Baucum, A.J., 2nd, Bass, M.A. and Colbran, R.J. (2008). Selective targeting of the gamma1 isoform of protein phosphatase 1 to F-actin in intact cells requires multiple domains in spinophilin and neurabin. *FASEB journal : official publication of the Federation of American Societies for Experimental Biology* **22,** 1660-1671.

Cartier, C., Deckert, M., Grangeasse, C., Trauger, R., Jensen, F., Bernard, A.*, et al.* (1997). Association of ERK2 mitogen-activated protein kinase with human immunodeficiency virus particles. *Journal of virology* **71,** 4832-4837.

Castelli, J., Wood, K.A. and Youle, R.J. (1998). The 2-5A system in viral infection and apoptosis. *Biomedicine & pharmacotherapy = Biomedecine & pharmacotherapie* **52,** 386-390.

Chantler, J.K. and Tingle, A.J. (1980). Replication and expression of rubella virus in human lymphocyte populations. *The Journal of general virology* **50,** 317-328.

Charrier, S., Ferrand, M., Zerbato, M., Precigout, G., Viornery, A., Bucher-Laurent, S.*, et al.* (2011). Quantification of lentiviral vector copy numbers in individual hematopoietic colony-forming cells shows vector dose-dependent effects on the frequency and level of transduction. *Gene therapy* **18,** 479-487.

Chattopadhyay, D. and Banerjee, A.K. (1987). Phosphorylation within a specific domain of the phosphoprotein of vesicular stomatitis virus regulates transcription in vitro. *Cell* **49,** 407-414.

Chattopadhyay, S., Marques, J.T., Yamashita, M., Peters, K.L., Smith, K., Desai, A.*, et al.* (2010a). Viral apoptosis is induced by IRF-3-mediated activation of Bax. *The EMBO journal* **29,** 1762-1773.

Chattopadhyay, S., Marques, J.T., Yamashita, M., Peters, K.L., Smith, K., Desai, A.*, et al.* (2010b). Viral apoptosis is induced by IRF-3-mediated activation of Bax. *Embo Journal* **29,** 1762-1773.

Chawla-Sarkar, M., Leaman, D.W. and Borden, E.C. (2001). Preferential induction of apoptosis by interferon (IFN)-beta compared with IFN-alpha2: correlation with TRAIL/Apo2L induction in melanoma cell lines. *Clinical cancer research : an official journal of the American Association for Cancer Research* **7,** 1821-1831.

Chen, H., Gill, A., Dove, B.K., Emmett, S.R., Kemp, C.F., Ritchie, M.A.*, et al.* (2005). Mass spectroscopic characterization of the coronavirus infectious bronchitis virus nucleoprotein and elucidation of the role of phosphorylation in RNA binding by using surface plasmon resonance. *Journal of virology* **79,** 1164-1179.

Chen, L., Zhang, S., Banerjee, A.K. and Chen, M. (2013). N-terminal phosphorylation of phosphoprotein of vesicular stomatitis virus is required for preventing nucleoprotein from binding to cellular RNAs and for functional template formation. *Journal of virology* **87,** 3177-3186.

Chen, M.H. and Frey, T.K. (1999). Mutagenic analysis of the 3' cis-acting elements of the rubella virus genome. *Journal of virology* **73,** 3386-3403.

Chen, M.H., Frolov, I., Icenogle, J. and Frey, T.K. (2004a). Analysis of the 3' cis-acting elements of rubella virus by using replicons expressing a puromycin resistance gene. *Journal of virology* **78,** 2553-2561.

Chen, M.H. and Icenogle, J.P. (2004b). Rubella virus capsid protein modulates viral genome replication and virus infectivity. *Journal of virology* **78,** 4314-4322.

Chen, Q., Gong, B., Mahmoud-Ahmed, A.S., Zhou, A., Hsi, E.D., Hussein, M. and Almasan, A. (2001). Apo2L/TRAIL and Bcl-2-related proteins regulate type I interferon-induced apoptosis in multiple myeloma. *Blood* **98,** 2183-2192.

Cheong, Y.K. and Ng, M.L. (2011). Dephosphorylation of West Nile virus capsid protein enhances the processes of nucleocapsid assembly. *Microbes and infection / Institut Pasteur* **13,** 76-84.

Chiang, C.W., Kanies, C., Kim, K.W., Fang, W.B., Parkhurst, C., Xie, M.*, et al.* (2003). Protein phosphatase 2A dephosphorylation of phosphoserine 112 plays the gatekeeper role for BAD-mediated apoptosis. *Molecular and cellular biology* **23,** 6350-6362.

Chiang, S.F., Huang, C.Y., Lin, T.Y., Chiou, S.H. and Chow, K.C. (2012). An alternative import pathway of AIF to the mitochondria. *International journal of molecular medicine* **29,** 365-372.

Chinnaiyan, A.M., O'Rourke, K., Tewari, M. and Dixit, V.M. (1995). FADD, a novel death domain-containing protein, interacts with the death domain of Fas and initiates apoptosis. *Cell* **81,** 505-512.

Cho, K.I., Cai, Y., Yi, H., Yeh, A., Aslanukov, A. and Ferreira, P.A. (2007). Association of the kinesin-binding domain of RanBP2 to KIF5B and KIF5C determines mitochondria localization and function. *Traffic* **8,** 1722-1735.

Choi, H.K., Tong, L., Minor, W., Dumas, P., Boege, U., Rossmann, M.G. and Wengler, G. (1991). Structure of Sindbis virus core protein reveals a chymotrypsin-like serine proteinase and the organization of the virion. *Nature* **354,** 37-43.

Chowdhury, A.R., Ghosh, I. and Datta, K. (2008). Excessive reactive oxygen species induces apoptosis in fibroblasts: role of mitochondrially accumulated hyaluronic acid binding protein 1 (HABP1/p32/gC1qR). *Experimental cell research* **314,** 651-667.

Choy, M.S., Page, R. and Peti, W. (2012). Regulation of protein phosphatase 1 by intrinsically disordered proteins. *Biochemical Society transactions* **40,** 969-974.

Chu, T.H., Liou, A.T., Su, P.Y., Wu, H.N. and Shih, C. (2014). Nucleic acid chaperone activity associated with the arginine-rich domain of human hepatitis B virus core protein. *Journal of virology* **88,** 2530-2543.

Cipolat, S., Rudka, T., Hartmann, D., Costa, V., Serneels, L., Craessaerts, K.*, et al.* (2006). Mitochondrial rhomboid PARL regulates cytochrome c release during apoptosis via OPA1-dependent cristae remodeling. *Cell* **126,** 163-175.

Clarke, D.M., Loo, T.W., Hui, I., Chong, P. and Gillam, S. (1987). Nucleotide sequence and in vitro expression of rubella virus 24S subgenomic messenger RNA encoding the structural proteins E1, E2 and C. *Nucleic acids research* **15,** 3041-3057.

Claus, C., Chey, S., Heinrich, S., Reins, M., Richardt, B., Pinkert, S.*, et al.* (2011). Involvement of p32 and microtubules in alteration of mitochondrial functions by rubella virus. *Journal of virology* **85,** 3881-3892.

Claus, C., Hofmann, J., Uberla, K. and Liebert, U.G. (2006). Rubella virus pseudotypes and a cell-cell fusion assay as tools for functional analysis of the rubella virus E2 and E1 envelope glycoproteins. *Journal of General Virology* **87,** 3029-3037.

Clem, R.J. (2015). Viral IAPs, then and now. *Seminars in cell & developmental biology*.

Cohen, B., Peretz, D., Vaiman, D., Benech, P. and Chebath, J. (1988). Enhancer-like interferon responsive sequences of the human and murine (2'-5') oligoadenylate synthetase gene promoters. *The EMBO journal* **7,** 1411-1419.

Coltharp, C. and Xiao, J. (2012). Superresolution microscopy for microbiology. *Cellular microbiology* **14,** 1808-1818.

Cong, H.L., Jiang, Y. and Tien, P. (2011). Identification of the Myelin Oligodendrocyte Glycoprotein as a Cellular Receptor for Rubella Virus. *Journal of virology* **85,** 11038-11047.

Cotlier, E., Fox, J., Bohigian, G., Beaty, C. and Du Pree, A. (1968). Pathogenic effects of rubella virus on embryos and newborn rats. *Nature* **217,** 38-40.

Cougot, D., Allemand, E., Riviere, L., Benhenda, S., Duroure, K., Levillayer, F.*, et al.* (2012). Inhibition of PP1 phosphatase activity by HBx: a mechanism for the activation of hepatitis B virus transcription. *Science signaling* **5,** ra1.

Cristofari, G., Ivanyi-Nagy, R., Gabus, C., Boulant, S., Lavergne, J.P., Penin, F. and Darlix, J.L. (2004). The hepatitis C virus Core protein is a potent nucleic acid chaperone that directs dimerization of the viral (+) strand RNA in vitro. *Nucleic acids research* **32,** 2623-2631.

Cruz, J.L., Sola, I., Becares, M., Alberca, B., Plana, J., Enjuanes, L. and Zuniga, S. (2011). Coronavirus gene 7 counteracts host defenses and modulates virus virulence. *PLoS pathogens* **7,** e1002090.

Danial, N.N., Gramm, C.F., Scorrano, L., Zhang, C.Y., Krauss, S., Ranger, A.M.*, et al.* (2003). BAD and glucokinase reside in a mitochondrial complex that integrates glycolysis and apoptosis. *Nature* **424,** 952-956.

Dansen, T.B., Whitfield, J., Rostker, F., Brown-Swigart, L. and Evan, G.I. (2006). Specific requirement for Bax, not Bak, in Myc-induced apoptosis and tumor suppression in vivo. *Journal of Biological Chemistry* **281,** 10890-10895.

Darlix, J.L., Vincent, A., Gabus, C., de Rocquigny, H. and Roques, B. (1993). Trans-activation of the 5' to 3' viral DNA strand transfer by nucleocapsid protein during reverse transcription of HIV1 RNA. *Comptes rendus de l'Academie des sciences. Serie III, Sciences de la vie* **316,** 763-771.

Davis, M.E., Wang, M.K., Rennick, L.J., Full, F., Gableske, S., Mesman, A.W.*, et al.* (2014). Antagonism of the phosphatase PP1 by the measles virus V protein is required for innate immune escape of MDA5. *Cell host & microbe* **16,** 19-30.

Dawson, J.F. and Holmes, C.F. (1999). Molecular mechanisms underlying inhibition of protein phosphatases by marine toxins. *Frontiers in bioscience : a journal and virtual library* **4,** D646-658.

Dedio, J., Jahnen-Dechent, W., Bachmann, M. and Muller-Esterl, W. (1998). The multiligand-binding protein gC1qR, putative C1q receptor, is a mitochondrial protein. *Journal of immunology* **160,** 3534-3542.

Dejean, L.M., Martinez-Caballero, S., Guo, L., Hughes, C., Teijido, O., Ducret, T.*, et al.* (2005). Oligomeric Bax is a component of the putative cytochrome c release channel MAC, mitochondrial apoptosis-induced channel. *Molecular biology of the cell* **16,** 2424-2432.

Delahunt, C.S. and Rieser, N. (1967). Rubella-induced embryopathies in monkeys. *American journal of obstetrics and gynecology* **99,** 580-588.

Depraetere, V. and Golstein, P. (1997). Fas and other cell death signaling pathways. *Seminars in immunology* **9,** 93-107.

Der, S.D., Yang, Y.L., Weissmann, C. and Williams, B.R. (1997). A double-stranded RNA-activated protein kinase-dependent pathway mediating stress-induced apoptosis. *Proceedings of the National Academy of Sciences of the United States of America* **94,** 3279-3283.

Deroubaix, A., Osseman, Q., Cassany, A., Begu, D., Ragues, J., Kassab, S.*, et al.* (2015). Expression of viral polymerase and phosphorylation of core protein determine core and capsid localization of the human hepatitis B virus. *The Journal of general virology* **96,** 183-195.

Devasthanam, A.S. (2014). Mechanisms underlying the inhibition of interferon signaling by viruses. *Virulence* **5,** 270-277.

Dewson, G., Kratina, T., Czabotar, P., Day, C.L., Adams, J.M. and Kluck, R.M. (2009). Bak activation for apoptosis involves oligomerization of dimers via their alpha6 helices. *Molecular cell* **36,** 696-703.

Dewson, G., Kratina, T., Sim, H.W., Puthalakath, H., Adams, J.M., Colman, P.M. and Kluck, R.M. (2008). To trigger apoptosis, Bak exposes its BH3 domain and homodimerizes via BH3:groove interactions. *Molecular cell* **30,** 369-380.

Domegan, L.M. and Atkins, G.J. (2002). Apoptosis induction by the Therien and vaccine RA27/3 strains of rubella virus causes depletion of oligodendrocytes from rat neural cell cultures. *The Journal of general virology* **83,** 2135-2143.

Dominguez, G., Wang, C.Y. and Frey, T.K. (1990). Sequence of the genome RNA of rubella virus: evidence for genetic rearrangement during togavirus evolution. *Virology* **177,** 225-238.

Drake, J.W., Charlesworth, B., Charlesworth, D. and Crow, J.F. (1998). Rates of spontaneous mutation. *Genetics* **148,** 1667-1686.

Dube, M., Rey, F.A. and Kielian, M. (2014). Rubella virus: first calcium-requiring viral fusion protein. *PLoS pathogens* **10,** e1004530.

DuBois, R.M., Vaney, M.C., Tortorici, M.A., Kurdi, R.A., Barba-Spaeth, G., Krey, T. and Rey, F.A. (2013). Functional and evolutionary insight from the crystal structure of rubella virus protein E1. *Nature* **493,** 552-556.

Duncan, R., Esmaili, A., Law, L.M., Bertholet, S., Hough, C., Hobman, T.C. and Nakhasi, H.L. (2000). Rubella virus capsid protein induces apoptosis in transfected RK13 cells. *Virology* **275,** 20-29.

Duncan, R., Muller, J., Lee, N., Esmaili, A. and Nakhasi, H.L. (1999). Rubella virus-induced apoptosis varies among cell lines and is modulated by Bcl-XL and caspase inhibitors. *Virology* **255,** 117-128.

Edlich, R.F., Winters, K.L., Long, W.B., 3rd and Gubler, K.D. (2005). Rubella and congenital rubella (German measles). *Journal of long-term effects of medical implants* **15,** 319-328.

Egloff, M.P., Johnson, D.F., Moorhead, G., Cohen, P.T., Cohen, P. and Barford, D. (1997). Structural basis for the recognition of regulatory subunits by the catalytic subunit of protein phosphatase 1. *The EMBO journal* **16,** 1876-1887.

Elgizoli, M., Dai, Y., Kempf, C., Koblet, H. and Michel, M.R. (1989). Semliki Forest virus capsid protein acts as a pleiotropic regulator of host cellular protein synthesis. *Journal of virology* **63,** 2921-2928.

Eliseeva, I.A., Lyabin, D.N. and Ovchinnikov, L.P. (2013). Poly(A)-binding proteins: structure, domain organization, and activity regulation. *Biochemistry. Biokhimiia* **78,** 1377-1391.

Erickson, S.L. and Lykke-Andersen, J. (2011). Cytoplasmic mRNP granules at a glance. *Journal of cell science* **124,** 293-297.

Esterly, J.R. and Oppenheimer, E.H. (1967). Vascular lesions in infants with congenital rubella. *Circulation* **36,** 544-554.

Everett, H. and McFadden, G. (2002). Poxviruses and apoptosis: a time to die. *Current opinion in microbiology* **5,** 395-402.

Fadok, V.A., Voelker, D.R., Campbell, P.A., Cohen, J.J., Bratton, D.L. and Henson, P.M. (1992). Exposure of phosphatidylserine on the surface of apoptotic lymphocytes triggers specific recognition and removal by macrophages. *Journal of immunology* **148,** 2207-2216.

Favre, D., Studer, E. and Michel, M.R. (1994). Two nucleolar targeting signals present in the N-terminal part of Semliki Forest virus capsid protein. *Archives of virology* **137,** 149-155.

Feigenblum, D. and Schneider, R.J. (1993). Modification of eukaryotic initiation factor 4F during infection by influenza virus. *Journal of virology* **67,** 3027-3035.

Fletcher, J.I., Meusburger, S., Hawkins, C.J., Riglar, D.T., Lee, E.F., Fairlie, W.D.*, et al.* (2008). Apoptosis is triggered when prosurvival Bcl-2 proteins cannot restrain Bax. *Proceedings of the National Academy of Sciences of the United States of America* **105,** 18081-18087.

Fliedl, L., Kast, F., Grillari, J., Wieser, M. and Grillari-Voglauer, R. (2015). Optimization of a quantitative PCR based method for plasmid copy number determination in human cell lines. *New biotechnology*.

Fontana, J., Lopez-Iglesias, C., Tzeng, W.P., Frey, T.K., Fernandez, J.J. and Risco, C. (2010). Three-dimensional structure of Rubella virus factories. *Virology* **405,** 579-591.

Fontana, J., Tzeng, W.P., Calderita, G., Fraile-Ramos, A., Frey, T.K. and Risco, C. (2007). Novel replication complex architecture in rubella replicon-transfected cells. *Cellular microbiology* **9,** 875-890.

Forng, R.Y. and Atreya, C.D. (1999). Mutations in the retinoblastoma protein-binding LXCXE motif of rubella virus putative replicase affect virus replication. *The Journal of general virology* **80 (Pt 2),** 327-332.

Forng, R.Y. and Frey, T.K. (1995). Identification of the rubella virus nonstructural proteins. *Virology* **206,** 843-853.

Forrest, J.M., Turnbull, F.M., Sholler, G.F., Hawker, R.E., Martin, F.J., Doran, T.T. and Burgess, M.A. (2002). Gregg's congenital rubella patients 60 years later. *The Medical journal of Australia* **177,** 664-667.

Fransson, A., Ruusala, A. and Aspenstrom, P. (2003). Atypical Rho GTPases have roles in mitochondrial homeostasis and apoptosis. *The Journal of biological chemistry* **278,** 6495-6502.

Fransson, S., Ruusala, A. and Aspenstrom, P. (2006). The atypical Rho GTPases Miro-1 and Miro-2 have essential roles in mitochondrial trafficking. *Biochem Biophys Res Commun* **344,** 500-510.

Frey, T.K. (1994). Molecular-Biology of Rubella-Virus. *Adv Virus Res* **44,** 69-160.

Frey, T.K. and Marr, L.D. (1988). Sequence of the region coding for virion proteins C and E2 and the carboxy terminus of the nonstructural proteins of rubella virus: comparison with alphaviruses. *Gene* **62,** 85-99.

Frey, T.K., Marr, L.D., Hemphill, M.L. and Dominguez, G. (1986). Molecular cloning and sequencing of the region of the rubella virus genome coding for glycoprotein E1. *Virology* **154,** 228-232.

Fricker, M., O'Prey, J., Tolkovsky, A.M. and Ryan, K.M. (2010). Phosphorylation of Puma modulates its apoptotic function by regulating protein stability. *Cell death & disease* **1,** e59.

Fros, J.J., Major, L.D., Scholte, F.E., Gardner, J., van Hemert, M.J., Suhrbier, A. and Pijlman, G.P. (2015). Chikungunya virus non-structural protein 2-mediated host shut-off disables the unfolded protein response. *The Journal of general virology* **96,** 580-589.

Galindo, I., Hernaez, B., Munoz-Moreno, R., Cuesta-Geijo, M.A., Dalmau-Mena, I. and Alonso, C. (2012). The ATF6 branch of unfolded protein response and apoptosis are activated to promote African swine fever virus infection. *Cell death & disease* **3,** e341.

Galluzzi, L., Brenner, C., Morselli, E., Touat, Z. and Kroemer, G. (2008). Viral control of mitochondrial apoptosis. *PLoS pathogens* **4,** e1000018.

Garbutt, M., Law, L.M., Chan, H. and Hobman, T.C. (1999). Role of rubella virus glycoprotein domains in assembly of virus-like particles. *Journal of virology* **73,** 3524-3533.

Garcia, M.A., Meurs, E.F. and Esteban, M. (2007). The dsRNA protein kinase PKR: virus and cell control. *Biochimie* **89,** 799-811.

Gavathiotis, E., Reyna, D.E., Davis, M.L., Bird, G.H. and Walensky, L.D. (2010). BH3-triggered structural reorganization drives the activation of proapoptotic BAX. *Molecular cell* **40,** 481-492.

George, N.M., Evans, J.J. and Luo, X. (2007). A three-helix homo-oligomerization domain containing BH3 and BH1 is responsible for the apoptotic activity of Bax. *Genes & development* **21,** 1937-1948.

Ghebrehiwet, B., Lim, B.L., Kumar, R., Feng, X. and Peerschke, E.I. (2001). gC1q-R/p33, a member of a new class of multifunctional and multicompartmental cellular proteins, is involved in inflammation and infection. *Immunological reviews* **180,** 65-77.

Ghebrehiwet, B. and Peerschke, E.I. (1998). Structure and function of gC1q-R: a multiligand binding cellular protein. *Immunobiology* **199,** 225-238.

Giam, M., Huang, D.C. and Bouillet, P. (2008). BH3-only proteins and their roles in programmed cell death. *Oncogene* **27 Suppl 1,** S128-136.

Gibbons, J.A., Kozubowski, L., Tatchell, K. and Shenolikar, S. (2007). Expression of human protein phosphatase-1 in Saccharomyces cerevisiae highlights the role of phosphatase isoforms in regulating eukaryotic functions. *The Journal of biological chemistry* **282,** 21838-21847.

Gillissen, B., Essmann, F., Graupner, V., Starck, L., Radetzki, S., Dorken, B.*, et al.* (2003). Induction of cell death by the BH3-only Bcl-2 homolog Nbk/Bik is mediated by an entirely Bax-dependent mitochondrial pathway. *The EMBO journal* **22,** 3580-3590.

Gitlin, L., Barchet, W., Gilfillan, S., Cella, M., Beutler, B., Flavell, R.A.*, et al.* (2006). Essential role of mda-5 in type I IFN responses to polyriboinosinic:polyribocytidylic acid and encephalomyocarditis picornavirus. *Proceedings of the National Academy of Sciences of the United States of America* **103,** 8459-8464.

Glasgow, G.M., McGee, M.M., Tarbatt, C.J., Mooney, D.A., Sheahan, B.J. and Atkins, G.J. (1998). The Semliki Forest virus vector induces p53-independent apoptosis. *The Journal of general virology* **79 (Pt 10),** 2405-2410.

Goldberg, J., Huang, H.B., Kwon, Y.G., Greengard, P., Nairn, A.C. and Kuriyan, J. (1995). Three-dimensional structure of the catalytic subunit of protein serine/threonine phosphatase-1. *Nature* **376,** 745-753.

Goldstein, J.C., Waterhouse, N.J., Juin, P., Evan, G.I. and Green, D.R. (2000). The coordinate release of cytochrome c during apoptosis is rapid, complete and kinetically invariant. *Nature cell biology* **2,** 156-162.

Gorbalenya, A.E., Enjuanes, L., Ziebuhr, J. and Snijder, E.J. (2006). Nidovirales: Evolving the largest RNA virus genome. *Virus Res* **117,** 17-37.

Gorbalenya, A.E., Koonin, E.V. and Lai, M.M. (1991). Putative papain-related thiol proteases of positive-strand RNA viruses. Identification of rubi- and aphthovirus proteases and delineation of a novel conserved domain associated with proteases of rubi-, alpha- and coronaviruses. *FEBS letters* **288,** 201-205.

Gregg, N. (1941). Congenital cataract following German measles in the mother. *Trans Ophthalmol Soc Aust***,** 35-46.

Griffiths, G.J., Dubrez, L., Morgan, C.P., Jones, N.A., Whitehouse, J., Corfe, B.M.*, et al.* (1999a). Cell damage-induced conformational changes of the pro-apoptotic protein bak in vivo precede the onset of apoptosis. *Journal of Cell Biology* **144,** 903-914.

Griffiths, G.J., Dubrez, L., Morgan, C.P., Jones, N.A., Whitehouse, J., Corfe, B.M.*, et al.* (1999b). Cell damage-induced conformational changes of the pro-apoptotic protein Bak in vivo precede the onset of apoptosis. *The Journal of cell biology* **144,** 903-914.

Gupta, A.K., Das, T. and Banerjee, A.K. (1995). Casein Kinase-Ii Is the P-Protein Phosphorylating Cellular Kinase Associated with the Ribonucleoprotein Complex of Purified Vesicular Stomatitis-Virus. *Journal of General Virology* **76,** 365-372.

Haneda, M., Kojima, E., Nishikimi, A., Hasegawa, T., Nakashima, I. and Isobe, K. (2004). Protein phosphatase 1, but not protein phosphatase 2A, dephosphorylates DNA-damaging stress-induced phospho-serine 15 of p53. *FEBS letters* **567,** 171-174.

Happo, L., Strasser, A. and Cory, S. (2012). BH3-only proteins in apoptosis at a glance. *Journal of cell science* **125,** 1081-1087.

Hayajneh, W.A., Colberg-Poley, A.M., Skaletskaya, A., Bartle, L.M., Lesperance, M.M., Contopoulos-Ioannidis, D.G.*, et al.* (2001). The sequence and antiapoptotic functional domains of the human cytomegalovirus UL37 exon 1 immediate early protein are conserved in multiple primary strains. *Virology* **279,** 233-240.

Hemphill, M.L., Forng, R.Y., Abernathy, E.S. and Frey, T.K. (1988). Time course of virus-specific macromolecular synthesis during rubella virus infection in Vero cells. *Virology* **162,** 65-75.

Hendrickx, A., Beullens, M., Ceulemans, H., Den Abt, T., Van Eynde, A., Nicolaescu, E.*, et al.* (2009). Docking motif-guided mapping of the interactome of protein phosphatase-1. *Chemistry & biology* **16,** 365-371.

Henke, A., Launhardt, H., Klement, K., Stelzner, A., Zell, R. and Munder, T. (2000). Apoptosis in coxsackievirus B3-caused diseases: interaction between the capsid protein VP2 and the proapoptotic protein siva. *Journal of virology* **74,** 4284-4290.

Henke, A., Nestler, M., Strunze, S., Saluz, H.P., Hortschansky, P., Menzel, B*., et al.* (2001). The apoptotic capability of coxsackievirus B3 is influenced by the efficient interaction between the capsid protein VP2 and the proapoptotic host protein Siva. *Virology* **289,** 15-22.

Heroes, E., Lesage, B., Gornemann, J., Beullens, M., Van Meervelt, L. and Bollen, M. (2013). The PP1 binding code: a molecular-lego strategy that governs specificity. *The FEBS journal* **280,** 584-595.

Hobman, T. (2013) Rubella Virus. In *Field's Virology*, D.M. Knipe (ed.) 6th edn. Philadelphia, Wolters Kluwer Health/Lippincott Williams & Wilkins, pp. 1069-1099.

Hobman, T.C. and Gillam, S. (1989). In vitro and in vivo expression of rubella virus glycoprotein E2: the signal peptide is contained in the C-terminal region of capsid protein. *Virology* **173,** 241-250.

Hobman, T.C., Lemon, H.F. and Jewell, K. (1997). Characterization of an endoplasmic reticulum retention signal in the rubella virus E1 glycoprotein. *Journal of virology* **71,** 7670-7680.

Hobman, T.C., Lundstrom, M.L. and Gillam, S. (1990). Processing and intracellular transport of rubella virus structural proteins in COS cells. *Virology* **178,** 122-133.

Hobman, T.C., Lundstrom, M.L., Mauracher, C.A., Woodward, L., Gillam, S. and Farquhar, M.G. (1994). Assembly of rubella virus structural proteins into virus-like particles in transfected cells. *Virology* **202,** 574-585.

Hobman, T.C., Qiu, Z.Y., Chaye, H. and Gillam, S. (1991). Analysis of rubella virus E1 glycosylation mutants expressed in COS cells. *Virology* **181,** 768-772.

Hobman, T.C., Shukin, R. and Gillam, S. (1988). Translocation of rubella virus glycoprotein E1 into the endoplasmic reticulum. *Journal of virology* **62,** 4259-4264.

Hobman, T.C., Woodward, L. and Farquhar, M.G. (1992). The rubella virus E1 glycoprotein is arrested in a novel post-ER, pre-Golgi compartment. *The Journal of cell biology* **118,** 795-811.

Hobman, T.C., Woodward, L. and Farquhar, M.G. (1993). The rubella virus E2 and E1 spike glycoproteins are targeted to the Golgi complex. *The Journal of cell biology* **121,** 269-281.

Hobman, T.C., Woodward, L. and Farquhar, M.G. (1995). Targeting of a heterodimeric membrane protein complex to the Golgi: rubella virus E2 glycoprotein contains a transmembrane Golgi retention signal. *Molecular biology of the cell* **6,** 7-20.

Hofmann, J., Pletz, M.W. and Liebert, U.G. (1999). Rubella virus-induced cytopathic effect in vitro is caused by apoptosis. *The Journal of general virology* **80 (Pt 7),** 1657-1664.

Horstmann, D.M. (1965). Rubella and the Rubella Syndrome. New Epidemiologic and Virologic Observations. *California medicine* **102,** 397-403.

Horstmann, D.M. (1969). Discussion paper: the use of primates in experimental viral infections--rubella and the rubella syndrome. *Annals of the New York Academy of Sciences* **162,** 594-597.

Hovi, T. and Vaheri, A. (1970). Rubella virus-specific ribonucleic acids in infected BHK21 cells. *The Journal of general virology* **6,** 77-83.

Hsu, Y.T., Wolter, K.G. and Youle, R.J. (1997a). Cytosol-to-membrane redistribution of Bax and Bcl-X-L during apoptosis. *Proceedings of the National Academy of Sciences of the United States of America* **94,** 3668-3672.

Hsu, Y.T. and Youle, R.J. (1997b). Nonionic detergents induce dimerization among members of the Bcl-2 family. *The Journal of biological chemistry* **272,** 13829-13834.

Hu, M., Crawford, S.A., Henstridge, D.C., Ng, I.H., Boey, E.J., Xu, Y.*, et al.* (2013). p32 protein levels are integral to mitochondrial and endoplasmic reticulum morphology, cell metabolism and survival. *The Biochemical journal* **453,** 381-391.

Hu, Y., Benedict, M.A., Ding, L. and Nunez, G. (1999). Role of cytochrome c and dATP/ATP hydrolysis in Apaf-1-mediated caspase-9 activation and apoptosis. *The EMBO journal* **18,** 3586-3595.

Hurley, T.D., Yang, J., Zhang, L., Goodwin, K.D., Zou, Q., Cortese, M.*, et al.* (2007). Structural basis for regulation of protein phosphatase 1 by inhibitor-2. *The Journal of biological chemistry* **282,** 28874-28883.

Hwang, L.N., Englund, N., Das, T., Banerjee, A.K. and Pattnaik, A.K. (1999). Optimal replication activity of vesicular stomatitis virus RNA polymerase requires phosphorylation of a residue(s) at carboxy-terminal domain II of

its accessory subunit, phosphoprotein P. *Journal of virology* **73,** 5613-5620.

Ilkow, C.S., Goping, I.S. and Hobman, T.C. (2011). The Rubella virus capsid is an anti-apoptotic protein that attenuates the pore-forming ability of Bax. *PLoS pathogens* **7,** e1001291.

Ilkow, C.S., Mancinelli, V., Beatch, M.D. and Hobman, T.C. (2008). Rubella virus capsid protein interacts with poly(a)-binding protein and inhibits translation. *Journal of virology* **82,** 4284-4294.

Ilkow, C.S., Weckbecker, D., Cho, W.J., Meier, S., Beatch, M.D., Goping, I.S*., et al.* (2010a). The rubella virus capsid protein inhibits mitochondrial import. *Journal of virology* **84,** 119-130.

Ilkow, C.S., Willows, S.D. and Hobman, T.C. (2010b). Rubella virus capsid protein: a small protein with big functions. *Future microbiology* **5,** 571-584.

Isenmann, S., Khew-Goodall, Y., Gamble, J., Vadas, M. and Wattenberg, B.W. (1998). A splice-isoform of vesicle-associated membrane protein-1 (VAMP-1) contains a mitochondrial targeting signal. *Molecular biology of the cell* **9,** 1649-1660.

Itahana, K. and Zhang, Y. (2008). Mitochondrial p32 is a critical mediator of ARF-induced apoptosis. *Cancer cell* **13,** 542-553.

Ivanyi-Nagy, R., Lavergne, J.P., Gabus, C., Ficheux, D. and Darlix, J.L. (2008). RNA chaperoning and intrinsic disorder in the core proteins of Flaviviridae. *Nucleic acids research* **36,** 712-725.

Jan, J.T. and Griffin, D.E. (1999). Induction of apoptosis by sindbis virus occurs at cell entry and does not require virus replication. *Journal of virology* **73,** 10296-10302.

Ji, X., Klarmann, G.J. and Preston, B.D. (1996). Effect of human immunodeficiency virus type 1 (HIV-1) nucleocapsid protein on HIV-1 reverse transcriptase activity in vitro. *Biochemistry* **35,** 132-143.

Joe, A.K., Foo, H.H., Kleeman, L. and Levine, B. (1998). The transmembrane domains of Sindbis virus envelope glycoproteins induce cell death. *Journal of virology* **72,** 3935-3943.

Kao, C.F., Chen, S.Y., Chen, J.Y. and Wu Lee, Y.H. (2004). Modulation of p53 transcription regulatory activity and post-translational modification by hepatitis C virus core protein. *Oncogene* **23,** 2472-2483.

Karasawa, S., Azuma, M., Kasama, T., Sakamoto, S., Kabe, Y., Imai, T.*, et al.* (2013). Vitamin K2 covalently binds to Bak and induces Bak-mediated apoptosis. *Molecular pharmacology* **83,** 613-620.

Katow, S. and Sugiura, A. (1985). Antibody response to individual rubella virus proteins in congenital and other rubella virus infections. *Journal of clinical microbiology* **21,** 449-451.

Katow, S. and Sugiura, A. (1988). Low pH-induced conformational change of rubella virus envelope proteins. *The Journal of general virology* **69 (Pt 11),** 2797-2807.

Kaufmann, T., Schlipf, S., Sanz, J., Neubert, K., Stein, R. and Borner, C. (2003). Characterization of the signal that directs Bcl-x(L), but not Bcl-2, to the mitochondrial outer membrane. *The Journal of cell biology* **160,** 53-64.

Kayagaki, N., Yamaguchi, N., Nakayama, M., Eto, H., Okumura, K. and Yagita, H. (1999). Type I interferons (IFNs) regulate tumor necrosis factor-related apoptosis-inducing ligand (TRAIL) expression on human T cells: A novel mechanism for the antitumor effects of type I IFNs. *The Journal of experimental medicine* **189,** 1451-1460.

Kazemi, S., Papadopoulou, S., Li, S., Su, Q., Wang, S., Yoshimura, A.*, et al.* (2004). Control of alpha subunit of eukaryotic translation initiation factor 2 (eIF2 alpha) phosphorylation by the human papillomavirus type 18 E6 oncoprotein: implications for eIF2 alpha-dependent gene expression and cell death. *Molecular and cellular biology* **24,** 3415-3429.

Kee, S.H., Cho, E.J., Song, J.W., Park, K.S., Baek, L.J. and Song, K.J. (2004). Effects of endocytosis inhibitory drugs on rubella virus entry into VeroE6 cells. *Microbiology and immunology* **48,** 823-829.

Kischkel, F.C., Hellbardt, S., Behrmann, I., Germer, M., Pawlita, M., Krammer, P.H. and Peter, M.E. (1995). Cytotoxicity-dependent APO-1 (Fas/CD95)-associated proteins form a death-inducing signaling complex (DISC) with the receptor. *The EMBO journal* **14,** 5579-5588.

Kock, J., Kann, M., Putz, G., Blum, H.E. and von Weizsacker, F. (2003). Central role of a serine phosphorylation site within duck hepatitis B virus core protein for capsid trafficking and genome release. *Journal of Biological Chemistry* **278,** 28123-28129.

Kono, R., Hayakawa, Y., Hibi, M. and Ishii, K. (1969). Experimental vertical transmission of rubella virus in rabbits. *Lancet* **1,** 343-347.

Koonin, E.V. and Dolja, V.V. (1993). Evolution and taxonomy of positive-strand RNA viruses: implications of comparative analysis of amino acid sequences. *Critical reviews in biochemistry and molecular biology* **28,** 375-430.

Korrodi-Gregorio, L., Esteves, S.L. and Fardilha, M. (2014). Protein phosphatase 1 catalytic isoforms: specificity toward interacting proteins. *Translational research : the journal of laboratory and clinical medicine* **164,** 366-391.

Krainer, A.R., Mayeda, A., Kozak, D. and Binns, G. (1991). Functional expression of cloned human splicing factor SF2: homology to RNA-binding proteins, U1 70K, and Drosophila splicing regulators. *Cell* **66,** 383-394.

Kujala, P., Ahola, T., Ehsani, N., Auvinen, P., Vihinen, H. and Kaariainen, L. (1999). Intracellular distribution of rubella virus nonstructural protein P150. *Journal of virology* **73,** 7805-7811.

Kuroda, R., Ikenoue, T., Honsho, M., Tsujimoto, S., Mitoma, J.Y. and Ito, A. (1998). Charged amino acids at the carboxyl-terminal portions determine the intracellular locations of two isoforms of cytochrome b5. *The Journal of biological chemistry* **273,** 31097-31102.

Kuwana, T., Bouchier-Hayes, L., Chipuk, J.E., Bonzon, C., Sullivan, B.A., Green, D.R. and Newmeyer, D.D. (2005). BH3 domains of BH3-only proteins differentially regulate Bax-mediated mitochondrial membrane permeabilization both directly and indirectly. *Molecular cell* **17,** 525-535.

Kuwana, T., Mackey, M.R., Perkins, G., Ellisman, M.H., Latterich, M., Schneiter, R.*, et al.* (2002). Bid, Bax, and lipids cooperate to form supramolecular openings in the outer mitochondrial membrane. *Cell* **111,** 331-342.

Kuyumcu-Martinez, M., Belliot, G., Sosnovtsev, S.V., Chang, K.O., Green, K.Y. and Lloyd, R.E. (2004). Calicivirus 3C-like proteinase inhibits cellular translation by cleavage of poly(A)-binding protein. *Journal of virology* **78,** 8172-8182.

Law, L.J., Ilkow, C.S., Tzeng, W.P., Rawluk, M., Stuart, D.T., Frey, T.K. and Hobman, T.C. (2006). Analyses of phosphorylation events in the rubella virus capsid protein: role in early replication events. *Journal of virology* **80,** 6917-6925.

Law, L.M., Everitt, J.C., Beatch, M.D., Holmes, C.F. and Hobman, T.C. (2003). Phosphorylation of rubella virus capsid regulates its RNA binding activity and virus replication. *Journal of virology* **77,** 1764-1771.

Law, L.M.J., Duncan, R., Esmaili, A., Nakhasi, H.L. and Hobman, T.C. (2001). Rubella virus E2 signal peptide is required for perinuclear localization of capsid protein and virus assembly. *Journal of virology* **75,** 1978-1983.

Lee, J.Y. and Bowden, D.S. (2000). Rubella virus replication and links to teratogenicity. *Clinical microbiology reviews* **13,** 571-587.

Lee, J.Y., Bowden, D.S. and Marshall, J.A. (1996a). Membrane junctions associated with rubella virus infected cells. *Journal of submicroscopic cytology and pathology* **28,** 101-108.

Lee, J.Y., Hwang, D. and Gillam, S. (1996b). Dimerization of rubella virus capsid protein is not required for virus particle formation. *Virology* **216,** 223-227.

Lee, J.Y., Marshall, J.A. and Bowden, D.S. (1992). Replication complexes associated with the morphogenesis of rubella virus. *Archives of virology* **122,** 95-106.

Lee, J.Y., Marshall, J.A. and Bowden, D.S. (1994). Characterization of rubella virus replication complexes using antibodies to double-stranded RNA. *Virology* **200,** 307-312.

Lee, J.Y., Marshall, J.A. and Bowden, D.S. (1999). Localization of rubella virus core particles in vero cells. *Virology* **265,** 110-119.

Lei, K. and Davis, R.J. (2003). JNK phosphorylation of Bim-related members of the Bcl2 family induces Bax-dependent apoptosis. *Proceedings of the National Academy of Sciences of the United States of America* **100,** 2432-2437.

Levy, D.E., Kessler, D.S., Pine, R., Reich, N. and Darnell, J.E., Jr. (1988). Interferon-induced nuclear factors that bind a shared promoter element correlate with positive and negative transcriptional control. *Genes & development* **2,** 383-393.

Li, H., Zhu, H., Xu, C.J. and Yuan, J. (1998). Cleavage of BID by caspase 8 mediates the mitochondrial damage in the Fas pathway of apoptosis. *Cell* **94,** 491-501.

Li, M.L. and Stollar, V. (2004). Alphaviruses and apoptosis. *International reviews of immunology* **23,** 7-24.

Li, P., Nijhawan, D., Budihardjo, I., Srinivasula, S.M., Ahmad, M., Alnemri, E.S. and Wang, X. (1997). Cytochrome c and dATP-dependent formation of Apaf-

1/caspase-9 complex initiates an apoptotic protease cascade. *Cell* **91,** 479-489.

Li, Y., Zhang, C., Chen, X., Yu, J., Wang, Y., Yang, Y.*, et al.* (2011). ICP34.5 protein of herpes simplex virus facilitates the initiation of protein translation by bridging eukaryotic initiation factor 2alpha (eIF2alpha) and protein phosphatase 1. *The Journal of biological chemistry* **286,** 24785-24792.

Liang, Y. and Gillam, S. (2000a). Mutational analysis of the rubella virus nonstructural polyprotein and its cleavage products in virus replication and RNA synthesis. *Journal of virology* **74,** 5133-5141.

Liang, Y., Yao, J. and Gillam, S. (2000b). Rubella virus nonstructural protein protease domains involved in trans- and cis-cleavage activities. *Journal of virology* **74,** 5412-5423.

Lievano, F., Galea, S.A., Thornton, M., Wiedmann, R.T., Manoff, S.B., Tran, T.N.*, et al.* (2012). Measles, mumps, and rubella virus vaccine (M-M-RII): a review of 32 years of clinical and postmarketing experience. *Vaccine* **30,** 6918-6926.

Lin, R.J., Chang, B.L., Yu, H.P., Liao, C.L. and Lin, Y.L. (2006). Blocking of interferon-induced Jak-Stat signaling by Japanese encephalitis virus NS5 through a protein tyrosine phosphatase-mediated mechanism. *Journal of virology* **80,** 5908-5918.

Liu, X., Yang, J., Ghazi, A.M. and Frey, T.K. (2000). Characterization of the zinc binding activity of the rubella virus nonstructural protease. *Journal of virology* **74,** 5949-5956.

Liu, Z., Yang, D., Qiu, Z., Lim, K.T., Chong, P. and Gillam, S. (1996). Identification of domains in rubella virus genomic RNA and capsid protein necessary for specific interaction. *Journal of virology* **70,** 2184-2190.

Llanos, S., Royer, C., Lu, M., Bergamaschi, D., Lee, W.H. and Lu, X. (2011). Inhibitory member of the apoptosis-stimulating proteins of the p53 family (iASPP) interacts with protein phosphatase 1 via a noncanonical binding motif. *The Journal of biological chemistry* **286,** 43039-43044.

Llorian, M., Beullens, M., Andres, I., Ortiz, J.M. and Bollen, M. (2004). SIPP1, a novel pre-mRNA splicing factor and interactor of protein phosphatase-1. *The Biochemical journal* **378,** 229-238.

Loew, L.M. (1994). Characterization of Potentiometric Membrane Dyes. *Adv Chem Ser* **235,** 151-173.

Loo, Y.M. and Gale, M., Jr. (2011). Immune signaling by RIG-I-like receptors. *Immunity* **34,** 680-692.

Lu, W., Lo, S.Y., Chen, M., Wu, K., Fung, Y.K. and Ou, J.H. (1999). Activation of p53 tumor suppressor by hepatitis C virus core protein. *Virology* **264,** 134-141.

Lu, W. and Ou, J.H. (2002). Phosphorylation of hepatitis C virus core protein by protein kinase A and protein kinase C. *Virology* **300,** 20-30.

Lund, K.D. and Chantler, J.K. (2000). Mapping of genetic determinants of rubella virus associated with growth in joint tissue. *Journal of virology* **74,** 796-804.

Lundstrom, M.L., Mauracher, C.A. and Tingle, A.J. (1991). Characterization of carbohydrates linked to rubella virus glycoprotein E2. *The Journal of general virology* **72 (Pt 4),** 843-850.

Luo, X., Budihardjo, I., Zou, H., Slaughter, C. and Wang, X. (1998). Bid, a Bcl2 interacting protein, mediates cytochrome c release from mitochondria in response to activation of cell surface death receptors. *Cell* **94,** 481-490.

Ma, J., Edlich, F., Bermejo, G.A., Norris, K.L., Youle, R.J. and Tjandra, N. (2012). Structural mechanism of Bax inhibition by cytomegalovirus protein vMIA. *Proceedings of the National Academy of Sciences of the United States of America* **109,** 20901-20906.

Maassab, H.F. and Veronelli, J.A. (1966). Characteristics of serially propagated monkey kidney cell cultures with persistent rubella infection. *Journal of bacteriology* **91,** 436-441.

Maes, R., Vaheri, A., Sedwick, D. and Plotkin, S. (1966). Synthesis of virus and macromolecules by rubella-infected cells. *Nature* **210,** 384-385.

Magliano, D., Marshall, J.A., Bowden, D.S., Vardaxis, N., Meanger, J. and Lee, J.Y. (1998). Rubella virus replication complexes are virus-modified lysosomes. *Virology* **240,** 57-63.

Mamiya, N. and Worman, H.J. (1999). Hepatitis C virus core protein binds to a DEAD box RNA helicase. *The Journal of biological chemistry* **274,** 15751-15756.

Mammas, I.N., Sourvinos, G., Giannoudis, A. and Spandidos, D.A. (2008). Human papilloma virus (HPV) and host cellular interactions. *Pathology oncology research : POR* **14,** 345-354.

Mangala Prasad, V., Willows, S.D., Fokine, A., Battisti, A.J., Sun, S., Plevka, P.*, et al.* (2013). Rubella virus capsid protein structure and its role in virus assembly and infection. *Proceedings of the National Academy of Sciences of the United States of America* **110,** 20105-20110.

Marr, L.D., Sanchez, A. and Frey, T.K. (1991). Efficient in vitro translation and processing of the rubella virus structural proteins in the presence of microsomes. *Virology* **180,** 400-405.

Marr, L.D., Wang, C.Y. and Frey, T.K. (1994). Expression of the rubella virus nonstructural protein ORF and demonstration of proteolytic processing. *Virology* **198,** 586-592.

Mastromarino, P., Cioe, L., Rieti, S. and Orsi, N. (1990). Role of Membrane Phospholipids and Glycolipids in the Vero Cell-Surface Receptor for Rubella-Virus. *Med Microbiol Immun* **179,** 105-114.

Maton, W. (1815). Some account of a rash liable to be mistaken for scarlatina. *Med Trans Coll Physicians (London)* **5,** 149-165.

Matthews, D.A. and Russell, W.C. (1998). Adenovirus core protein V interacts with p32--a protein which is associated with both the mitochondria and the nucleus. *The Journal of general virology* **79 (Pt 7),** 1677-1685.

Matthews, J.D., Tzeng, W.P. and Frey, T.K. (2009). Determinants of subcellular localization of the rubella virus nonstructural replicase proteins. *Virology* **390,** 315-323.

Matthews, J.D., Tzeng, W.P. and Frey, T.K. (2010). Analysis of the function of cytoplasmic fibers formed by the rubella virus nonstructural replicase proteins. *Virology* **406,** 212-227.

Mauracher, C.A., Gillam, S., Shukin, R. and Tingle, A.J. (1991). pH-dependent solubility shift of rubella virus capsid protein. *Virology* **181,** 773-777.

Mavinakere, M.S. and Colberg-Poley, A.M. (2004). Dual targeting of the human cytomegalovirus UL37 exon 1 protein during permissive infection. *The Journal of general virology* **85,** 323-329.

Mavinakere, M.S., Williamson, C.D., Goldmacher, V.S. and Colberg-Poley, A.M. (2006). Processing of human cytomegalovirus UL37 mutant glycoproteins

in the endoplasmic reticulum lumen prior to mitochondrial importation. *Journal of virology* **80,** 6771-6783.

McDonald, H., Hobman, T.C. and Gillam, S. (1991). The influence of capsid protein cleavage on the processing of E2 and E1 glycoproteins of rubella virus. *Virology* **183,** 52-60.

Medigeshi, G.R., Lancaster, A.M., Hirsch, A.J., Briese, T., Lipkin, W.I., Defilippis, V.*, et al.* (2007). West Nile virus infection activates the unfolded protein response, leading to CHOP induction and apoptosis. *Journal of virology* **81,** 10849-10860.

Megyeri, K., Berencsi, K., Halazonetis, T.D., Prendergast, G.C., Gri, G., Plotkin, S.A.*, et al.* (1999). Involvement of a p53-dependent pathway in rubella virus-induced apoptosis. *Virology* **259,** 74-84.

Melancon, P. and Garoff, H. (1987). Processing of the Semliki Forest virus structural polyprotein: role of the capsid protease. *Journal of virology* **61,** 1301-1309.

Menser, M.A., Forrest, J.M. and Bransby, R.D. (1978). Rubella infection and diabetes mellitus. *Lancet* **1,** 57-60.

Merrill, R.A., Dagda, R.K., Dickey, A.S., Cribbs, J.T., Green, S.H., Usachev, Y.M. and Strack, S. (2011). Mechanism of neuroprotective mitochondrial remodeling by PKA/AKAP1. *PLoS biology* **9,** e1000612.

Mesman, A.W., Zijlstra-Willems, E.M., Kaptein, T.M., de Swart, R.L., Davis, M.E., Ludlow, M.*, et al.* (2014). Measles virus suppresses RIG-I-like receptor activation in dendritic cells via DC-SIGN-mediated inhibition of PP1 phosphatases. *Cell host & microbe* **16,** 31-42.

Mi, J., Li, Z.Y., Ni, S., Steinwaerder, D. and Lieber, A. (2001). Induced apoptosis supports spread of adenovirus vectors in tumors. *Human gene therapy* **12,** 1343-1352.

Mifune, K., Desmyter, J. and Rawls, W.E. (1970). Effect of exogenous interferon on rubella virus production in carrier cultures of cells defective in interferon production. *Infection and immunity* **2,** 132-138.

Miki, N.P. and Chantler, J.K. (1992). Differential ability of wild-type and vaccine strains of rubella virus to replicate and persist in human joint tissue. *Clinical and experimental rheumatology* **10,** 3-12.

Mir, M.A. and Panganiban, A.T. (2006). Characterization of the RNA chaperone activity of hantavirus nucleocapsid protein. *Journal of virology* **80,** 6276-6285.

Misumi, S., Inoue, M., Dochi, T., Kishimoto, N., Hasegawa, N., Takamune, N. and Shoji, S. (2010). Uncoating of human immunodeficiency virus type 1 requires prolyl isomerase Pin1. *The Journal of biological chemistry* **285,** 25185-25195.

Mitzner, D., Dudek, S.E., Studtrucker, N., Anhlan, D., Mazur, I., Wissing, J.*, et al.* (2009). Phosphorylation of the influenza A virus protein PB1-F2 by PKC is crucial for apoptosis promoting functions in monocytes. *Cellular microbiology* **11,** 1502-1516.

Mohan, K.V., Ghebrehiwet, B. and Atreya, C.D. (2002). The N-terminal conserved domain of rubella virus capsid interacts with the C-terminal region of cellular p32 and overexpression of p32 enhances the viral infectivity. *Virus Res* **85,** 151-161.

Mondal, A., Potts, G.K., Dawson, A.R., Coon, J.J. and Mehle, A. (2015). Phosphorylation at the homotypic interface regulates nucleoprotein oligomerization and assembly of the influenza virus replication machinery. *PLoS pathogens* **11,** e1004826.

Moorhead, G.B., Trinkle-Mulcahy, L. and Ulke-Lemee, A. (2007). Emerging roles of nuclear protein phosphatases. *Nature reviews. Molecular cell biology* **8,** 234-244.

Murphy, F.A., Halonen, P.E. and Harrison, A.K. (1968). Electron Microscopy of Development of Rubella Virus in Bhk-21 Cells. *Journal of virology* **2,** 1223-&.

Muta, T., Kang, D., Kitajima, S., Fujiwara, T. and Hamasaki, N. (1997). p32 protein, a splicing factor 2-associated protein, is localized in mitochondrial matrix and is functionally important in maintaining oxidative phosphorylation. *The Journal of biological chemistry* **272,** 24363-24370.

Muzio, M., Chinnaiyan, A.M., Kischkel, F.C., O'Rourke, K., Shevchenko, A., Ni, J.*, et al.* (1996). FLICE, a novel FADD-homologous ICE/CED-3-like protease, is recruited to the CD95 (Fas/APO-1) death--inducing signaling complex. *Cell* **85,** 817-827.

Naeye, R.L. and Blanc, W. (1965). Pathogenesis of congenital rubella. *Jama* **194,** 1277-1283.

Nakhasi, H.L., Singh, N.K., Pogue, G.P., Cao, X.Q. and Rouault, T.A. (1994). Identification and characterization of host factor interactions with cis-acting elements of rubella virus RNA. *Archives of virology. Supplementum* **9,** 255-267.

Nakhasi, H.L., Thomas, D., Zheng, D.X. and Liu, T.Y. (1989). Nucleotide sequence of capsid, E2 and E1 protein genes of Rubella virus vaccine strain RA27/3. *Nucleic acids research* **17,** 4393-4394.

Nechushtan, A., Smith, C.L., Hsu, Y.T. and Youle, R.J. (1999). Conformation of the Bax C-terminus regulates subcellular location and cell death. *The EMBO journal* **18,** 2330-2341.

Nemoto, Y. and De Camilli, P. (1999). Recruitment of an alternatively spliced form of synaptojanin 2 to mitochondria by the interaction with the PDZ domain of a mitochondrial outer membrane protein. *The EMBO journal* **18,** 2991-3006.

Neu, N., Duchon, J. and Zachariah, P. (2015). TORCH Infections. *Clinics in perinatology* **42,** 77-103.

Neznanov, N., Kondratova, A., Chumakov, K.M., Angres, B., Zhumabayeva, B., Agol, V.I. and Gudkov, A.V. (2001). Poliovirus protein 3A inhibits tumor necrosis factor (TNF)-induced apoptosis by eliminating the TNF receptor from the cell surface. *Journal of virology* **75,** 10409-10420.

Nguyen, M., Millar, D.G., Yong, V.W., Korsmeyer, S.J. and Shore, G.C. (1993). Targeting of Bcl-2 to the mitochondrial outer membrane by a COOH-terminal signal anchor sequence. *The Journal of biological chemistry* **268,** 25265-25268.

Nomura-Takigawa, Y., Nagano-Fujii, M., Deng, L., Kitazawa, S., Ishido, S., Sada, K. and Hotta, H. (2006). Non-structural protein 4A of Hepatitis C virus accumulates on mitochondria and renders the cells prone to undergoing mitochondria-mediated apoptosis. *The Journal of general virology* **87,** 1935-1945.

Oker-Blom, C. (1984). The gene order for rubella virus structural proteins is NH2-C-E2-E1-COOH. *Journal of virology* **51,** 354-358.

Oker-Blom, C., Ulmanen, I., Kaariainen, L. and Pettersson, R.F. (1984). Rubella virus 40S genome RNA specifies a 24S subgenomic mRNA that codes for a precursor to structural proteins. *Journal of virology* **49,** 403-408.

Ontiveros, S.J., Li, Q. and Jonsson, C.B. (2010). Modulation of apoptosis and immune signaling pathways by the Hantaan virus nucleocapsid protein. *Virology* **401,** 165-178.

Otsuka, M., Kato, N., Lan, K., Yoshida, H., Kato, J., Goto, T*., et al.* (2000). Hepatitis C virus core protein enhances p53 function through augmentation of DNA binding affinity and transcriptional ability. *The Journal of biological chemistry* **275,** 34122-34130.

Ott, M., Norberg, E., Walter, K.M., Schreiner, P., Kemper, C., Rapaport, D*., et al.* (2007). The mitochondrial TOM complex is required for tBid/Bax-induced cytochrome c release. *The Journal of biological chemistry* **282,** 27633-27639.

Pappas, C.L., Tzeng, W.P. and Frey, T.K. (2006). Evaluation of cis-acting elements in the rubella virus subgenomic RNA that play a role in its translation. *Archives of virology* **151,** 327-346.

Park, S.W., Han, M.G., Park, C., Ju, Y.R., Ahn, B.Y. and Ryou, J. (2013). Hantaan virus nucleocapsid protein stimulates MDM2-dependent p53 degradation. *The Journal of general virology* **94,** 2424-2428.

Parkman, P.D., Meyer, H.M., Jr., Kirschstein, R.L. and Hopps, H.E. (1966). Attenuated rubella virus. I. Development and laboratory characterization. *The New England journal of medicine* **275,** 569-574.

Pattnaik, A.K., Hwang, L., Li, T., Englund, N., Mathur, M., Das, T. and Banerjee, A.K. (1997). Phosphorylation within the amino-terminal acidic domain I of the phosphoprotein of vesicular stomatitis virus is required for transcription but not for replication. *Journal of virology* **71,** 8167-8175.

Pauleau, A.L., Larochette, N., Giordanetto, F., Scholz, S.R., Poncet, D., Zamzami, N*., et al.* (2007). Structure-function analysis of the interaction between Bax and the cytomegalovirus-encoded protein vMIA. *Oncogene* **26,** 7067-7080.

Pederson, T. (2011). The nucleolus. *Cold Spring Harbor perspectives in biology* **3**.

Peetermans, J. and Huygelen, C. (1967). Attenuation ob rubella virus by serial passage in primary rabbit kidney cell cultures. I. Growth characteristics in vitro and production of experimental vaccines at different passage levels. *Archiv fur die gesamte Virusforschung* **21,** 133-143.

Peliska, J.A., Balasubramanian, S., Giedroc, D.P. and Benkovic, S.J. (1994). Recombinant HIV-1 nucleocapsid protein accelerates HIV-1 reverse transcriptase catalyzed DNA strand transfer reactions and modulates RNase H activity. *Biochemistry* **33,** 13817-13823.

Perelygina, L., Zheng, Q., Metcalfe, M. and Icenogle, J. (2013). Persistent infection of human fetal endothelial cells with rubella virus. *PloS one* **8,** e73014.

Perkins, G.A., Renken, C.W., van der Klei, I.J., Ellisman, M.H., Neupert, W. and Frey, T.G. (2001). Electron tomography of mitochondria after the arrest of protein import associated with Tom19 depletion. *European journal of cell biology* **80,** 139-150.

Peter, M.E. and Krammer, P.H. (2003). The CD95(APO-1/Fas) DISC and beyond. *Cell death and differentiation* **10,** 26-35.

Peti, W., Nairn, A.C. and Page, R. (2013). Structural basis for protein phosphatase 1 regulation and specificity. *The FEBS journal* **280,** 596-611.

Petit, E., Oliver, L. and Vallette, F.M. (2009). The mitochondrial outer membrane protein import machinery: a new player in apoptosis? *Frontiers in bioscience* **14,** 3563-3570.

Petruzziello, R., Orsi, N., Macchia, S., Rieti, S., Frey, T.K. and Mastromarino, P. (1996). Pathway of rubella virus infectious entry into Vero cells. *The Journal of general virology* **77 (Pt 2),** 303-308.

Peyerl, F.W., Dai, S., Murphy, G.A., Crawford, F., White, J., Marrack, P. and Kappler, J.W. (2007). Elucidation of some Bax conformational changes through crystallization of an antibody-peptide complex. *Cell death and differentiation* **14,** 447-452.

Phillips, C.A., Melnick, J.L., Yow, M.D., Bayatpour, M. and Burkhardt, M. (1965). Persistence of Virus in Infants with Congenital Rubella and in Normal Infants with a History of Maternal Rubella. *Jama* **193,** 1027-1029.

Plotkin, S.A., Farquhar, J., Katz, M. and Ingalls, T.H. (1967). A new attenuated rubella virus grown in human fibroblasts: evidence for reduced nasopharyngeal excretion. *American journal of epidemiology* **86,** 468-477.

Plotkin, S.A., Farquhar, J.D. and Ogra, P.L. (1973). Immunologic properties of RA27-3 rubella virus vaccine. A comparison with strains presently licensed in the United States. *Jama* **225,** 585-590.

Pogue, G.P., Cao, X.Q., Singh, N.K. and Nakhasi, H.L. (1993). 5' sequences of rubella virus RNA stimulate translation of chimeric RNAs and specifically interact with two host-encoded proteins. *Journal of virology* **67,** 7106-7117.

Poncet, D., Larochette, N., Pauleau, A.L., Boya, P., Jalil, A.A., Cartron, P.F.*, et al.* (2004). An anti-apoptotic viral protein that recruits Bax to mitochondria. *The Journal of biological chemistry* **279,** 22605-22614.

Porter, A.C., Chernajovsky, Y., Dale, T.C., Gilbert, C.S., Stark, G.R. and Kerr, I.M. (1988). Interferon response element of the human gene 6-16. *The EMBO journal* **7,** 85-92.

Porter, A.G. (1993). Picornavirus nonstructural proteins: emerging roles in virus replication and inhibition of host cell functions. *Journal of virology* **67,** 6917-6921.

Preblud, S.R. and Williams, N.M. (1985). Fetal risk associated with rubella vaccine: implications for vaccination of susceptible women. *Obstetrics and gynecology* **66,** 121-123.

Prikhod'ko, E.A., Prikhod'ko, G.G., Siegel, R.M., Thompson, P., Major, M.E. and Cohen, J.I. (2004). The NS3 protein of hepatitis C virus induces caspase-8-mediated apoptosis independent of its protease or helicase activities. *Virology* **329,** 53-67.

Pugachev, K.V., Abernathy, E.S. and Frey, T.K. (1997). Improvement of the specific infectivity of the rubella virus (RUB) infectious clone: determinants of cytopathogenicity induced by RUB map to the nonstructural proteins. *Journal of virology* **71,** 562-568.

Pugachev, K.V. and Frey, T.K. (1998). Rubella virus induces apoptosis in culture cells. *Virology* **250,** 359-370.

Putcha, G.V., Le, S., Frank, S., Besirli, C.G., Clark, K., Chu, B.*, et al.* (2003). JNK-mediated BIM phosphorylation potentiates BAX-dependent apoptosis. *Neuron* **38,** 899-914.

Qiu, Z., Hobman, T.C., McDonald, H.L., Seto, N.O. and Gillam, S. (1992). Role of N-linked oligosaccharides in processing and intracellular transport of E2 glycoprotein of rubella virus. *Journal of virology* **66,** 3514-3521.

Qiu, Z., Ou, D., Hobman, T.C. and Gillam, S. (1994). Expression and characterization of virus-like particles containing rubella virus structural proteins. *Journal of virology* **68,** 4086-4091.

Ramanathan, M.P., Chambers, J.A., Pankhong, P., Chattergoon, M., Attatippaholkun, W., Dang, K.*, et al.* (2006). Host cell killing by the West Nile Virus NS2B-NS3 proteolytic complex: NS3 alone is sufficient to recruit caspase-8-based apoptotic pathway. *Virology* **345,** 56-72.

Rathore, A.P., Ng, M.L. and Vasudevan, S.G. (2013). Differential unfolded protein response during Chikungunya and Sindbis virus infection: CHIKV nsP4 suppresses eIF2alpha phosphorylation. *Virology journal* **10,** 36.

Rawls, W.E. and Melnick, J.L. (1966). Rubella virus carrier cultures derived from congenitally infected infants. *The Journal of experimental medicine* **123,** 795-816.

Ray, R.B., Steele, R., Meyer, K. and Ray, R. (1997). Transcriptional repression of p53 promoter by hepatitis C virus core protein. *The Journal of biological chemistry* **272,** 10983-10986.

Rintahaka, J., Wiik, D., Kovanen, P.E., Alenius, H. and Matikainen, S. (2008a). Cytosolic antiviral RNA recognition pathway activates caspases 1 and 3. *Journal of immunology* **180,** 1749-1757.

Rintahaka, J., Wiik, D., Kovanen, P.E., Alenius, H. and Matikainen, S. (2008b). Cytosolic antiviral RNA recognition pathway activates caspases 1 and 3. *Journal of immunology* **180,** 1749-1757.

Risco, C., Carrascosa, J.L. and Frey, T.K. (2003). Structural maturation of rubella virus in the Golgi complex. *Virology* **312,** 261-269.

Rogne, M., Stokka, A.J., Tasken, K., Collas, P. and Kuntziger, T. (2009). Mutually exclusive binding of PP1 and RNA to AKAP149 affects the mitochondrial network. *Human molecular genetics* **18,** 978-987.

Rossmann, M.G. and Johnson, J.E. (1989). Icosahedral RNA virus structure. *Annual review of biochemistry* **58,** 533-573.

Roulston, A., Marcellus, R.C. and Branton, P.E. (1999). Viruses and apoptosis. *Annual review of microbiology* **53,** 577-628.

Rozanov, M.N., Koonin, E.V. and Gorbalenya, A.E. (1992). Conservation of the putative methyltransferase domain: a hallmark of the 'Sindbis-like'

supergroup of positive-strand RNA viruses. *The Journal of general virology* **73 (Pt 8),** 2129-2134.

Ruffolo, S.C., Breckenridge, D.G., Nguyen, M., Goping, I.S., Gross, A., Korsmeyer, S.J*., et al.* (2000). BID-dependent and BID-independent pathways for BAX insertion into mitochondria. *Cell death and differentiation* **7,** 1101-1108.

Ruffolo, S.C. and Shore, G.C. (2003). BCL-2 selectively interacts with the BID-induced open conformer of BAK, inhibiting BAK auto-oligomerization. *The Journal of biological chemistry* **278,** 25039-25045.

Rutherford, M.N., Hannigan, G.E. and Williams, B.R. (1988). Interferon-induced binding of nuclear factors to promoter elements of the 2-5A synthetase gene. *The EMBO journal* **7,** 751-759.

Saito, M., Korsmeyer, S.J. and Schlesinger, P.H. (2000). BAX-dependent transport of cytochrome c reconstituted in pure liposomes. *Nature cell biology* **2,** 553-555.

Sakata, M., Otsuki, N., Okamoto, K., Anraku, M., Nagai, M., Takeda, M. and Mori, Y. (2014). Short self-interacting N-terminal region of rubella virus capsid protein is essential for cooperative actions of capsid and nonstructural p150 proteins. *Journal of virology* **88,** 11187-11198.

Salaun, B., Coste, I., Rissoan, M.C., Lebecque, S.J. and Renno, T. (2006). TLR3 can directly trigger apoptosis in human cancer cells. *Journal of immunology* **176,** 4894-4901.

Salaun, B., Lebecque, S., Matikainen, S., Rimoldi, D. and Romero, P. (2007). Toll-like receptor 3 expressed by melanoma cells as a target for therapy? *Clinical cancer research : an official journal of the American Association for Cancer Research* **13,** 4565-4574.

Saleh, A., Srinivasula, S.M., Acharya, S., Fishel, R. and Alnemri, E.S. (1999). Cytochrome c and dATP-mediated oligomerization of Apaf-1 is a prerequisite for procaspase-9 activation. *The Journal of biological chemistry* **274,** 17941-17945.

Santel, A. and Fuller, M.T. (2001). Control of mitochondrial morphology by a human mitofusin. *Journal of cell science* **114,** 867-874.

Sarosiek, K.A., Chi, X.K., Bachman, J.A., Sims, J.J., Montero, J., Patel, L*., et al.* (2013). BID Preferentially Activates BAK while BIM Preferentially Activates BAX, Affecting Chemotherapy Response. *Molecular cell* **51,** 751-765.

Sato, M., Tanaka, H., Yamada, T. and Yamamoto, N. (1977). Persistent infection of BHK21/WI-2 cells with rubella virus and characterization of rubella variants. *Archives of virology* **54,** 333-343.

Sattler, M., Liang, H., Nettesheim, D., Meadows, R.P., Harlan, J.E., Eberstadt, M*., et al.* (1997). Structure of Bcl-xL-Bak peptide complex: recognition between regulators of apoptosis. *Science* **275,** 983-986.

Scaffidi, C., Fulda, S., Srinivasan, A., Friesen, C., Li, F., Tomaselli, K.J*., et al.* (1998). Two CD95 (APO-1/Fas) signaling pathways. *The EMBO journal* **17,** 1675-1687.

Scheele, C.M. and Pfefferkorn, E.R. (1969). Kinetics of incorporation of structural proteins into Sindbis virions. *Journal of virology* **3,** 369-375.

Sedwick, W.D. and Sokol, F. (1970). Nucleic acid of rubella virus and its replication in hamster kidney cells. *Journal of virology* **5,** 478-489.

Siemen, D. and Ziemer, M. (2013). What is the nature of the mitochondrial permeability transition pore and what is it not? *IUBMB life* **65,** 255-262.

Simons, K. and Garoff, H. (1980). The budding mechanisms of enveloped animal viruses. *The Journal of general virology* **50,** 1-21.

Siskind, L.J., Mullen, T.D., Romero Rosales, K., Clarke, C.J., Hernandez-Corbacho, M.J., Edinger, A.L. and Obeid, L.M. (2010). The BCL-2 protein BAK is required for long-chain ceramide generation during apoptosis. *The Journal of biological chemistry* **285,** 11818-11826.

Smith, R.W. and Gray, N.K. (2010). Poly(A)-binding protein (PABP): a common viral target. *The Biochemical journal* **426,** 1-12.

Stanwick, T.L. and Hallum, J.V. (1974). Role of interferon in six cell lines persistently infected with rubella virus. *Infection and immunity* **10,** 810-815.

Stojanovski, D., Koutsopoulos, O.S., Okamoto, K. and Ryan, M.T. (2004). Levels of human Fis1 at the mitochondrial outer membrane regulate mitochondrial morphology. *Journal of cell science* **117,** 1201-1210.

Street, A., Macdonald, A., Crowder, K. and Harris, M. (2004). The Hepatitis C virus NS5A protein activates a phosphoinositide 3-kinase-dependent survival signaling cascade. *The Journal of biological chemistry* **279,** 12232-12241.

Su, H.L., Liao, C.L. and Lin, Y.L. (2002). Japanese encephalitis virus infection initiates endoplasmic reticulum stress and an unfolded protein response. *Journal of virology* **76,** 4162-4171.

Suhrbier, A., Jaffar-Bandjee, M.C. and Gasque, P. (2012). Arthritogenic alphaviruses-an overview. *Nat Rev Rheumatol* **8,** 420-429.

Sukumaran, L., McNeil, M.M., Moro, P.L., Lewis, P.W., Winiecki, S.K. and Shimabukuro, T.T. (2015). Adverse Events Following Measles, Mumps, and Rubella Vaccine in Adults Reported to the Vaccine Adverse Event Reporting System (VAERS), 2003-2013. *Clinical infectious diseases : an official publication of the Infectious Diseases Society of America*.

Sunayama, J., Ando, Y., Itoh, N., Tomiyama, A., Sakurada, K., Sugiyama, A*., et al.* (2004). Physical and functional interaction between BH3-only protein Hrk and mitochondrial pore-forming protein p32. *Cell death and differentiation* **11,** 771-781.

Suomalainen, M., Garoff, H. and Baron, M.D. (1990a). The E2 Signal Sequence of Rubella-Virus Remains Part of the Capsid Protein and Confers Membrane Association Invitro. *Journal of virology* **64,** 5500-5509.

Suomalainen, M., Garoff, H. and Baron, M.D. (1990b). The E2 signal sequence of rubella virus remains part of the capsid protein and confers membrane association in vitro. *Journal of virology* **64,** 5500-5509.

Suppiah, S., Mousa, H.A., Tzeng, W.P., Matthews, J.D. and Frey, T.K. (2012). Binding of cellular p32 protein to the rubella virus P150 replicase protein via PxxPxR motifs. *The Journal of general virology* **93,** 807-816.

Surjit, M., Kumar, R., Mishra, R.N., Reddy, M.K., Chow, V.T. and Lal, S.K. (2005). The severe acute respiratory syndrome coronavirus nucleocapsid protein is phosphorylated and localizes in the cytoplasm by 14-3-3-mediated translocation. *Journal of virology* **79,** 11476-11486.

Suzuki, M., Youle, R.J. and Tjandra, N. (2000). Structure of Bax: Coregulation of dimer formation and intracellular localization. *Cell* **103,** 645-654.

Svedmyr, A. (1965). Persistent Infection with Rubella Virus in Rk 13 Cells. *Archiv fur die gesamte Virusforschung* **16,** 464-465.

Takenaka, I., Morin, F., Seizinger, B.R. and Kley, N. (1995). Regulation of the sequence-specific DNA binding function of p53 by protein kinase C and

protein phosphatases. *The Journal of biological chemistry* **270,** 5405-5411.

Taylor, R.C., Cullen, S.P. and Martin, S.J. (2008). Apoptosis: controlled demolition at the cellular level. *Nature reviews. Molecular cell biology* **9,** 231-241.

Thayyullathil, F., Chathoth, S., Shahin, A., Kizhakkayil, J., Hago, A., Patel, M. and Galadari, S. (2011). Protein phosphatase 1-dependent dephosphorylation of Akt is the prime signaling event in sphingosine-induced apoptosis in Jurkat cells. *Journal of cellular biochemistry* **112,** 1138-1153.

Theodorakis, P., Lomonosova, E. and Chinnadurai, G. (2002). Critical requirement of BAX for manifestation of apoptosis induced by multiple stimuli in human epithelial cancer cells. *Cancer research* **62,** 3373-3376.

Thomas, M. and Banks, L. (1999). Human papillomavirus (HPV) E6 interactions with Bak are conserved amongst E6 proteins from high and low risk HPV types. *The Journal of general virology* **80 (Pt 6),** 1513-1517.

Thomas, S., Rai, J., John, L., Schaefer, S., Putzer, B.M. and Herchenroder, O. (2013). Chikungunya virus capsid protein contains nuclear import and export signals. *Virology journal* **10,** 269.

Tingle, A.J., Allen, M., Petty, R.E., Kettyls, G.D. and Chantler, J.K. (1986). Rubella-associated arthritis. I. Comparative study of joint manifestations associated with natural rubella infection and RA 27/3 rubella immunisation. *Annals of the rheumatic diseases* **45,** 110-114.

Tondury, G. and Smith, D.W. (1966). Fetal rubella pathology. *The Journal of pediatrics* **68,** 867-879.

Trinkle-Mulcahy, L., Ajuh, P., Prescott, A., Claverie-Martin, F., Cohen, S., Lamond, A.I. and Cohen, P. (1999). Nuclear organisation of NIPP1, a regulatory subunit of protein phosphatase 1 that associates with pre-mRNA splicing factors. *Journal of cell science* **112 (Pt 2),** 157-168.

Tyor, W. and Harrison, T. (2014). Mumps and rubella. *Handbook of clinical neurology* **123,** 591-600.

Tzeng, W.P., Chen, M.H., Derdeyn, C.A. and Frey, T.K. (2001). Rubella virus DI RNAs and replicons: requirement for nonstructural proteins acting in cis for amplification by helper virus. *Virology* **289,** 63-73.

Tzeng, W.P. and Frey, T.K. (2003). Complementation of a deletion in the rubella virus p150 nonstructural protein by the viral capsid protein. *Journal of virology* **77,** 9502-9510.

Tzeng, W.P. and Frey, T.K. (2005). Rubella virus capsid protein modulation of viral genomic and subgenomic RNA synthesis. *Virology* **337,** 327-334.

Tzeng, W.P. and Frey, T.K. (2009). Functional replacement of a domain in the rubella virus p150 replicase protein by the virus capsid protein. *Journal of virology* **83,** 3549-3555.

Tzeng, W.P., Matthews, J.D. and Frey, T.K. (2006). Analysis of rubella virus capsid protein-mediated enhancement of replicon replication and mutant rescue. *Journal of virology* **80,** 3966-3974.

Ueda, K., Shingaki, Y., Sato, T., Tokugawa, K. and Sasaki, H. (1985). Hemolytic anemia following postnatally acquired rubella during the 1975-1977 rubella epidemic in Japan. *Clinical pediatrics* **24,** 155-157.

Urbanowski, M.D. and Hobman, T.C. (2013). The West Nile virus capsid protein blocks apoptosis through a phosphatidylinositol 3-kinase-dependent mechanism. *Journal of virology* **87,** 872-881.

Vaheri, A. and Cristofalo, V.J. (1967). Metabolism of rubella virus-infected BHK 21 cells. Enhanced glycolysis and late cellular inhibition. *Archiv fur die gesamte Virusforschung* **21,** 425-436.

Van Opdenbosch, N., Van den Broeke, C., De Regge, N., Tabares, E. and Favoreel, H.W. (2012). The IE180 protein of pseudorabies virus suppresses phosphorylation of translation initiation factor eIF2alpha. *Journal of virology* **86,** 7235-7240.

van Steeg, H., Kasperaitis, M., Voorma, H.O. and Benne, R. (1984). Infection of neuroblastoma cells by Semliki Forest virus. The interference of viral capsid protein with the binding of host messenger RNAs into initiation complexes is the cause of the shut-off of host protein synthesis. *European journal of biochemistry / FEBS* **138,** 473-478.

Virshup, D.M. and Shenolikar, S. (2009). From promiscuity to precision: protein phosphatases get a makeover. *Molecular cell* **33,** 537-545.

Vives-Bauza, C., Zhou, C., Huang, Y., Cui, M., de Vries, R.L., Kim, J.*, et al.* (2010). PINK1-dependent recruitment of Parkin to mitochondria in mitophagy.

Proceedings of the National Academy of Sciences of the United States of America **107,** 378-383.

Voiland, A. and Bardeletti, G. (1980). Fatty acid composition of rubella virus and BHK21/13S infected cells. *Archives of virology* **64,** 319-328.

von Bonsdorff, C.H. and Vaheri, A. (1969). Growth of rubella virus in BHK21 cells: electron microscopy of morphogenesis. *The Journal of general virology* **5,** 47-51.

Wang, C.Y., Mayo, M.W., Korneluk, R.G., Goeddel, D.V. and Baldwin, A.S., Jr. (1998). NF-kappaB antiapoptosis: induction of TRAF1 and TRAF2 and c-IAP1 and c-IAP2 to suppress caspase-8 activation. *Science* **281,** 1680-1683.

Waris, G., Livolsi, A., Imbert, V., Peyron, J.F. and Siddiqui, A. (2003). Hepatitis C virus NS5A and subgenomic replicon activate NF-kappaB via tyrosine phosphorylation of IkappaBalpha and its degradation by calpain protease. *The Journal of biological chemistry* **278,** 40778-40787.

Washington, K., Ammosova, T., Beullens, M., Jerebtsova, M., Kumar, A., Bollen, M. and Nekhai, S. (2002). Protein phosphatase-1 dephosphorylates the C-terminal domain of RNA polymerase-II. *The Journal of biological chemistry* **277,** 40442-40448.

Waxham, M.N. and Wolinsky, J.S. (1985a). Detailed immunologic analysis of the structural polypeptides of rubella virus using monoclonal antibodies. *Virology* **143,** 153-165.

Waxham, M.N. and Wolinsky, J.S. (1985b). A model of the structural organization of rubella virions. *Reviews of infectious diseases* **7 Suppl 1,** S133-139.

Webster, W.S. (1998). Teratogen update: congenital rubella. *Teratology* **58,** 13-23.

Wei, M.C., Zong, W.X., Cheng, E.H., Lindsten, T., Panoutsakopoulou, V., Ross, A.J., *et al.* (2001). Proapoptotic BAX and BAK: a requisite gateway to mitochondrial dysfunction and death. *Science* **292,** 727-730.

Westphal, D., Dewson, G., Czabotar, P.E. and Kluck, R.M. (2011). Molecular biology of Bax and Bak activation and action. *Biochimica et biophysica acta* **1813,** 521-531.

White, E. (2006). Mechanisms of apoptosis regulation by viral oncogenes in infection and tumorigenesis. *Cell death and differentiation* **13,** 1371-1377.

Wies, E., Wang, M.K., Maharaj, N.P., Chen, K., Zhou, S., Finberg, R.W. and Gack, M.U. (2013). Dephosphorylation of the RNA sensors RIG-I and MDA5 by the phosphatase PP1 is essential for innate immune signaling. *Immunity* **38,** 437-449.

Wild, N.J., Sheppard, S., Smithells, R.W., Holzel, H. and Jones, G. (1989). Onset and severity of hearing loss due to congenital rubella infection. *Archives of disease in childhood* **64,** 1280-1283.

Willis, S.N., Chen, L., Dewson, G., Wei, A., Naik, E., Fletcher, J.I.*, et al.* (2005). Proapoptotic Bak is sequestered by Mcl-1 and Bcl-xL, but not Bcl-2, until displaced by BH3-only proteins. *Genes & development* **19,** 1294-1305.

Willows, S., Hou, S.M. and Hobman, T.C. (2013). RNA virus capsid proteins: more than just a shell. *Future Virol* **8,** 435-450.

Willows, S., Ilkow, C.S. and Hobman, T.C. (2014). Phosphorylation and membrane association of the Rubella virus capsid protein is important for its anti-apoptotic function. *Cellular microbiology* **16,** 1201-1210.

Wolter, K.G., Hsu, Y.T., Smith, C.L., Nechushtan, A., Xi, X.G. and Youle, R.J. (1997). Movement of Bax from the cytosol to mitochondria during apoptosis. *Journal of Cell Biology* **139,** 1281-1292.

Wong, K.T., Baron, S. and Ward, T.G. (1967). Rubella virus: role of interferon during infection of African green monkey kidney tissue cultures. *Journal of immunology* **99,** 1140-1149.

World_Health_Organization (2014) Rubella. W.H. Organization (ed.).

Xu, L., Xiao, N., Liu, F., Ren, H. and Gu, J. (2009). Inhibition of RIG-I and MDA5-dependent antiviral response by gC1qR at mitochondria. *Proceedings of the National Academy of Sciences of the United States of America* **106,** 1530-1535.

Xu, W., Yuan, X., Jung, Y.J., Yang, Y., Basso, A., Rosen, N.*, et al.* (2003). The heat shock protein 90 inhibitor geldanamycin and the ErbB inhibitor ZD1839 promote rapid PP1 phosphatase-dependent inactivation of AKT in ErbB2 overexpressing breast cancer cells. *Cancer research* **63,** 7777-7784.

Yang, J.S., Ramanathan, M.P., Muthumani, K., Choo, A.Y., Jin, S.H., Yu, Q.C.*, et al.* (2002). Induction of inflammation by West Nile virus capsid through the caspase-9 apoptotic pathway. *Emerging infectious diseases* **8,** 1379-1384.

Yang, M.R., Lee, S.R., Oh, W., Lee, E.W., Yeh, J.Y., Nah, J.J*., et al.* (2008). West Nile virus capsid protein induces p53-mediated apoptosis via the sequestration of HDM2 to the nucleolus. *Cellular microbiology* **10,** 165-176.

Yao, J. and Gillam, S. (1999). Mutational analysis, using a full-length rubella virus cDNA clone, of rubella virus E1 transmembrane and cytoplasmic domains required for virus release. *Journal of virology* **73,** 4622-4630.

Yao, J., Yang, D., Chong, P., Hwang, D., Liang, Y. and Gillam, S. (1998). Proteolytic processing of rubella virus nonstructural proteins. *Virology* **246,** 74-82.

Yokota, S., Saito, H., Kubota, T., Yokosawa, N., Amano, K. and Fujii, N. (2003). Measles virus suppresses interferon-alpha signaling pathway: suppression of Jak1 phosphorylation and association of viral accessory proteins, C and V, with interferon-alpha receptor complex. *Virology* **306,** 135-146.

Yoneyama, M., Kikuchi, M., Natsukawa, T., Shinobu, N., Imaizumi, T., Miyagishi, M*., et al.* (2004). The RNA helicase RIG-I has an essential function in double-stranded RNA-induced innate antiviral responses. *Nat Immunol* **5,** 730-737.

Zacks, M.A. and Paessler, S. (2010). Encephalitic alphaviruses. *Vet Microbiol* **140,** 281-286.

Zamarin, D., Garcia-Sastre, A., Xiao, X., Wang, R. and Palese, P. (2005). Influenza virus PB1-F2 protein induces cell death through mitochondrial ANT3 and VDAC1. *PLoS pathogens* **1,** e4.

Zhang, C., Tang, J., Xie, J., Zhang, H., Li, Y., Zhang, J*., et al.* (2008). A conserved domain of herpes simplex virus ICP34.5 regulates protein phosphatase complex in mammalian cells. *FEBS letters* **582,** 171-176.

Zhang, H.M., Ye, X., Su, Y., Yuan, J., Liu, Z., Stein, D.A. and Yang, D. (2010). Coxsackievirus B3 infection activates the unfolded protein response and induces apoptosis through downregulation of p58IPK and activation of CHOP and SREBP1. *Journal of virology* **84,** 8446-8459.

Zheng, D.P., Frey, T.K., Icenogle, J., Katow, S., Abernathy, E.S., Song, K.J*., et al.* (2003). Global distribution of rubella virus genotypes. *Emerging infectious diseases* **9,** 1523-1530.

Zheng, D.X., Dickens, L., Liu, T.Y. and Nakhasi, H.L. (1989). Nucleotide sequence of the 24S subgenomic messenger RNA of a vaccine strain (HPV77) of

rubella virus: comparison with a wild-type strain (M33). *Gene* **82,** 343-349.

Zheng, W., Li, J., Wang, S., Cao, S., Jiang, J., Chen, C*., et al.* (2015). Phosphorylation controls the nuclear-cytoplasmic shuttling of influenza A virus nucleoprotein. *Journal of virology*.

Zheng, Y. and Kielian, M. (2013). Imaging of the alphavirus capsid protein during virus replication. *Journal of virology* **87,** 9579-9589.

Zong, W.X., Lindsten, T., Ross, A.J., MacGregor, G.R. and Thompson, C.B. (2001). BH3-only proteins that bind pro-survival Bcl-2 family members fail to induce apoptosis in the absence of Bax and Bak. *Genes & development* **15,** 1481-1486.

Zou, H., Li, Y., Liu, X. and Wang, X. (1999). An APAF-1.cytochrome c multimeric complex is a functional apoptosome that activates procaspase-9. *The Journal of biological chemistry* **274,** 11549-11556.